MARTENSITIC PHASE TRANSITIONS WITH SURFACE EFFECTS

Thesis by

Mark T. Lusk

In Partial Fulfillment of the

Requirements for the Degree of

Doctor of Philosophy

California Institute of Technology

Pasadena, California

1992

(Submitted April 14, 1992)

ACKNOWLEDGEMENTS

I remember dreaming about going to graduate school and becoming a research scientist. That was in the old days, when I used to float around in the ocean for a living, and a huge number of people have helped my dream materialize since then.

It has been a wonderful privelege to have had Jim Knowles as my advisor. He has guided my research and has taught me how to conduct a scientific investigation. A great person is measured by both his professional achievements and his works of human compassion. My mentor certainly is such a man.

Eliot Fried taught me the fundamentals of continuum mechanics and has always been willing to share and explore new ideas with me. I think it is probably rare to have a good friend for a research partner.

I am pleased to acknowledge Morton Gurtin, Rohan Abeyaratne, Qing Jiang, Phoebus Rosakis and Andrew Lewis for a number of productive discussions that helped to shape my thesis research.

It is remarkable that Caltech has so many nice people associated with it. In particular, I am grateful to Dana Young, Jackie Beard, Susan Burns, Cecilia Lin, Sharon Bekenbach, Carol Mastin, Lorrie Mack and Ruth Sustaita. Thank you for your help and, more importantly, your friendship. Thanks is also in order to John Wissler for our weekly return to sanity over coffee. I savored these times.

I am one of those lucky people who are part of a large and loving family. Thank you Mom and Dad Lusk, Mom and Dad Asbell, Joe and Kathleen Hall, Joan and Buck, Gail and Jeff, Lois and Wayne, Lori and Steve, Barri and John, Caryn and Anton, Tracie and Eric.

My research has been supported under a National Science Foundation Graduate Fellowship as well as an A.R.C.S. Fellowship.

This thesis is dedicated to my wife, Kimberly, and our little tribe. Graduate school is hard on family, and all the things we have accomplished over the last few years have been a team effort. Research is fun. Family comes first.

ABSTRACT

Continuum treatments of martensitic phase transformations are capable of accounting for a variety of important surface effects attributable to the spatially localized interaction of coexisting material phases. Such phenomena are thought to play a critical role in determining the size, shape, and stability of nucleated embryos as well as to affect the conditions under which nucleation events occur. These issues are examined within a purely mechanical context wherein the special properties are modeled as traction and energy fields defined on a two-dimensional abstraction of the interface region. Materials that undergo martensitic phase changes are modeled as having a hyperelastic character in both the bulk and interface. The characterization of such bodies is examined in detail and a representation theorem is presented for describing the interfaces of isotropic, hyperelastic media. A class of isotropic, nonlinearly hyperelastic bulk material is introduced that is capable of modeling the dilatative component of martensitic phase transformations. Such materials are considered within a noninertial setting referred to as *The Cylinder Problem.* This problem provides a means of exploring a variety of surface effects, and a criterion for nucleation based on energy is presented towards this end. Here nucleation events are modeled as deterministic, temporal shocks that are global in spatial extent. The fundamental development presented does more than capture the desired surface effects. It shows how they are related to specific assumptions regarding interface and bulk constitution. Four different interface characterizations are presented that serve to illustrate this.

TABLE OF CONTENTS

Acknowledgements iii

Abstract iv

Table of Contents v

1. Introduction 1

1.1 Martensitic phase transitions 1

1.2 Continuum models of martensitic phenomena 3

1.3 Surface effects and phase transitions 5

1.4 Material surfaces in fluids and solids 6

1.5 Phase interfaces in deformable and non-deformable media 9

1.6 Scope of the present work 12

2. Preliminaries 15

2.1 Notation and definitions 15

2.2 Bulk and surface gradients 17

2.3 Smooth, superficial fields and surface divergence 18

2.4 Surface motion 18

2.5 Latticed bodies and interfaces 20

3. Balance Postulates 23

3.1 Primitive fields 23

3.2 Balance postulates 23

3.3 Referential formulation 25

3.4 Implications of parameterization invariance 27

3.5 Referential localizations and interface driving traction 28

4. Hyperelastic Materials With Interfaces 30

4.1 Material constitution 30

4.2 A remark on the accretive stress, $\hat{\mathbf{C}}$ 33

4.3 A kinetic relation for interfaces 33

5. Mechanical Symmetry For Hyperelastic Materials With Interfaces 35

5.1 Mechanical equivalence 35

5.2 Material isotropy 36

5.3 Further insights regarding $\hat{\mathbf{C}}$ 40

6. Slow Dilative Phase Transitions 42

6.1 Dilatation in martensitic phase transitions 42

6.2 Loss of ellipticity under pure dilatation 43

6.3 Two-phase, dilative solids 43

6.4 A reduced form for the driving traction 45

6.5 Two-phase linearly dilative solids 46

7. The Cylinder Problem For 2-PLD Solids 48

7.1 Temporal shocks 48

7.2 Problem setting 48

7.3 Single-phase solutions 52

7.4 Two-phase solutions: no surface fields 53

7.5 Nucleation events 55

7.6 A nucleation criterion 57

7.7 The nucleation problem: no surface fields 58

7.8 Embryo stability 60

8. The Cylinder Problem: Interfaces With Bonding Energy 62

8.1 Two-phase solutions: interfaces with bonding energy 62

8.2 Nucleation with bonding energy 65

8.3 Embryo stability 66

9. The Cylinder Problem: Interfaces With A Fluid Nature 68

9.1 Two-phase solutions: fluid-like interfaces 68

9.2 Nucleation with fluid-like interfaces 71

9.3 Embryo stability 72

10. The Cylinder Problem: Interfaces With A Membrane Nature 73

10.1 A membrane-like interface 73

10.2 Macroscopic response: membrane-like interfaces 74

11. Concluding Remarks 77

Appendices 79

A. Galilean objectivity 79

B. Invariance lemma 80

C. Interface representation for isotropic, hyperelastic materials 81

D. Fluid-surface theorem 91

E. Strain dependence of the nucleation energy 94

References 100

Figures 113

1. INTRODUCTION

1.1. Martensitic Phase Transitions.

> A given material may exist in different states, and changes of state, or *phase transformations*, may be induced by sufficiently altering the material environment.

This statement seems reasonable because it reflects a wealth of physical experiences wherein the properties of a substance are observed to abruptly change. A common example is the liquid-to-vapor phase transformation of a fluid in response to heating—a *thermally induced* reaction—or a drop in pressure—the same reaction but now *mechanically induced.*

The process by which a material accomplishes a change of phase is called a *phase transition.* Transitions are therefore associated with the formation and growth of a new phase partitioned from the original phase by an interfacial region, and these interfaces may be either sharp or diffuse, depending on the nature of the reaction. If no cracks, voids, or slippage are associated with an interface, it is referred to as *coherent.*

The present investigation focuses on non-diffusive transitions that involve two solid phases of a material separated by a sharp, coherent interface. These *martensitic* processes are most common in Fe-C systems, but are found in Ni-Ti, Ag-Cd, Au-Cd, Cu-Zn, Cu-Zn-Al, Cu-Al-Ni, In-Tl and other alloys as well.[1.1] In addition, ceramic materials such as partially stabilized zirconia (ZrO_2) exhibit this type of phase transition.[1.2]

In recent years the materials science community has developed a wide variety of products whose working properties rely on martensitic phase transitions.

[1.1] For a basic text of work in this area see NISHIYAMA[1978]. For investigations of specific systems see, for example, KRISHNAN & BROWN[1973]; CHANG[1952]; AHLERS[1986]; OTSUKA, TAKAHASHI & SHIMIZU[1973]; GRUJICIC, OLSON & OWEN[1985]; BURKART & READ[1953].

[1.2] See PORTER & HEUER[1977]; BUDIANSKY, HUTCHINSON & LAMBROPOULOS[1983]; LAMBROPOULOS[1983]; RUF & EVANS[1983].

These include shape-memory materials[1.3] like the Nitinol and Tinel alloys that are used to make, among other things, Cryofit couplings and heat-to-shrink fasteners. Shape-memory materials also constitute an important component of the emerging discipline of smart materials and systems. Here *smart* refers to the idea that a component is able to sense its environment and actuate an appropriate self-control procedure. Vibration suppressors, structural damage warning devices, and robotic muscle are potential applications that are currently being investigated.[1.4]

Another technology based on martensitic phase transitions is that of transformation-toughened materials.[1.2] Here ceramic beads of, for instance, partially stabilized zirconia are embedded in a ceramic matrix. High stress regions near cracks cause the beads to change phase; this is found to inhibit further crack growth. The fracture toughness of the composite is thus increased.

The number of existing and potential uses for martensitic materials has motivated a number of theoretical investigations attempting to better understand these phase transitions through modeling from a continuum physics perspective. Such a macroscopic viewpoint is only one means of gaining insight into the nature of martensitic phenomena and is certainly not intended to supplant atomistic approaches. The utility of embracing such a treatment to investigate complex phenomena is well established, however, as summarized in the following appraisal of Conyers Herring:[1.5]

> These concepts, besides being simpler and neater to work with than those of atomistic theory, have the great advantage that they often lead to soundly based conclusions independent of any detailed assumptions regarding the atomic mechanisms of the phenomena being studied. Ofcourse, this does not mean that the user of macroscopic concepts should

---

1.3 DELAEY, KRISHNAN, TAS & WARLIMONT[1974a,b,c] provide a review of the shape-memory effect.

1.4 AMATO[1992]; ROGERS, LIANG, & FULLER[1991]; WANG & ROGERS[1991].

1.5 HERRING[1952] p.70.

think no atomistic thoughts! It merely means that he should, wherever possible, use such thoughts as a guide to his intuition in formulating macroscopic laws and deciding the range of their validity.

1.2. Continuum Models of Martensitic Phase Transitions. In the simplest sense, the various phases of a body may be identified by their differing material properties.[1.6] More detailed consideration of phase transitions involves a number of subtleties, however, and even a precise definition of phase is elusive. Continuum physics provides a foundation for investigating such phenomena and offers a criterion for distinguishing various phases of a material. Here *phases* refer to disjoint domains of a single energy functional that characterizes the material of interest.[1.7] This is in line with the intuitive picture that individual phases are just differing configurations of a single substance and provides a means of distinguishing variation in a given phase from a phase transition. The classical example of this type of material description is that for the Van der Waals fluid.[1.8] From the continuum perspective, an interface is coherent if the multiphase configuration can be described as a continuous deformation of some homogeneous reference state.

Material constitution generally imposes severe restrictions—*phase segregation requirements*—on the ways coherent coexistence can be accommodated. Only certain environments will support multiphase states, and the shape of each phase is often restricted as well.[1.9] The interface between phases may *accrete*—that is, move relative to the underlying material so as to effect a transfer of mass from one phase to another. However, it is not a free boundary because of the phase segregation requirements, and certain materials may call for supplementary information

---

1.6 GIBBS[1928] p.96.

1.7 GIBBS[1928] p.31, COLEMAN & NOLL[1959] p.103, FOSDICK[1986] p.137. A different viewpoint is taken by ESHELBY[1961] and ROBIN[1974], among others, wherein each phase is characterized by a distinct constitutive law.

1.8 See, for instance, CALLEN[1960] Ch. 9.

1.9 ROSAKIS[1991].

regarding interface position.

Continuum investigations of martensitic phenomena have proved both challenging and productive. ERICKSEN[1975], and from a completely different perspective, KNOWLES & STERNBERG[1975, 1977, 1978], pioneered such work, and a rich line of research ensued. Within special settings, ABEYARATNE[1980, 1981] and FOSDICK & MACSITHIGH[1983] studied the existence and uniqueness of elastostatic solutions with discontinuous deformation gradients in incompressible hyperelastic materials. JAMES[1979] considered stability issues within a one-dimensional static setting and GURTIN[1983], extending this development, found necessary conditions for equilibrium with piecewise homogeneous solutions for a class of hyperelastic materials. JAMES[1981, 1986a,b], PARRY[1980], and KINDERLEHRER[1984, 1988] investigated piecewise homogeneous equilibria associated with mechanical twinning. necessary and sufficient conditions for general hyperelastic materials to sustain a loss of ellipticity were derived by ROSAKIS[1990]. The existence of two-phase equilibria involving inhomogeneous, two-dimensional anti-plane shear deformation was studied by SILLING[1988a,b] and by FRIED[1991a]. A nonlinear elasticity framework was used by ROSAKIS[1991] to account for observed shapes of embedded phases in shear transitions of anisotropic material. Non-convex strain-energy densities have been successfully used to model transformation-toughening in ceramic composites by BUDIANSKY, HUTCHINSON, & LAMBROPOULOS[1983], SILLING[1987], and ABEYARATNE & JIANG[1988a,b] and by BALL & JAMES[1987] to study fine phase mixtures. SILLING[1988c] provided numerical studies of interface dynamics. Phase-boundary interactions with acoustic waves were studied by JAMES[1980] and PENCE[1991]. The dissipative nature of martensitic phase transitions was considered by KNOWLES[1979], YATOMI & NISHIMURA[1983], and ABEYARATNE & KNOWLES[1987a,b], and was placed within a fully thermodynamical framework by ABEYARATNE & KNOWLES[1990a].

Within nonlinear constitutive settings, there may be a number of states of a body satisfying given boundary conditions. Such a lack of uniqueness may,

for instance, be manifested in a range of possible interface positions. This issue was addressed by ABEYARATNE & KNOWLES[1987a,b, 1988] within special settings where a lack of solution uniqueness was established. Motivated by the internal variable work of RICE[1971, 1975] in plasticity, they suggested a class of supplementary *kinetic relations* and found them sufficient to guarantee the uniqueness of solutions. Kinetic relations were then used by ABEYARATNE & KNOWLES[1989, 1990b,c] to study one-dimensional phase-boundary dynamics, by JIANG[1989] to model creep in a thermoelastic setting, and by FRIED[1991b, 1991c] to study the stability of planar phase boundaries. ABEYARATNE & KNOWLES[1990a] discuss the role of kinetic relations within a thermodynamical framework.

1.3. Surface Effects and Phase Transitions. The continuum models described above do not capture certain key phenomena, known as *surface effects*, associated with phase transitions. These phenomena are attributable to the spatially localized interaction of coexisting material phases. Such properties are particularly relevant in situations where the interface curvature is very large—as in the initial formation of a new phase embryo.[1.10]

One such surface effect is the existence of a jump in the traction exerted on either side of an interface. An example of this for fluids is that the pressure inside a vapor bubble is higher than that of its surrounding liquid, but in solids it is reasonable to think that interfaces may resist shear as well since this is a characteristic of the bulk phases on either side.

A second important effect attributable to special interface properties is the occurrence of *supercritical phenomena.*[1.11] It is found that conditions capable of initiating a phase change with planar interface geometry cannot produce a phase embryo with a highly curved boundary. If the relevant environmental parameter is temperature, for instance, a phase change might not occur until the body is

[1.10] CHALMERS[1964] Ch. 3.

[1.11] DUNNING[1969] p.3, gives a brief historical survey of supercritical phenomena. Also see the discussions of PIPPARD[1981] pp.114-115; MULLER[1985] p.251; and CHALMERS[1964] p.62, p.85.

superheated above its normal transition temperature. Likewise, for mechanically induced reactions, a body may require straining beyond that known to induce phase changes when inhomogeneities allow the formation of low curvature interfaces.

It is observed that symmetry properties associated with an interface should influence the shape of a phase embryo, and this is especially true when the nucleus is so small that bulk effects do not dominate. The surface properties of an interface can thus play an important role in the determination of embryo shape.

A final surface effect of interest in this work pertains to the stability of newly formed nuclei. It is observed that the stability of multiphase equilibria may depend upon the embryo size as well as on conditions at the system boundary. This behavior, and often the existence of such equilibria themselves, are attributable to localized properties at phase interfaces.[1.12]

Continuum treatments of phase transitions may be modified to account for these important surface effects. Interface properties are modeled by fields defined on the interface itself, which are collectively referred to as *interfacial structure.* Here the interface is usually treated as a surface.[1.13] Balance principles are postulated that restrict the way in which bulk and surface fields may interact, and a characterization of the body via constitutive response functions completes the development. Though this provides a mathematically tractable model, it requires physical motivation, especially in regard to what types of interfacial fields should be included and the way in which they should interact.

1.4. Material Surfaces in Fluids and Solids[1.14]

The development of continuum theories of interfacial structure has its roots in considerations

1.12 UBRICHT, SCHMELZER, MAHNKE & SCHWEITZER[1988]; PIPPARD[1981].

1.13 A different approach is to treat the interface as a thin bulk region. See SLATTERY[1990] or ALTS & HUTTER[1988a,b,c] for investigations of how these differing approaches may be resolved.

1.14 The following motivational sketch of the development of continuum theories of surface and interfacial structure is by no means intended to include all of the important contributions that such a vast development necessarily entails.

of the localized surface properties of materials not involved in a change of phase. It is often reasonable to model such boundaries as distinct, lower-dimensional bodies themselves—that is, as material skins with their own constitutive properties. These regions are referred to as *material surfaces.* Common to all such work is the allowance for a surface energy. This has a compelling molecular motivation since atoms in layers nearest to the surface have a different bonding arrangement than those in the material bulk.

Consider a wire frame suspending a liquid film.[1.15] Suppose that the film has a constant energy per unit area, γ, and is in equilibrium with area, A. Hamilton's principle—energy stationarity with respect to virtual system changes[1.16]—dictates that such an equilibrium can exist only if $d(\gamma A)/dA = 0$. For the molecularly motivated assumption that γ be constant for such a fluid film, this condition implies the existence of an unbalanced surface tension in the film, equal in magnitude to the surface energy, which disallows an equilibrium configuration *unless* the wire frame offers a reactive tension of equal magnitude. This is found to be the case experimentally. Thus, Hamilton's principle motivates an adoption of surface traction as a primitive field which, for fluid films, is just a surface tension. Certainly this is not how the concept of surface tension was derived since its advent actually proceeded any idea of surface energy,[1.17] but the approach has proved productive in establishing the utility of additional surface primitives. Application of this idea to such a film sandwiched between two fluid bodies yields the classic Gibbs-Thomson relation:[1.18]

$$\Delta P = 2H\gamma,$$

1.15 See ADAMSON[1967] Ch. 1; PORTER & EASTERLING[1981] Ch. 3. Here the film is used to illustrate a two-dimensional continuum, though in reality it is two fluid surfaces sandwiching a thin layer of bulk fluid.

1.16 To quote Gibbs on the matter: " For the equilibrium of any isolated system it is necessary and sufficient that, in all possible variations in the state of the system which do not alter its entropy, the variation of its energy shall either vanish or be positive."
GIBBS[1928] p.56.

1.17 SHUTTLEWORTH[1950] gives a brief historical sketch of surface tension and surface energy.

1.18 GIBBS[1928] p.229.

where ΔP is the difference in pressure across the film and H is its mean curvature.

A more complex situation arises in solid-material membranes, where atomistic considerations suggest that surface stress should be tensorial in nature. In fluids, atoms are free to migrate to and from the surface so that shear stresses cannot be supported. Solids, however, do not have this property and the atom migration necessary to maintain unchanged surface energy happens only very slowly. Surfaces may be modeled as conserving their mass with deformation measured relative to some arbitrary reference state. SHUTTLEWORTH[1950] and HERRING[1951a,b] supposed the surface energy of such a membrane to be a function of the deformation gradient, $\mathbf{F}_s$, and they applied Hamilton's principle to find that the membrane boundary must support a surface stress, $\mathbf{T}_s = \gamma \mathbf{1}_s + d\gamma/d\mathbf{F}_s$, as a necessary condition for equilibrium. Here $\mathbf{1}_s$ is the identity tensor for the surface. Thus for solid surfaces, the tensile contribution from surface energy is only a part of the total tensorial stress. In association with this is a straightforward vectorial generalization of the Gibbs-Thomson relation.[1.19]

Such reasoning has been used extensively in early treatments of material surfaces[1.20] and eventually led to the formation by GURTIN & MURDOCH[1975] of a complete dynamical theory of material surfaces with both surface energy and surface stress taken as primitives. This theory was used to consider stress on the surface of crystals by GURTIN & MURDOCH[1976]. MOECKEL[1975] independently developed the same approach but considered only fluid constitutions. His work, however, embraced a fully thermodynamic description of material surfaces by introducing a surface heat flux and surface entropy field. MURDOCH[1976] later extended his earlier work to include these thermal effects. MULLER[1985] gives a detailed presentation of the complete theromodynamic theory and studies a number of fluid surface applications.

1.19 See, for instance, discussions in CAHN[1980] and CAHN & LARCHE[1982].

1.20 For examples, see ADAM[1941]; HERRING[1951a,b]; SCRIVEN[1960]; ARIS[1962]; and LANGER[1989].

1.5 Phase Interfaces in Deformable and Non-deformable Media.

While similar in many respects to material surfaces, phenomena associated with interfaces between phases of a material are more complex because of the potential for accretion and the constraints of phase segregation. Accretion embodies a new type of material interaction, and it is not obvious what new fields are necessary in order to account for observed phenomena. MOECKEL[1975] took the stance that accreting interfaces should be treated in the same manner as deforming material surfaces—an approach discredited in later investigations, which benefited from considerations of energy stationarity. Accretion represents a kinematic process distinct from classical notions of motion and calls for a non-classical notion of both traction and power expenditure where interfacial properties are accounted for.

Non-deformable media

The first efforts to develop a model of the structured accreting interface focused on temperature-induced transitions in non-deformable media. This greatly simplified investigations because only one kinematic process was involved, and work was primarily focused on solidification and melting—the *Two-phase Stefan Problem.*[1.21] Based on the assumption of constant interfacial energy, a variational argument involving virtual accretion and the Gibbs-Thomson relation gave the classic *capillarity relation*[1.22]:

$$\Delta\theta = 2Hh,$$

where $\Delta\theta$ is the departure of interface temperature from the melting temperature associated with a planar interface, H is the interface mean curvature, and h is a material constant. The physical interpretation is that on the boundary of a convex solid phase, particles have weaker bonds than on a flat interface.[1.23] Thus,

---

1.21 RUBENSTEIN[1971].

1.22 Due to THOMSON[1886]. See also the discussion of DUNNING[1969] pp.8-10. Though somewhat confusing, this equality is commonly referred to as the Gibbs-Thomson relation as well.

1.23 CHALMERS[1964] pp.63-64.

the thermal energy required to remove atoms from curved surfaces is smaller, and consequently the corresponding equilibrium temperature is smaller than for a flat interface. Within the statical theory, the capillarity relation provides supplementary information regarding interface geometry.[1.24]

FERNANDEZ-DIAZ & WILLIAMS[1979] and later GURTIN[1986] developed axiomatic frameworks that accounted for interfacial structure in phase transitions of non-deformable media. Gurtin showed that within a fully dynamical theory, if the interface produces no entropy, then the capillarity relation can be derived under a specific set of constitutive assumptions. As in the statical setting, this relation provides information characterizing the interface morphology. The isentropic assumption, while implicit in variational considerations of equilibrium, takes the form of a balance postulate in Gurtin's dynamical theory. An important feature of the energy balance postulated is the explicit accounting of surface energy outflow that is due to interface motion relative to the subbody considered. This would later be accounted for via an accretive stress field.

Experimental evidence showed the capillarity relation to be too simple to account for an observed dependence of interface temperature on solidification melting rate.[1.25] CAHN, HILLIG & SEARS[1964] proposed several relations between accretive velocity and the departure of interface temperature from its static value on the basis of molecular considerations. Independently, VORONKOV[1965] proposed that a constitutively determined relation should exist between the accretive velocity of the phase boundary and melting temperature. With an empirical requirement for such a *kinetic relation*[1.26] established, a large number of investigations focused on its implications in problems previously considered using only the

---

1.24 Applications abound. For examples see CHALMERS[1964]; MULLINS & SEKERKA[1963, 1964]; DELVES[1974].

1.25 See related discussions in CAHN, HILLIG & SEARS[1964]; CHALMERS[1964] Chapter 2.4.

1.26 The term *kinetic relation* was proposed by ABEYARATNE & KNOWLES[1988] within the context of displacive phase transitions. CAHN, HILLIG & SEARS[1964], for instance, refer to a *kinetic law* while VISINTIN[1987,1989] uses the term *kinetic response function*. Neither VORONKOV[1965] nor GURTIN[1988a] assign a name to this type of relation.

capillarity relation.[1.27] GURTIN[1988a] generalized his earlier theory by giving up isentropic interfaces in favor of the assumption that a kinetic relation is a required part of the characterization of a material. He showed that under near equilibrium conditions, his rather general kinetic relation reduces to the linear form typically utilized in earlier works.

An additional development in the theory that appeared in Gurtin's work was the allowance for a mechanical energy flux within the interface. This flux is distinct from the energy-outflow term introduced earlier. Within a reasonble constitutive setting, restrictions imposed by entropy imbalance allowed the flux to be expressed as a traction expending power in association with the motion of anisotropic interfaces. This interpretation pointed towards a fundamentally new concept of work associated only with accretion, and not with particle motion. The idea is in line with the earlier developments of CAHN & HOFFMAN[1972, 1974], in turn based on the investigations of HERRING[1951a,b], who adopted a capillary traction to account for interface orientation effects.

Though well motivated physically, the introduction of a kinetic relation is ad hoc insofar as it is not derivable from axiomatic foundations. Based on the premise that there must exist a general balance framework from which a kinetic relation could be derived, GURTIN[1988b] abandoned his earlier, constitutive procedure in favor of an *Accretive Force Balance*. This new balance principle, representing bulk-interface interaction, provides a relation between conditions at the interface and accretive velocity that is independent of material constitution. An *accretive stress* expends power in association with accretion. The normal component of this stress corresponds to the capillary traction of CAHN & HOFFMAN[1972, 1974]. Power expenditure associated with the tangential component of the accretive stress is an alternate way of accounting for the outflow of surface energy that is due to the relative motion of the interface with respect to the subbody under

[1.27] See, for instance, CORIELL & PARKER[1966]; VISINTIN[1987,1989]; XIE[1990]; STRAIN [1988, 1990].

consideration. The theory was applied to study the evolution of interfaces in an isothermal environment by ANGENENT & GURTIN[1989].

Deformable media

In considering phase transitions involving both accretion and deformation, physical intuition suggests a marriage of the developments from material surfaces and non-deforming interfaces. CAHN[1980] and CAHN & LARCHE[1982] examined deforming, accreting interfaces within the context of spherical symmetry and isotropic media. ALEXANDER & JOHNSON[1985, 1986] generalized their variational approach to include dependence of interfacial energy on surface orientation but did not properly account for virtual accretion. LEO & SEKERKA[1989] continued the development and provided a correct method of accounting for accretive variation. In allowing interfacial energy to depend on orientation, surface deformation, and temperature, they identified a traction associated with the resistance to rotations of the interface during accretion. This was then shown to be directly related to the capillary traction of Cahn and Hoffman's investigations of non-deformable bodies. GURTIN & STRUTHERS[1990] incorporated these results into a complete thermodynamical theory of phase transitions in deformable media. Their work draws on Gurtin's earlier development for non-deformable media and includes an accretive force balance. Interfacial structure includes a deformational traction akin to that associated with material surfaces and an accretive stress that accounts for both surface energy outflow and power expenditure due to anisotropic interface accretion. The resulting theory has been successfully applied in an investigation of melting-freezing waves.[1.28]

1.6. Scope of the Present Work. Comprehensive continuum models that account for localized interface properties have yet to be used to study a number of interesting surface effects that may exist in martensitic phase transitions, and experimental data suggest that such a continuum investigation is in

[1.28] GURTIN[1990].

order. Solid material surfaces, for instance, have long been known to support surface stresses so that it is physically reasonable to suppose that solid-solid phase interfaces may indeed generate a traction jump whose effect is significant in high curvature regions. Another important surface effect, supercritical phenomena, has been experimentally documented in martensitic reactions through the small particle experiments of CECH & TURNBULL[1956]. Finally, on the basis of investigations of phase transitions in fluids, it is likely that special interface properties play an important role in determining the size, shape and stability of martensite nuclei. Most materials science investigations of martensitic phase transitions do make some attempt to account for surface energy, though this is done in an ad hoc manner. The development presented here does more than capture the desired surface effects. It shows how they are related to specific assumptions regarding interface and bulk constitution.

For simplicity, attention is restricted to martensitic transitions that are mechanically induced, and a theoretical development is presented that does not account for temperature effects. The theory is a modified version of that developed by GURTIN & STRUTHERS[1990] and discussed in the previous section.

Materials that undergo martensitic phase changes are modeled here as hyperelastic in both bulk and interface response to deformation. The characterization of such bodies is examined in detail, and a representation theorem is presented for describing the interfaces of isotropic, hyperelastic bodies in terms of the two fundamental scalar invariants of the deformation gradient of the surface.

A class of isotropic, nonlinearly hyperelastic bulk materials is introduced that is capable of modeling the dilatation component of martensitic phase changes. The materials are considered within a non-inertial context referred to as *The Cylinder Problem.* This setting provides a means of exploring a variety of surface effects, and a *nucleation criterion* is presented towards this end that is based on system energy. Here nucleation events are modeled as deterministic, temporal shocks that are global in spatial extent. Such a model is in line with the continuum

viewpoint in that it is utilized to better understand the relationship between macroscopic material properties and observed material response to loading. This work is intended to be synergistic with investigations that consider martensitic nucleation from a statistical perspective.[1.29]

Four different interface characterizations are presented that illustrate how various interface properties and surface effects are related. Interfaces with a *bonding energy* nature, for instance, yield no traction jump, while *fluid-like* and *membrane-like* interfaces do. The latter two interface constitutions, in conjunction with the phase segregation constraints, imply the existence of a lower limit on embryo size that the system can support independent of any nucleation criterion. For all three interfaces, however, the embryo size at the instant of formation must be finite, and it is found that the number and stability of two-phase equilibria are affected in each case. The Cylinder Problem is also capable of exhibiting supercritical phenomena, which in this mechanical context, is referred to as *superstraining.*

[1.29] See the excellent review article of THADHANI & MEYERS[1986] as well as the more recent work of ROITBURD[1990].

2. PRELIMINARIES

Within a purely mechanical theory of phase transitions, phase interfaces are associated with kinematic singularities that partition the body of interest. For clarity of presentation, a theory is presented for which there exists at most one such partition in a given body. Since the theory is well understood in the absence of phase transitions, only processes associated with the presence of an interface are considered.[2.1]

2.1. Notation and Definitions.

$\mathbb{R}^N$	set of all N-tuples of real numbers
$\mathcal{V}^N, \mathcal{U}^N$	N-dimensional inner product spaces
$\mathbb{E}^N$	N-dimensional Euclidean space
$\mathrm{Unit}(\mathcal{V}^N)$	set of all unit length elements of $\mathcal{V}^N$
$\mathrm{Lin}(\mathcal{V}^N, \mathcal{V}^M)$	set of all linear maps of $\mathcal{V}^N \to \mathcal{V}^M$
$\mathrm{Lin}^{ns}(\mathcal{V}^N, \mathcal{V}^M)$	set of all non-singular elements of $\mathrm{Lin}(\mathcal{V}^N, \mathcal{V}^M)$
$\mathrm{Lin}_+(\mathcal{V}^N, \mathcal{U}^N)$	set of all elements of $\mathrm{Lin}(\mathcal{V}^N, \mathcal{U}^N)$ with positive determinant
$\mathrm{Sym}(\mathcal{V}^N)$	set of all symmetric elements of $\mathrm{Lin}(\mathcal{V}^N, \mathcal{V}^N)$
$\mathrm{Sym}^+(\mathcal{V}^N)$	set of all positive definite elements of $\mathrm{Sym}(\mathcal{V}^N)$
$\mathrm{Unim}(\mathcal{V}^N, \mathcal{U}^N)$	set of all elements of $\mathrm{Lin}_+(\mathcal{V}^N, \mathcal{U}^N)$ with unit determinant
$\mathrm{Orth}(\mathcal{V}^N, \mathcal{U}^N)$	set of all orthogonal elements of $\mathrm{Lin}(\mathcal{V}^N, \mathcal{U}^N)$
$\mathrm{Orth}_+(\mathcal{V}^N, \mathcal{U}^N)$	set of all orthogonal elements of $\mathrm{Lin}_+(\mathcal{V}^N, \mathcal{U}^N)$

The *inner product* of $\mathbf{a}, \mathbf{b} \in \mathcal{V}^N$ is denoted by $<\mathbf{a}, \mathbf{b}>$ or $\mathbf{a} \cdot \mathbf{b}$.

The *outer product*, $\mathbf{c} \otimes \mathbf{d} \in \mathrm{Lin}(\mathcal{V}^N, \mathcal{V}^M)$, of $\mathbf{c} \in \mathcal{V}^N$ and $\mathbf{d} \in \mathcal{V}^M$ is defined by

$$(\mathbf{c} \otimes \mathbf{d})\mathbf{e} = <\mathbf{d}, \mathbf{e}> \mathbf{c} \quad \forall \mathbf{c} \in \mathcal{V}^N, \quad \forall \mathbf{d}, \mathbf{e} \in \mathcal{V}^M. \tag{2.1.1}$$

2.1 The preliminary concepts developed in Sections 2.1-2.4 are presented in more detail by GURTIN & MURDOCH[1975]; GURTIN[1988a]; and GURTIN & STRUTHERS[1990]. An attempt is made to use notation consistent with these works wherever possible.

The *vector product* of $\mathbf{f}, \mathbf{g} \in \mathcal{V}^N$ is denoted by $(\mathbf{f} \wedge \mathbf{g}) \in \mathcal{V}^N$ and is the unique bilinear operator satisfying

$$\begin{aligned} \mathbf{f} \wedge \mathbf{g} &= -\mathbf{g} \wedge \mathbf{f} \\ (\mathbf{f} \wedge \mathbf{g}) \cdot (\mathbf{f} \wedge \mathbf{g}) &= (\mathbf{f} \cdot \mathbf{f})(\mathbf{g} \cdot \mathbf{g}) - (\mathbf{f} \cdot \mathbf{g})^2 \\ \mathbf{f} \cdot (\mathbf{f} \wedge \mathbf{g}) &= 0. \end{aligned} \tag{2.1.2}$$

The *transpose* of $\mathbf{A} \in \mathrm{Lin}(\mathcal{V}^N, \mathcal{V}^M)$ is denoted A^T and is defined by

$$(\mathbf{A}\mathbf{b}) \cdot \mathbf{c} = \mathbf{b} \cdot (\mathbf{A}^T \mathbf{c}) \quad \forall \mathbf{b} \in \mathcal{V}^N, \quad \forall \mathbf{c} \in \mathcal{V}^M. \tag{2.1.3}$$

The *inner product* on $\mathrm{Lin}(\mathcal{V}^N, \mathcal{V}^M)$ is defined by

$$\begin{aligned} \mathbf{A} \cdot \mathbf{B} &:= \mathrm{Trace}(\mathbf{A}\mathbf{B}^T) \\ &= \langle \mathbf{A}, \mathbf{B} \rangle \end{aligned} \qquad \forall \mathbf{A}, \mathbf{B} \in \mathrm{Lin}(\mathcal{V}^N, \mathcal{V}^M) \tag{2.1.4}$$

so that all of the sets of linear transformations defined are endowed with an inner product space structure. The *norm* of $\mathbf{a} \in \mathcal{E}^N$ is given by

$$\|\mathbf{a}\| := \sqrt{\mathbf{a} \cdot \mathbf{a}} \quad \forall \mathbf{a} \in \mathcal{E}^N. \tag{2.1.5}$$

In general, scalar fields are denoted by lower-case letters, vector fields by lower-case bold type, and tensor fields by bold-type, upper-case letters. A superscript '$\cdot$' denotes partial differentiation with respect to the second argument of a function.

Surface, $\mathcal{S}$	a subset of $\mathcal{E}^3$ locally diffeomorphic to $\mathcal{E}^2$.
Surface Normal, $\mathbf{n}(\mathbf{x})$	either of the two unit vectors perpendicular to a surface at the point $\mathbf{x}$.
Tangent Space, $\mathbf{n}^\perp(\mathbf{x})$, of $\mathcal{S}$ at $\mathbf{x}$	best linear approximation to $\mathcal{S}$ at $\mathbf{x}$.
Surface Boundary, $\partial\mathcal{S}$	the closed curve that delineates the edge of a surface.
Superficial Scalar or Vector Field	scalar of vector field defined on $\mathcal{S}$.
Tangential Vector Field	superficial vector field with values in $\mathbf{n}^\perp(\mathbf{x})$.
Superficial Tensor Field	field on $\mathcal{S}$ with values in $\mathrm{Lin}(\mathbf{n}^\perp(\mathbf{x}), \mathcal{E}^3)$.

Tangential Tensor Field	field on $\mathcal{S}$ with values in $\mathrm{Lin}\big(\mathbf{n}^{\perp}(\mathbf{x}), \mathbf{n}^{\perp}(\mathbf{x})\big)$.
Boundary Bi-normal, $\mathbf{m}(\mathbf{x})$	the outward pointing unit vector perpendicular to $\partial\mathcal{S}$ at $\mathbf{x}$ but within the tangent space of $\mathcal{S}$ at that point.
Projection Map, $\mathbf{P}$, of $\mathcal{S}$	tensor field on $\mathcal{S}$ with values in $\mathrm{Lin}(\mathbb{E}^3, \mathbf{n}^{\perp}(\mathbf{x}))$ defined by $\mathbf{P}(\mathbf{x})\mathbf{a} = \mathbf{a} - \big(\mathbf{a}\cdot\mathbf{n}(\mathbf{x})\big)\mathbf{n}(\mathbf{x})$ $\forall \mathbf{x} \in \mathcal{S}, \forall \mathbf{a} \in \mathbb{E}^3$.
Inclusion Map, $\mathbf{I}$, of $\mathcal{S}$	tensor field on $\mathcal{S}$ with values in $\mathrm{Lin}\big(\mathbf{n}^{\perp}(\mathbf{x}), \mathbb{E}^3\big)$ defined by $\mathbf{I}(\mathbf{x})\mathbf{a} = \mathbf{a} \quad \forall \mathbf{x} \in \mathcal{S}, \quad \forall \mathbf{a} \in \mathbf{n}^{\perp}(\mathbf{x})$. $\mathbf{P}(\mathbf{x})\mathbf{I}(\mathbf{x}) = \mathbf{1}_{\mathcal{S}}$, the tangent space identity map at $\mathbf{x}$, while $\mathbf{I}(\mathbf{x})\mathbf{P}(\mathbf{x}) = \mathbf{1} - \mathbf{n}(\mathbf{x}) \otimes \mathbf{n}(\mathbf{x})$. Also, $\mathbf{I} = \mathbf{P}^T$.

2.2. Bulk and Surface Gradients. Let $g : \mathbb{E}^K \to \mathbb{E}^N$. Then $\forall \mathbf{x} \in \mathbb{E}^K$ the gradient of g at $\mathbf{x}$, denoted $\nabla g(\mathbf{x})$, is the unique element of $\mathrm{Lin}(\mathbb{E}^K, \mathbb{E}^N)$ such that

$$\lim_{h \searrow 0} \Big(g(\mathbf{x} + h\mathbf{k}) - \big(\nabla g(\mathbf{x})\big) h\mathbf{k} \Big) = g(\mathbf{x}) \quad \forall \mathbf{k} \in \mathbb{E}^K. \tag{2.2.1}$$

Now consider a superficial scalar field, g, defined on $\mathcal{S}$ instead of $\mathbb{E}^K$. Let ϕ *parameterize* $\mathcal{S}$—that is, $\phi : \mathbb{E}^2 \to \mathcal{S}$ diffeomorphically. Then there exists $f : \mathbb{E}^2 \to \mathbb{E}^1$ given by the composition, $f := g \circ \phi$, which allows the gradient of superficial field g to be defined as

$$\nabla g(\mathbf{x}) := (\nabla f) \circ (\nabla \phi)^{-1}. \tag{2.2.2}$$

It is straightforward to show that this definition of the gradient of a superficial scalar field is independent of the parameterization, ϕ, of S. The idea is extendable to superficial vector and tensor fields as well.[2.2] For emphasis, denote by $\nabla_{\mathcal{S}}$ the *surface* gradient of a superficial field on $\mathcal{S}$. Note that if w, $\mathbf{b}$, and $\mathbf{A}$ are superficial

[2.2] An introductory text that covers these issues is GUILLEMIN & POLLACK[1974].

scalar, vector, and tensor fields, respectively, then

$$\begin{aligned} \nabla_{\mathcal{S}} w(\mathbf{x}) &\in \mathbf{n}^{\perp}(\mathbf{x}) \\ \nabla_{\mathcal{S}} \mathbf{b}(\mathbf{x}) &\in \mathrm{Lin}\big(\mathbf{n}^{\perp}(\mathbf{x}), I\!E^3\big) \\ \nabla_{\mathcal{S}} \mathbf{A}(\mathbf{x}) &\in \mathrm{Lin}\big(\mathbf{n}^{\perp}(\mathbf{x}), \mathrm{Lin}(I\!E^3, I\!E^3)\big). \end{aligned} \tag{2.2.3}$$

If $\mathbf{b}$ or $\mathbf{A}$ is tangential as well, then the codomain of their gradients is $\mathbf{n}^{\perp}$ instead of $I\!E^3$.

2.3. Smooth, Superficial Fields and Surface Divergence.

Let $w : \mathcal{S} \to I\!R$ be a map such that $\nabla_{\mathcal{S}} w$ is defined on $\mathcal{S}$. Then w is *smooth* on $\mathcal{S}$, denoted by $w \in C^1(\mathcal{S})$ or sometimes by $w : \mathcal{S} \xrightarrow{c^1} I\!R$. The extension to superficial vector and tensor fields is completely analogous.

Suppose $\mathbf{b}$ is a smooth, superficial vector field on $\mathcal{S}$. Then $\nabla_{\mathcal{S}} \cdot \mathbf{b} := \mathrm{Trace}\big(\mathbf{P}\nabla_{\mathcal{S}} \mathbf{b}\big)$ on $\mathcal{S}$ is the *surface divergence* of $\mathbf{b}$.

Suppose $\mathbf{C}$ is a smooth, superficial tensor field. Then the surface divergence of $\mathbf{C}$ is given by

$$(\nabla_{\mathcal{S}} \cdot \mathbf{C}) \cdot \mathbf{k} = \nabla_{\mathcal{S}} \cdot (\mathbf{C}^T k) \quad \forall \mathbf{k} \in I\!E^3. \tag{2.3.1}$$

The tangential tensor field $\mathbf{L} := -\mathbf{P}\nabla_{\mathcal{S}} \mathbf{n}$ provides curvature information intrinsic to the surface and is therefore called the *curvature tensor*. It can be shown that $\mathbf{L}$ is symmetric and that the scalar field $H := \frac{1}{2}\mathrm{Trace}(\mathbf{L})$ gives the surface *mean curvature*. A corollary to the Stokes Theorem, useful for surface considerations is the

Surface divergence theorem:

Let $\mathbf{f}$ be a smooth, superficial vector field on $\mathcal{S}$. Then

$$\int_{\mathcal{S}} \nabla_{\mathcal{S}} \cdot \mathbf{f}\, dA = \int_{\partial\mathcal{S}} \mathbf{f} \cdot \mathbf{m}\, dL - \int_{\mathcal{S}} 2H(\mathbf{f} \cdot \mathbf{n})\, dA. \tag{2.3.2}$$

2.4 Surface Motion. Consider a one-parameter family of surfaces, $\mathcal{S}(t)$, defined over some open time interval, $\mathcal{T}$. Let

$$\begin{aligned} \mathcal{S}_{\mathcal{T}} &:= \big\{(\mathbf{x}, t) \big| \mathbf{x} \in \mathcal{S}(t), \quad t \in \mathcal{T}\big\} \\ (\partial\mathcal{S})_{\mathcal{T}} &:= \big\{(\mathbf{x}, t) \big| \mathbf{x} \in \partial\mathcal{S}(t), \quad t \in \mathcal{T}\big\} \end{aligned} \tag{2.4.1}$$

define the *surface* and *surface-boundary trajectories*. Let $\phi : U \subset \mathbb{E}^2 \times \mathcal{T} \to \mathcal{S}_\mathcal{T}$ be a one-parameter family of surface parameterizations. Denote by ϕ_∂ the restriction of ϕ to $\partial U \times \mathcal{T}$. If there exists a ϕ such that $\dot{\phi}$ is defined on $U \times \mathcal{T}$ and $\dot{\phi}_\partial$ is defined on $\partial U \times \mathcal{T}$, then the surface is said to be *smoothly propagating*. It can be shown that while the *interface* and *edge velocities*

$$\begin{aligned} \mathbf{V}(\mathbf{x},t) &:= \dot{\phi}\big(\phi^{-1}(\mathbf{x},t),t\big) \\ \mathbf{V}_\partial(\mathbf{x},t) &:= \dot{\phi}_\partial\big(\phi^{-1}(\mathbf{x},t),t\big) \end{aligned} \tag{2.4.2}$$

depend on the choice of parameterization, ϕ, the *normal* and *intrinsic edge speeds*,

$$\begin{aligned} V_n &:= \mathbf{V}\cdot\mathbf{n} \quad \text{on} \quad \mathcal{S}_\mathcal{T} \\ V_m &:= \mathbf{V}\cdot\mathbf{m} \quad \text{on} \quad \partial\mathcal{S}_\mathcal{T}, \end{aligned} \tag{2.4.3}$$

are independent of parameterization. $V_n\mathbf{n}$ is the *normal velocity* of $\mathcal{S}$. $V_m\mathbf{m}$ is the *intrinsic, tangential edge velocity* of $\mathcal{S}$. On the surface boundary, the sum of these two velocity fields is referred to as the *intrinsic edge velocity* of $\mathcal{S}$.

Consider a *normal trajectory* of $\mathcal{S}_\mathcal{T}$ through $\mathbf{x} \in \mathcal{S}(t_0)$, $t_0 \in \mathcal{T}$. This is a smooth, t-parameterized curve, $\mathbf{z}$, in $\mathbb{E}^3$ such that

$$\mathbf{z}(t) \in \mathcal{S}(t), \quad \mathbf{P}\big(\mathbf{z}(t)\big)\dot{\mathbf{z}}(t) = \mathbf{0}, \quad \forall t \in \mathcal{T}. \tag{2.4.4}$$

The normal trajectory is used to define a *time derivative following* $\mathcal{S}$ by

$$\mathring{g}(\mathbf{x},t) := \frac{d}{d\beta} g\big(\mathbf{z}(\beta),\beta\big)\Big|_{\beta=t}, \tag{2.4.5}$$

where $\mathbf{z}$ is the normal trajectory of $\mathcal{S}_\mathcal{T}$ through $\mathbf{x} \in \mathcal{S}(t)$. A classical result is that

$$\mathring{\mathbf{n}} = -\nabla_\mathcal{S} V_n. \tag{2.4.6}$$

This derivative also finds application in the

Surface transport theorem:

Let g be a smooth, superficial scalar field on a smoothly propagating surface, $\mathcal{S}$. Then

$$\frac{d}{dt}\int_{\mathcal{S}(t)} g\,dA = \int_{\mathcal{S}(t)} \big[\mathring{g} - 2Hg V_n\big]\,dA + \int_{\partial\mathcal{S}(t)} g V_m\,dL \quad \forall t \in \mathcal{T}. \tag{2.4.7}$$

2.5 Latticed Bodies and Interfaces.[2.3] A collection, $\mathcal{B}$, of elements, p, is a *body* if there is a set, $\Omega(\mathcal{B})$, of continuous bijections, $\mathcal{X}$, such that:

(i) the gradient of the induced map between any two elements has positive determinant where it is defined;

(ii) $\Omega(\mathcal{B})$ contains all continuous bijections of its elements.

A *lattice*, $\mathcal{L}(\mathcal{B})$, of a body, $\mathcal{B}$, is a set of elements of $\Omega(\mathcal{B})$ such that:

(i) the gradient of the induced map between any two elements is smooth;

(ii) $\mathcal{L}(\mathcal{B})$ contains all smooth bijections (diffeomorphisms) of its elements.

A *latticed body* is any body along with one of its lattices. The view is taken that a body must be provided with a lattice—a preferred group of reference configurations—in order to identify phase interfaces kinematically.

A *two-phase deformation* with respect to $\mathcal{K} \in \Omega(\mathcal{B})$ is a configuration, $\mathcal{X} \in \Omega(\mathcal{B})$, such that the induced map between $\mathcal{K}$ and $\mathcal{X}$ is arbitrarily smooth everywhere except possibly on a partitioning surface. This surface, $\mathcal{S}$, is called a *phase interface*. A *two-phase motion*, $\mathcal{X}_\mathcal{T}$, is a one-parameter family of two-phase deformations, $\mathcal{X}(t) \in \Omega(\mathcal{B})$, with t ranging over an open interval, $\mathcal{T}$. It is *admissible* if there exists a reference configuration, $\mathcal{K} \in \Omega(\mathcal{B})$, such that

(i) each element of $\mathcal{X}_\mathcal{T}$ is a two-phase deformation with respect to $\mathcal{K}$;

(ii) $\mathcal{S}_\mathcal{T}$ is a smoothly propagating surface.

For a latticed body to undergo an admissible, two-phase deformation, it must be admissible with respect to one, and hence all, of the elements of its lattice.

Consider the two-phase deformation, shown in Figure 1, with induced map, $\bar{\mathbf{y}}$, and bulk deformation gradient, $\mathbf{F} := \nabla\bar{\mathbf{y}}$ defined where $\bar{\mathbf{y}}$ is smooth. Then the surface in the deformed configuration of the body,

$$\bar{\mathcal{S}} := \{\mathbf{y} | \mathbf{y} = \bar{\mathbf{y}}(\mathbf{x}), \quad \mathbf{x} \in \mathcal{S}\}, \tag{2.5.1}$$

[2.3] Here the development departs somewhat from that of GURTIN & STRUTHERS[1990].

is referred to as the *deformed interface* with $\{\bar{\mathbf{n}}, \bar{\mathbf{m}}\}$ and $\bar{\mathbf{P}}$ its surface orientations and projection map. The restriction of $\bar{\mathbf{y}}$ to $\mathcal{S}$, denoted $\hat{\mathbf{y}}$, is the invertible deformation map of the surface with an associated *surface-deformation gradient*, $\hat{\mathbf{F}} := \nabla_s \hat{\mathbf{y}}$ defined on $\mathcal{S}$. Note that $\hat{\mathbf{F}}(\mathbf{x}) \in \mathrm{Lin}_+\big(\mathbf{n}^\perp(\mathbf{x}), \bar{\mathbf{n}}^\perp(\mathbf{y})\big)$, $\mathbf{y} = \hat{\mathbf{y}}(\mathbf{x})$, even though $\mathbf{F}$ is not defined on $\mathcal{S}$. It is often convenient to use the linear transformation representing the surface gradient of $\bar{\mathbf{y}}$:

$$\mathit{I\!F} := \nabla_s \bar{\mathbf{y}} = \mathbf{F}^+\mathbf{I} = \mathbf{F}^-\mathbf{I}, \tag{2.5.2}$$

where

$$\mathbf{F}^{\pm} = \lim_{l \searrow 0}\big[\mathbf{F}\big(\mathbf{x} \pm l\mathbf{n}(\mathbf{x})\big)\big] \quad \forall \mathbf{x} \in \mathcal{S}. \tag{2.5.3}$$

Thus,

$$\hat{\mathbf{F}} = \bar{\mathbf{P}}\mathit{I\!F}, \quad \mathbf{F}^{\pm} = \mathit{I\!F}\mathbf{P} + \big(\mathbf{F}^{\pm}\big)\mathbf{n} \otimes \mathbf{n}, \tag{2.5.4}$$

and it is easy to show that

$$\mathit{I\!F} = \bar{\mathbf{I}}\hat{\mathbf{F}}. \tag{2.5.5}$$

Note that $\mathit{I\!F} \in \mathrm{Lin}^{NS}(\mathbf{n}^\perp, I\!E^3)$.

The orientations of the undeformed and deformed interfaces may be related using the determinants of the deformation-gradients,

$$\begin{aligned} J &:= \mathrm{Det}(\mathbf{F}) \\ j &:= \mathrm{Det}(\hat{\mathbf{F}}) = \frac{\mathrm{Det}(\mathbf{F})}{\|\mathbf{F}^{-T}\mathbf{n}\|}, \end{aligned} \tag{2.5.6}$$

where $\mathbf{F}$ may be either $\mathbf{F}^+$ or $\mathbf{F}^-$ in the second equality. The relations are

$$\bar{\mathbf{n}} = \frac{J}{j}\mathbf{F}^{-T}\mathbf{n}, \quad \bar{\mathbf{m}} = \frac{j}{h}\hat{\mathbf{F}}^{-T}\mathbf{m}, \tag{2.5.7}$$

where $\mathbf{F}$ may be either $\mathbf{F}^+$ or $\mathbf{F}^-$ and where h is the determinant of the gradient of the restriction of $\bar{\mathbf{y}}$ to $\partial\mathcal{S}$.

Define the *material* and *spatial velocity fields*, $\mathbf{v}$ and $\bar{\mathbf{v}}$, respectively, as

$$\begin{aligned} \mathbf{v}(\mathbf{x}, t) &:= \dot{\bar{\mathbf{y}}}(\mathbf{x}, t) \\ \bar{\mathbf{v}}(\mathbf{y}, t) &:= \mathbf{v}\big(\bar{\mathbf{y}}^{-1}(\mathbf{y}, t), t\big). \end{aligned} \tag{2.5.8}$$

If $\mathbf{V}$ is a surface velocity of $\mathcal{S}_T$, then the *induced interface velocity*

$$\bar{\mathbf{V}} := (\mathbf{F}^{\pm})\mathbf{V} + \mathbf{v}^{\pm} \tag{2.5.9}$$

is a surface velocity for $\bar{\mathcal{S}}_T$—the interface trajectory associated with deforming interface $\mathcal{S}$. As Equation (2.5.9) indicates, the definition of $\bar{\mathbf{V}}$ does not depend on the side of $\bar{\mathcal{S}}$ used, and in fact,

$$\bar{\mathbf{V}} = \mathbf{F}_c\mathbf{V} + \mathbf{v}_c \quad \forall c \in [0,1] \tag{2.5.10}$$

where

$$\begin{aligned} \mathbf{F}_c :=& c\mathbf{F}^+ + (1-c)\mathbf{F}^- \\ \mathbf{v}_c :=& c\mathbf{v}^+ + (1-c)\mathbf{v}^-. \end{aligned} \tag{2.5.11}$$

Let $\mathcal{K}_1$ and $\mathcal{K}_2$ be lattice elements related by the linear transformation $\mathbf{G}$: $\mathcal{K}_1(\mathcal{B}) \to \mathcal{K}_2(\mathcal{B})$. If $\mathbf{V}_1$ is an interface velocity for the motion with respect to $\mathcal{K}_1$, then $\mathbf{V}_2 = \mathbf{G}\mathbf{V}_1$ is an interface velocity for the motion with respect to $\mathcal{K}_2$ with $\mathbf{V}_1$ and $\mathbf{V}_2$ inducing the same interface trajectory, $\bar{\mathcal{S}}_T$.

3. BALANCE POSTULATES

3.1. Primitive Fields. Consider a latticed body, $\{\mathcal{B}, \mathcal{L}\}$, and an admissible two-phase motion, $\mathcal{X}_\mathcal{T}$. Let $\bar{\mathcal{R}}(t) := \mathcal{X}(t; \mathcal{B})$ represent the region occupied by $\mathcal{B}$ for all t in $\mathcal{T}$, with $\bar{\mathcal{S}}_\mathcal{T}$ the deformed interface trajectory partitioning $\bar{\mathcal{R}}(t)$ over $\mathcal{T}$. Define the *bulk trajectory* as

$$\bar{\mathcal{R}}_\mathcal{T} := \{(\mathbf{y}, t) \,|\, \mathbf{y} \in \bar{\mathcal{R}}(t), \quad t \in \mathcal{T}\}.$$

Stipulate that for every such motion the following smooth fields exist:[3.1]

Bulk Mass Density

$$\bar{\rho}: \quad (\bar{\mathcal{R}}_\mathcal{T} \setminus \bar{\mathcal{S}}_\mathcal{T}) \to \mathbb{R}_+$$

Bulk Energy Density

$$\bar{W}: \quad (\bar{\mathcal{R}}_\mathcal{T} \setminus \bar{\mathcal{S}}_\mathcal{T}) \to \mathbb{R}$$

Cauchy Stress

$$T: \quad (\bar{\mathcal{R}}_\mathcal{T} \setminus \bar{\mathcal{S}}_\mathcal{T}) \to \mathrm{Lin}(\mathbb{E}^3, \mathbb{E}^3)$$

Interface Energy Density

$$\bar{w}: \quad \bar{\mathcal{S}}_\mathcal{T} \to \mathbb{R}$$

Deformational Surface Stress

$$\hat{\mathbf{T}}: \quad (\mathbf{y}, t) \in \bar{\mathcal{S}}_\mathcal{T} \mapsto \hat{\mathbf{T}}(\mathbf{y}, t) \in \mathrm{Lin}\big(\bar{\mathbf{n}}^\perp(\mathbf{y}, t), \mathbb{E}^3\big)$$

Accretive Surface Stress

$$\hat{\bar{\mathbf{C}}}: \quad (\mathbf{y}, t) \in \bar{\mathcal{S}}_\mathcal{T} \mapsto \hat{\mathbf{T}}(\mathbf{y}, t) \in \mathrm{Lin}\big(\bar{\mathbf{n}}^\perp(\mathbf{y}, t), \mathbb{E}^3\big)$$

3.2. Balance Postulates. Let $\bar{\mathcal{P}}_\mathcal{T}$ be the bulk trajectory associated with an arbitrary subbody of $\mathcal{B}$ under the previous motion, $\mathcal{X}_\mathcal{T}$, as shown in Figure 2. Denote by $\bar{\mathcal{Q}}_\mathcal{T}$ the partitioning subinterface trajectory associated with $\bar{\mathcal{P}}_\mathcal{T}$. The boundary of $\bar{\mathcal{Q}}$ is denoted by $\partial\bar{\mathcal{Q}}$. Let $\bar{\nu}$ be the outward unit normal to $\partial\bar{\mathcal{P}}$—the boundary of $\bar{\mathcal{P}}$. Interface normal, $\bar{\mathbf{n}}$, and bi-normal, $\bar{\mathbf{m}}$, are as defined

[3.1] The theory presented here is a modified version of that developed by GURTIN & STRUTHERS[1990].

in Chapter two. The following postulates are imposed on all such subregions and motions and constitute the axiomatic foundation of a mechanical theory of dissipative phase transitions:

Mass Conservation

$$\frac{d}{dt}\int\limits_{\bar{\mathcal{P}}(t)} \bar{\rho}\, dV = 0$$

Momenta Balance

$$\frac{d}{dt}\int\limits_{\bar{\mathcal{P}}(t)} \bar{\rho}\bar{\mathbf{v}}\, dV = \int\limits_{\partial\bar{\mathcal{P}}(t)} \mathbf{T}\bar{\nu}\, dA + \int\limits_{\partial\bar{\mathcal{Q}}(t)} \hat{\mathbf{T}}\bar{\mathbf{m}}\, dL$$

$$\frac{d}{dt}\int\limits_{\bar{\mathcal{P}}(t)} \mathbf{y}\wedge\bar{\rho}\bar{\mathbf{v}}\, dV = \int\limits_{\partial\bar{\mathcal{P}}(t)} \mathbf{y}\wedge\mathbf{T}\bar{\nu}\, dA + \int\limits_{\partial\bar{\mathcal{Q}}(t)} \mathbf{y}\wedge\hat{\mathbf{T}}\bar{\mathbf{m}}\, dL$$

Mechanical Dissipation Imbalance

$$\dot{E} + \dot{K} \leq P,$$

where

$$E\big(t;\bar{\mathcal{P}}(t)\big) := \int\limits_{\bar{\mathcal{P}}(t)} \bar{W}\, dV + \int\limits_{\bar{\mathcal{Q}}(t)} \bar{w}\, dA$$

$$K\big(t;\bar{\mathcal{P}}(t)\big) := \int\limits_{\bar{\mathcal{P}}(t)} \frac{1}{2}\bar{\rho}\bar{\mathbf{v}}\cdot\bar{\mathbf{v}}\, dV$$

$$P\big(t;\bar{\mathcal{P}}(t)\big) := \int\limits_{\partial\bar{\mathcal{P}}(t)} \mathbf{T}\bar{\nu}\cdot\bar{\mathbf{v}}\, dA + \int\limits_{\partial\bar{\mathcal{Q}}(t)} \hat{\mathbf{T}}\bar{\mathbf{m}}\cdot\bar{\mathbf{V}}\, dL + \int\limits_{\partial\bar{\mathcal{Q}}(t)} \hat{\hat{\mathbf{C}}}\bar{\mathbf{m}}\cdot\big(\bar{\mathbf{V}} - \bar{\mathbf{v}}^{+}\big)\, dL$$
$$+ \int\limits_{\partial\bar{\mathcal{Q}}(t)} \hat{\hat{\mathbf{C}}}\bar{\mathbf{m}}\cdot\big(\bar{\mathbf{V}} - \bar{\mathbf{v}}^{-}\big)\, dL.$$

Parameterization Invariance

The power, P, expended at the boundary of $\bar{\mathcal{P}}$ is invariant with respect to the parameterization of $\bar{\mathcal{Q}}$ for all times in $\mathcal{T}$.

Objectivity

$\bar{W}$, $\bar{w}$, $\mathbf{T}$, $\hat{\mathbf{T}}$, and $\hat{\bar{\mathbf{C}}}$ exhibit Galilean objectivity as defined in Appendix A.

By Cauchy's theorem, the momenta balances imply that $\mathbf{T}$ is symmetric. A curvilinear triangle version of the theorem shows that $\hat{\mathbf{T}}$ is symmetric as well, and is therefore representable as a tangential tensor field as defined in Chapter two. Henceforth $\hat{\mathbf{T}}$ is taken to be a tangential. Note that requiring $\mathbf{T}$ and $\hat{\mathbf{T}}$ to be symmetric together with conservation of linear momentum implies the angular momentum balance.

The presence of two distinct interfacial stresses taxes physical intuition, and this issue is addressed at several points in the ensuing development. The deformational stress, $\hat{\mathbf{T}}$, expends power in association with the *absolute* movement of the interface. Even during a two-phase motion for which no new material changes phase, this stress may expend power. In contrast, the accretive stress, $\hat{\bar{\mathbf{C}}}$, expends power in association with the *relative* motion of the interface with respect to the underlying material—a process often referred to as *accretion.* In the limiting case (not covered by this theory) of a phase transition occurring with no material deformation, the accretive stress may still expend power. This stress is the Eulerian counterpart to that presented by GURTIN & STRUTHERS[1990] and is related to the capillary tractions of both LEO & SEKERKA[1989], CAHN & HOFFMAN[1972] and HOFFMAN & CAHN[1974]. Its physical significance for *hyperelastic* materials is elucidated in Chapters four and five with interfaces.

3.3. Referential Formulation. The derivation of local field equations is facilitated by re-expressing all primitive fields as quantities defined on an arbitrary element of the body lattice. To this end, define the following fields on such a reference configuration:

Referential Mass Density	$\rho := J\bar{\rho}$
Referential Bulk Energy	$W := J\bar{W}$

Piola-Kirchhoff Stress	$\mathbf{S} := J\mathbf{T}\mathbf{F}^{-T}$
Referential Interface Energy	$w := j\bar{w}$
Referential Deformational Surface Stress	$\hat{\mathbf{S}} := j\bar{\mathbf{I}}\hat{\mathbf{T}}\hat{\mathbf{F}}^{-T}, \quad j\hat{\mathbf{T}} = \bar{\mathbf{P}}\hat{\mathbf{S}}\hat{\mathbf{F}}^{T}$
Referential Accretive Surface Stress	$\hat{\mathbf{C}} := 2j\langle\!\langle \mathbf{F}^{T} \rangle\!\rangle \hat{\bar{\mathbf{C}}}\hat{\mathbf{F}}^{-T},$

where $\mathbf{F}$, $\hat{\mathbf{F}}$, j, and J are as defined in Section 2.5 and

$$\langle\!\langle \phi(\mathbf{x}) \rangle\!\rangle := \lim_{h \searrow 0} \frac{1}{2}\big\{\phi\big(\mathbf{x} + h\mathbf{n}(\mathbf{x})\big) + \phi\big(\mathbf{x} - h\mathbf{n}(\mathbf{x})\big)\big\} \quad \forall \mathbf{x} \in \mathcal{S}. \tag{3.3.1}$$

Using these fields, the Linear Momentum Balance and the Mechanical Dissipation Imbalance can be expressed as

$$\frac{d}{dt}\int_{\mathcal{P}} \rho\mathbf{v}\, dV = \int_{\partial\mathcal{P}} \mathbf{S}\nu\, dA + \int_{\partial\mathcal{Q}(t)} \hat{\mathbf{S}}\mathbf{m}\, dL \tag{3.3.2}$$

and

$$\begin{aligned} &\frac{d}{dt}\int_{\mathcal{P}} W\, dV + \frac{d}{dt}\int_{\mathcal{Q}(t)} w\, dA + \frac{d}{dt}\int_{\mathcal{P}} \frac{1}{2}\rho\mathbf{v}\cdot\mathbf{v}\, dV \\ &\qquad \leq \int_{\partial\mathcal{P}} \mathbf{S}\nu\cdot\mathbf{v}\, dA + \int_{\partial\mathcal{Q}(t)} \hat{\mathbf{S}}\mathbf{m}\cdot\big[\mathbf{F}_c\mathbf{V} + \mathbf{v}_c\big]\, dL + \int_{\partial\mathcal{Q}(t)} \hat{\mathbf{C}}\mathbf{m}\cdot\mathbf{V}\, dL, \end{aligned} \tag{3.3.3}$$

with $\mathbf{F}_c$ and $\mathbf{v}_c$ defined by Equation (2.4.16).

The localizations of the linear momentum balance away from and local to the interface are

$$\begin{aligned} \nabla\cdot\mathbf{S} &= \rho\mathbf{v} \\ [\![\rho\mathbf{v}]\!]V_n + [\![\mathbf{S}\mathbf{n}]\!] &= -\nabla_s\cdot\hat{\mathbf{S}}. \end{aligned} \tag{3.3.4}$$

Here

$$[\![\phi(\mathbf{x})]\!] := \lim_{h \searrow 0}\big\{\phi\big(\mathbf{x} + h\mathbf{n}(\mathbf{x})\big) - \phi\big(\mathbf{x} - h\mathbf{n}(\mathbf{x})\big)\big\} \quad \forall \mathbf{x} \in \mathcal{S}. \tag{3.3.5}$$

Analogous localizations for the dissipation imbalance are made after considering the field restrictions imposed by the principle of parameterization invariance.

3.4. Implications of Parameterization Invariance. Use of the Surface Divergence Theorem gives

$$\int_{\partial\mathcal{Q}(t)} \hat{\mathbf{C}}\mathbf{m}\cdot\mathbf{V}\,dL = \int_{\mathcal{Q}(t)} \nabla_s\cdot\big(\hat{\mathbf{C}}^T\mathbf{m}\cdot V_m\mathbf{m}\big)dA, \tag{3.4.1}$$

and application of the Product Rule then yields

$$\int_{\partial\mathcal{Q}(t)} \hat{\mathbf{C}}\mathbf{m}\cdot\mathbf{V}\,dL = \int_{\mathcal{Q}(t)} \left[-\hat{\mathbf{C}}\cdot\mathbf{L}V_n - \hat{\mathbf{C}}^T\mathbf{n}\cdot\mathring{\mathbf{n}} + (\nabla_s\cdot\hat{\mathbf{C}})\cdot\mathbf{n}V_n\right] dA + \int_{\partial\mathcal{Q}(t)} \hat{\mathbf{C}}\mathbf{m}\cdot\mathbf{m}V_m\,dL. \tag{3.4.2}$$

Now consider the second term in the referential dissipation inequality,

$$\int_{\partial\mathcal{Q}(t)} \hat{\mathbf{S}}\mathbf{m}\cdot\left[\mathbf{F}_c\mathbf{V}+\mathbf{v}_c\right] dL. \tag{3.4.3}$$

By the Surface Divergence Theorem this is equal to

$$\begin{aligned}
&\int_{\mathcal{Q}(t)} \nabla_s\cdot\left[\hat{\mathbf{S}}^T\mathbf{F}_c\mathbf{n}V_n\right]dA + \int_{\mathcal{Q}(t)} \nabla_s\cdot\left[\hat{\mathbf{S}}^T\mathbf{v}_c\right]dA + \int_{\partial\mathcal{Q}(t)} \hat{\mathbf{S}}\mathbf{m}\cdot\left[\mathbf{F}_c\mathbf{m}V_m\right]dL \\
&\quad= \int_{\partial\mathcal{Q}(t)} \hat{\mathbf{S}}\mathbf{m}\cdot\big(\mathbf{F}_c\mathbf{m}\big)V_m\,dL - \int_{\mathcal{Q}(t)} \left[(\mathcal{F}\hat{\mathbf{S}})\cdot\mathbf{L} + (\nabla_s\cdot\hat{\mathbf{S}})\cdot\big(\mathbf{F}_c\mathbf{n}\big)\right]V_n\,dA \\
&\qquad+ \int_{\mathcal{Q}(t)} \left\{(\hat{\mathbf{S}}\mathbf{P})\cdot\mathring{\mathbf{F}}_c - \big(\hat{\mathbf{S}}^T\mathbf{F}_c\mathbf{n}\big)\cdot\mathring{\mathbf{n}} + (\nabla_s\cdot\hat{\mathbf{S}})\cdot\mathbf{v}_c\right\}dA.
\end{aligned} \tag{3.4.4}$$

The Mechanical Dissipation Imbalance is now expressible in a form amenable to application of the *Invariance Lemma*[3.2] given in Appendix B. The result is a restriction imposed on the primitive fields by the Parameterization Invariance Postulate, which comes in the form of the

Tension-Energy Theorem:[3.2]

$$\mathcal{F}^T\hat{\mathbf{S}} + \mathbf{P}\hat{\mathbf{C}} = w\mathbf{1}_s. \tag{3.4.5}$$

[3.2] Due to GURTIN & STRUTHERS[1990].

Equations (3.3.3) and (3.4.2–3.4.5) then combine to give a form of the Mechanical Dissipation Imbalance that is consistent with the Parameterization Invariance Postulate:

$$\begin{aligned}\frac{d}{dt}\int_{\mathcal{P}} W\,dV + \frac{d}{dt}\int_{\partial\mathcal{Q}(t)} w\,dA + \frac{d}{dt}\int_{\mathcal{P}} \frac{1}{2}\rho\mathbf{v}\cdot\mathbf{v}\,dV \\ \leq \int_{\mathcal{Q}(t)} \left\{\hat{\mathbf{S}}\cdot\mathring{\hat{\mathbf{F}}}_c - \hat{\mathbf{a}}_c\cdot\mathring{\mathbf{n}} + \nabla_s\cdot\hat{\mathbf{S}}\cdot\mathbf{v}_c\right\}dA + \int_{\partial\mathcal{P}} \mathbf{S}\nu\cdot\mathbf{v}\,dA \\ + \int_{\partial\mathcal{Q}(t)} wV_m\,dL + \int_{\mathcal{Q}(t)} \left[(\nabla_s\cdot\hat{\mathbf{S}})\cdot(\mathbf{F}_c\mathbf{n}) + (\nabla_s\cdot\hat{\mathbf{C}})\cdot\mathbf{n} - 2Hw\right]V_n\,dA,\end{aligned} \tag{3.4.6}$$

where

$$\hat{\mathbf{a}}_c := (\hat{\mathbf{S}}^T\mathbf{F}_c + \hat{\mathbf{C}}^T)\mathbf{n}. \tag{3.4.7}$$

3.5. Referential Localizations and Interface Driving Traction. Application of the Surface Transport Theorem and Linear Momentum Balance to Equation (3.4.6) yields the

Reduced Dissipation Imbalance

$$\begin{aligned}\frac{d}{dt}\int_{\mathcal{P}} W\,dV \leq \int_{\mathcal{P}} \mathbf{S}\cdot\dot{\mathbf{F}}\,dV + \int_{\mathcal{Q}(t)} \left[(\nabla_s\cdot\hat{\mathbf{S}})\cdot\langle\!\langle\mathbf{Fn}\rangle\!\rangle + (\nabla_s\cdot\hat{\mathbf{C}})\cdot\mathbf{n}\right]V_n\,dA \\ - \int_{\mathcal{Q}(t)} \left[\mathring{w} - \hat{\mathbf{S}}\cdot\mathring{\hat{\mathbf{F}}}_c + \hat{\mathbf{a}}_c\cdot\mathring{\mathbf{n}}\right].\end{aligned} \tag{3.5.1}$$

Localized away from the interface, this implies that

$$\mathbf{S}\cdot\dot{\mathbf{F}} - \dot{W} \geq 0. \tag{3.5.2}$$

The implication local to the interface is

$$fV_n - \left[\mathring{w} - \hat{\mathbf{S}}\cdot\mathring{\hat{\mathbf{F}}}_c + \hat{\mathbf{a}}_c\cdot\mathring{\mathbf{n}}\right] \geq 0, \tag{3.5.3}$$

where

$$f := [\![W]\!] - \langle\!\langle\mathbf{S}\rangle\!\rangle\cdot[\![\mathbf{F}]\!] + (\nabla_s\cdot\hat{\mathbf{S}})\cdot\langle\!\langle\mathbf{Fn}\rangle\!\rangle + (\nabla_s\cdot\hat{\mathbf{C}})\cdot\mathbf{n} \tag{3.5.4}$$

is the interface *driving traction.*[3.2]

Equations (3.3.4), (3.4.5), (3.5.2), and (3.5.3) along with the Angular Momentum localizations,

$$\begin{aligned} \mathbf{S}\mathbf{F}^T &= \mathbf{F}\mathbf{S}^T \\ \hat{\mathbf{S}}\hat{\mathbf{F}}^T &= \hat{\mathbf{F}}\hat{\mathbf{S}}^T, \end{aligned} \tag{3.5.5}$$

comprise the local field equations for the mechanical theory of dissipative accretion.

[3.2] Equation (3.5.3) was first derived by KNOWLES[1979] within a setting devoid of surface effects. GURTIN & STRUTHERS[1990] derived Equation (3.5.3) in its present form, but their work differs from the present development in that a more extensive set of system postulates leads to a local balance principle with the form of Equation (3.5.4).

4. HYPERELASTIC MATERIALS WITH INTERFACES

4.1 Material Constitution. The mechanical theory summarized by Equations (3.3.4), (3.4.5) and (3.5.2 – 3.5.5) is incomplete since a means of characterizing the bulk and interface of a given material has yet to be provided. This is established by providing constitutive relationships between the primitive fields and the process kinematics. Though the form of such relations may be quite general, attention for the remainder of this work is restricted to *hyperelastic materials with interfaces*. For such materials, there exist energy response functions, $\tilde{W}$ and $\tilde{w}$ such that

$$\begin{aligned} W &= \tilde{W}(\mathbf{F}) \\ \mathbf{S} &= \partial\tilde{W}(\mathbf{F}) \end{aligned} \tag{4.1.1}$$

and

$$\begin{aligned} w &= \tilde{w}(\mathbf{F}_c, \mathbf{n}) \\ \hat{\mathbf{S}}\mathbf{P} &= \partial_1\tilde{w}(\mathbf{F}_c, \mathbf{n}) \\ \hat{\mathbf{a}}_c &= -\partial_2\tilde{w}(\mathbf{F}_c, \mathbf{n}), \end{aligned} \tag{4.1.2}$$

with

$$\begin{aligned} \tilde{W} &: \mathrm{Lin}_+(I\!E^3, I\!E^3) \xrightarrow{c^2} I\!R \\ \tilde{w}(\cdot, \mathbf{n}) &: \mathrm{Lin}_+(I\!E^3, I\!E^3) \xrightarrow{c^2} I\!R \quad \forall\, \mathbf{n} \in \mathrm{Unit}(I\!E^3), \end{aligned} \tag{4.1.3}$$

and where $\partial_i\phi$ refers to the partial derivative of ϕ with respect to its i^{th} argument. The symbol $\partial\phi$ refers to the derivative of a function, ϕ, of a single argument. Here and in the following development, $\mathbf{P}$ and $\mathbf{I}$ are treated as elements of $\mathrm{Lin}(I\!E^3, \mathbf{n}^\perp)$ and $\mathrm{Lin}(\mathbf{n}^\perp, I\!E^3)$, respectively, defined by

$$\mathbf{P}\mathbf{b} = \mathbf{b} - (\mathbf{b}\cdot\mathbf{n})\mathbf{n}, \quad \mathbf{I} = \mathbf{P}^T, \quad \forall\, \mathbf{b} \in I\!E^3. \tag{4.1.4}$$

The projection and inclusion maps, $\bar{\mathbf{P}}$, $\bar{\mathbf{I}}$, associated with the deformed surface normal, $\bar{\mathbf{n}}$, are treated analogously.

For such materials, Equation (3.5.2) is strictly satisfied, implying that the bulk material does not dissipate energy. The interface is still dissipative, however, with Equation (3.5.3) reducing to

$$fV_n \geq 0, \tag{4.1.5}$$

where the driving traction, f, is given by Equation (3.5.4). The power expended in association with accretion is thus the only way that hyperelastic materials can dissipate energy as is clear from both Equation (4.1.5) and the fact that

$$\dot{E} + \dot{K} - P = \int_{\partial \mathcal{Q}(t)} f V_n \, dA. \tag{4.1.6}$$

Here E, K, and P are as defined in the Mechanical Dissipation Imbalance.

The interface response functions of Equations (4.1.1) and (4.1.2) can be expressed in a more useful form, using the following[4.1]

Lemma 4.1:

Consider a function, $\breve{w}$, defined by

$$\begin{aligned} \breve{w}(\mathbb{F}, \mathbf{f}, \mathbf{n}) =& \tilde{w}(\mathbb{F}\mathbf{P} + \mathbf{f} \otimes \mathbf{n}, \mathbf{n}) \\ & \forall \mathbf{n} \in \text{Unit}(\mathbb{E}^3), \quad \forall \mathbf{f} \in \mathbb{E}^3, \quad \forall \mathbb{F} \in \text{Lin}^{NS}(\mathbf{n}^{\perp}, \mathbb{E}^3). \end{aligned} \tag{4.1.7}$$

Then

$$\begin{aligned} \partial_1 \breve{w}(\mathbb{F}, \mathbf{f}, \mathbf{n}) =& \partial_1 \tilde{w}(\mathbb{F}\mathbf{P} + \mathbf{f} \otimes \mathbf{n}, \mathbf{n})\mathbf{I} \\ \partial_2 \breve{w}(\mathbb{F}, \mathbf{f}, \mathbf{n}) =& \partial_1 \tilde{w}(\mathbb{F}\mathbf{P} + \mathbf{f} \otimes \mathbf{n}, \mathbf{n})\mathbf{n}. \end{aligned} \tag{4.1.8}$$

Lemma 4.1 and Equation $(4.1.2)_2$ imply that

$$\hat{\mathbf{S}} = \partial_1 \breve{w}(\mathbb{F}, \mathbf{f}, \mathbf{n}) \tag{4.1.9}$$

and that

$$\partial_2 \breve{w}(\mathbb{F}, \mathbf{f}, \mathbf{n}) = \mathbf{0}. \tag{4.1.10}$$

The surface fields are thus dependent only upon $\mathbf{n}$ and $\mathbb{F}$. This implies that the original dependence of the surface energy on $\mathbf{F}_c$ could just as well have been $\mathbf{F}^+$ or $\mathbf{F}^-$. Preference has not been given to the bulk on either side of the interface in describing the interfacial fields.

A final step in the material characterization is to express the referential accretive stress, $\hat{\mathbf{C}}$, in terms of the surface energy response function, $\tilde{w}$. This

[4.1] GURTIN & STRUTHERS[1990].

is facilitated by introducing $D_{\mathbf{n}}\tilde{w}$, the *partial derivative of* $\tilde{w}$ *with respect to* $\mathbf{n}$ *following the interface*—identified as the unique element of $\mathbf{n}^{\perp}$ such that

$$D_{\mathbf{n}}\tilde{w}(\mathbf{F},\mathbf{n})\cdot\mathbf{a} = \frac{d}{d\beta}\tilde{w}\Big(\mathbf{F}\tilde{\mathbf{Q}}\big(\mathbf{k}(\beta),\mathbf{n}\big),\mathbf{k}(\beta)\Big)\Big|_{\beta=0} \qquad \forall\,\mathbf{k}:\mathbb{R}\xrightarrow{c^1}\mathrm{Unit}(\mathbb{E}^3),\quad \mathbf{k}(0)=\mathbf{n},\quad \dot{\mathbf{k}}(0)=\mathbf{a}, \tag{4.1.11}$$

where

$$\tilde{\mathbf{Q}}:\mathrm{Unit}(\mathbb{E}^3)\times\mathrm{Unit}(\mathbb{E}^3)\to\mathrm{Orth}_+(\mathbb{E}^3,\mathbb{E}^3)$$

is the bilinear map defined by

$$\tilde{\mathbf{Q}}(\mathbf{e},\mathbf{f})\mathbf{e}=\mathbf{f},\quad \tilde{\mathbf{Q}}(\mathbf{e},\mathbf{f})\mathbf{g}=\mathbf{g}\qquad \forall\,\{\mathbf{e},\mathbf{f}\}\in\mathrm{Unit}(\mathbb{E}^3)\times\mathrm{Unit}(\mathbb{E}^3),$$

with $\mathbf{g}\cdot\mathbf{e}=\mathbf{g}\cdot\mathbf{f}=0$. Then it can be shown that[4.2]

$$D_{\mathbf{n}}\breve{w}(\mathbb{F},\mathbf{f},\mathbf{n}) = \partial_2\tilde{w}(\mathbb{F}\mathbf{P}+\mathbf{f}\otimes\mathbf{n},\mathbf{n})+[\partial_1\breve{w}(\mathbb{F},\mathbf{f},\mathbf{n})]^T\mathbf{f}-\mathbb{F}^T\partial_2\breve{w}(\mathbb{F},\mathbf{f},\mathbf{n}). \tag{4.1.12}$$

Since

$$\hat{\mathbf{C}} = \mathbf{I}\mathbf{P}\hat{\mathbf{C}}+\mathbf{n}\otimes\hat{\mathbf{C}}^T\mathbf{n}, \tag{4.1.13}$$

Equations (3.4.5) and (3.4.7) plus the fact that $\mathbf{P}\mathbf{I}=\mathbf{1}_{\mathcal{S}}$ combine to give

$$\hat{\mathbf{C}} = w\mathbf{I}-\mathbf{I}\mathbb{F}^T\hat{\mathbf{S}}+\mathbf{n}\otimes\big(\hat{\mathbf{a}}_c-\hat{\mathbf{S}}^T\mathbf{F}_c\mathbf{n}\big). \tag{4.1.14}$$

Equations (4.1.2), (4.1.7), (4.1.9) and (4.1.10) then give that

$$\hat{\mathbf{C}} = \breve{w}(\mathbb{F},\mathbf{f},\mathbf{n})\mathbf{I}-\mathbf{I}\mathbb{F}^T\partial_1\breve{w}(\mathbb{F},\mathbf{f},\mathbf{n})-\mathbf{n}\otimes D_{\mathbf{n}}\breve{w}(\mathbb{F},\mathbf{f},\mathbf{n}). \tag{4.1.15}$$

Dropping the dependence of $\breve{w}$ on its second argument by virtue of Equation (4.1.8) then gives the following characterization of hyperelastic materials with interfaces:

$$\begin{aligned} W &= \tilde{W}(\mathbf{F})\\ \mathbf{S} &= \partial\tilde{W}(\mathbf{F}), \end{aligned} \tag{4.1.16}$$

[4.2] GURTIN & STRUTHERS[1990].

and

$$\begin{aligned} w &= \breve{w}(\mathbb{F}, \mathbf{n}) \\ \hat{\mathbf{S}} &= \partial_1 \breve{w}(\mathbb{F}, \mathbf{n}) \\ \hat{\mathbf{C}} &= \breve{w}(\mathbb{F}, \mathbf{n})\mathbf{I} - \mathbf{I}\mathbb{F}^T \partial_1 \breve{w}(\mathbb{F}, \mathbf{n}) - \mathbf{n} \otimes D_{\mathbf{n}} \breve{w}(\mathbb{F}, \mathbf{n}). \end{aligned} \tag{4.1.17}$$

Note that the system response is independent of the scalar, c, introduced in Equation (3.3.3).

4.2 A Remark on the Accretive Stress, $\hat{\mathbf{C}}$. Recall that the local power expenditure associated with $\hat{\mathbf{C}}$ is given by $\hat{\mathbf{C}}\mathbf{m} \cdot \mathbf{V}$. For hyperelastic materials, then, Equation $(4.1.17)_3$ implies that

$$\hat{\mathbf{C}}\mathbf{m} \cdot \mathbf{V} = \{\breve{w} - [(\mathbb{F}^T \partial_1 \breve{w})\mathbf{m}] \cdot \mathbf{m}\} V_m - [(D_{\mathbf{n}} \breve{w}) \cdot \mathbf{m}] V_n. \tag{4.2.1}$$

The first term represents power expended in extending the interface boundary via tangential accretion. The second term represents a power expenditure accompanying changes in interface orientation in association with normal accretion. As is shown in the following chapter, this latter power expenditure is zero for isotropic media, implying that it is material anisotropy that offers such a resistance to accretive reorientations of an interface.

4.3 A Kinetic Relation for Interfaces. The mechanical theory of hyperelastic materials summarized by Equations (3.3.4), (3.5.4), (4.1.5) and (4.1.16–4.1.17) is still incomplete. As shown by ERICKSEN[1975] and ABEYARATNE & KNOWLES [1987(a,b), 1988, 1989] for the case of no surface effects, there exist settings for which the interface location cannot be determined uniquely for prescribed boundary data. Abeyaratne and Knowles suggest that this may be interpreted as a constitutive deficiency. Motivated by the internal variable work of RICE[1971, 1975] and the form of Equation (4.1.5), they offer a simple remedy in the form of a constitutive relation between the driving traction, f, and the accretive velocity of the interface, V_n:

$$\begin{aligned} &V_n = \hat{V}(f), \\ &\hat{V} : \mathbb{R} \to \mathbb{R}, \quad \hat{V}(f) f \geq 0 \quad \forall f \in \mathbb{R}. \end{aligned} \tag{4.3.1}$$

Equation $(4.3.1)_1$ is referred to as a *kinetic relation* with the inequality restricting $\hat{V}$ imposed by the dissipation imbalance, Equation (4.1.5). Supplementing the system postulates and material constitution with such a relation has been shown, in certain settings, to resolve the uniqueness problem.[4.3] Though developed without considering surface effects, the rationale for adopting a kinetic relation is still valid within the setting of interfacial structure. Such a constitutive remedy is therefore adopted in the present work. [4.4]

[4.3] ABEYARATNE & KNOWLES[1988, 1989, 1990(a,b,c)].

[4.4] GURTIN & STRUTHERS[1990] have *derived* an equation with the form of Equation (4.3.1) from a more elaborate set of balance postulates.

5. MECHANICAL SYMMETRY FOR HYPERELASTIC MATERIALS WITH INTERFACES

5.1. Mechanical Equivalence. Consider two lattice elements, $\mathcal{K}_1$ and $\mathcal{K}_2$, with respect to which a body is hyperelastic, that are related by linear transformation, $\mathbf{H}$, where $\mathcal{K}_2 = \mathbf{H}\mathcal{K}_1$. These two reference configurations are said to be *mechanically equivalent* if first,

$$\rho_1(\mathbf{x},t) = \rho_2(\mathbf{H}\mathbf{x},t) \quad \forall \mathbf{x} \in \mathcal{R}_1(t)\backslash\mathcal{S}_1(t), \quad \forall t \in \mathcal{T} \tag{5.1.1}$$

and, second, they are characterized by the same response functions:

$$\begin{aligned} \tilde{W}_2 &= \tilde{W}_1 \\ \breve{w}_2 &= \breve{w}_1. \end{aligned} \tag{5.1.2}$$

By virtue of the construction of referential fields given in Section 3.3, the following formulae relate mass density and energy fields independent of any constitutive considerations:

$$\begin{aligned} \rho_2(\mathbf{x},t) &= \mathrm{Det}(\mathbf{H})\rho_1(\mathbf{H}\mathbf{x},t) \\ W_2(\mathbf{x},t) &= \frac{1}{\mathrm{Det}(\mathbf{H})} W_1(\mathbf{H}\mathbf{x},t) \end{aligned} \quad \forall \mathbf{x} \in \mathcal{R}_1\backslash\mathcal{S}_1(t), \quad \forall t \in \mathcal{T} \tag{5.1.3}$$

and

$$w_2(\mathbf{x},t) = \frac{|\mathbf{H}^T\mathbf{n}(\mathbf{x},t)|}{\mathrm{Det}(\mathbf{H})} w_1(\mathbf{H}\mathbf{x},t) \quad \forall \mathbf{x} \in \mathcal{S}_1(t), \quad \forall t \in \mathcal{T}. \tag{5.1.4}$$

Equations (5.1.1)–(5.1.4) collectively imply that two reference configurations are mechanically equivalent if and only if

$$\begin{aligned} &\mathrm{Det}(\mathbf{H}) = 1 \\ &\tilde{W}_1(\mathbf{F}) = \tilde{W}_1(\mathbf{H}\mathbf{F}) \\ &\tilde{w}_1(\mathbf{F},\mathbf{n}) = \|\mathbf{H}^T\mathbf{n}\|\tilde{w}_1\left(\mathbf{F}\mathbf{H}, \frac{\mathbf{H}^T\mathbf{n}}{\|\mathbf{H}^T\mathbf{n}\|}\right) \end{aligned} \quad \forall \mathbf{F} \in \mathrm{Lin}_+(\mathbb{E}^3,\mathbb{E}^3), \quad \forall \mathbf{n} \in \mathrm{Unit}(\mathbb{E}^3). \tag{5.1.5}$$

Define the *Material Symmetry Group*, $\mathcal{G}_\mathcal{K}$, of a latticed body with respect to lattice element, $\mathcal{K}$, to be the set of all lattice elements that are mechanically

equivalent to $\mathcal{K}$. If $\mathcal{G}_{\mathcal{K}} = \text{Unim}(I\!E^3, I\!E^3)$, the material is called a *fluid*. If $\mathcal{G}_{\mathcal{K}} = \text{Orth}_+(I\!E^3, I\!E^3)$, the material is called a *solid*.

The kinetic relation does not play a role in determining the mechanical equivalence of two lattice elements. An appropriate change of configuration formula can, however, be established. Let J_H and j_H be the bulk and surface determinants associated with the linear transformation, $\mathbf{H}$. Then

$$V_n^{(2)} = \frac{J_H}{j_H} V_n^{(1)} \tag{5.1.6}$$

and

$$f_2 = J_H f_1 \tag{5.1.7}$$

so that

$$\hat{V}_2\left(\frac{f}{J_H}\right) = \frac{J_H}{j_H}\hat{V}_1(f) \qquad \forall f \in I\!R. \tag{5.1.8}$$

5.2 Material Isotropy. A standard result in classical continuum mechanics is that hyperelastic materials are isotropic with respect to a given reference configuration if and only if the bulk energy can be represented by a function of the three fundamental scalar invariants of the Right Cauchy-Green Tensor, $\mathbf{C} := \mathbf{F}^T\mathbf{F}$, or its square root, $\mathbf{U}$. These scalar invariants are defined as

$$\begin{aligned} I_1(\mathbf{U}) &:= \text{Trace}(\mathbf{U}) \\ I_2(\mathbf{U}) &:= \frac{1}{2}\left[\left(\text{Trace}(\mathbf{U})\right)^2 - \text{Trace}(\mathbf{U}^2)\right] \qquad \forall \mathbf{U} \in \text{Sym}^+(I\!E^3), \\ I_3(\mathbf{U}) &:= \text{Det}(\mathbf{U}) \end{aligned} \tag{5.2.1}$$

so that in the absence of surface fields, a hyperelastic material is isotropic if and only if it is characterized by

$$\begin{aligned} W &= \breve{W}(I_1, I_2, I_3) \\ S &= (\partial_1\breve{W} + I_1\partial_2\breve{W})\mathbf{F}\mathbf{U}^{-1} - (\partial_2\breve{W})\mathbf{F} + (I_3\partial_3\breve{W})\mathbf{F}^{-T} \\ T &= \frac{1}{I_3}(\partial_1\breve{W} + I_1\partial_2\breve{W})\mathbf{V} - \frac{1}{I_3}(\partial_2\breve{W})\mathbf{V}^2 + (\partial_3\breve{W})\mathbf{1}, \end{aligned} \tag{5.2.2}$$

where

$$I_k := I_k(\mathbf{U}) = I_k(\mathbf{V}), \quad \mathbf{U} := \sqrt{\mathbf{F}^T\mathbf{F}}, \quad \text{and} \quad \mathbf{V} := \sqrt{\mathbf{F}\mathbf{F}^T}. \tag{5.2.3}$$

Material isotropy also imposes restrictions on the interfacial response functions and these are now investigated. One such restriction is on the accretive surface stress, $\hat{\mathbf{C}}$, and is a direct result of the following important

Proposition 5.1:

Material isotropy implies that $D_{\mathbf{n}}\breve{w} = 0$.

Proof:

By Equation (5.1.5), isotropy implies that

$$\begin{aligned}&\tilde{w}(\mathbf{F},\mathbf{n}) = \tilde{w}(\mathbf{FQ},\mathbf{Q}^T\mathbf{n})\\ &\quad \forall\,\mathbf{Q}\in \mathrm{Orth}_+(\mathbb{E}^3,\mathbb{E}^3),\quad \forall\,\mathbf{F}\in \mathrm{Lin}_+(\mathbb{E}^3,\mathbb{E}^3),\quad \forall\,\mathbf{n}\in \mathrm{Unit}(\mathbb{E}^3).\end{aligned} \tag{5.2.4}$$

Recalling Equation (4.1.11), let

$$\mathbf{Q} = \tilde{\mathbf{Q}}\big(\mathbf{k}(\beta),\mathbf{n}\big)$$

for some

$$\mathbf{k} : \mathbb{R} \overset{\mathcal{C}^1}{\mapsto} \mathrm{Unit}(\mathbb{E}^3),\quad \mathbf{k}(0) = \mathbf{n}.$$

Then,

$$\tilde{\mathbf{Q}}^T\big(\mathbf{k}(\beta),\mathbf{n}\big)\mathbf{n} = \mathbf{k}(\beta) \tag{5.2.5}$$

so that Equation (5.2.4) implies that

$$\tilde{w}\Big(\mathbf{F}\tilde{\mathbf{Q}}\big(\mathbf{k}(\beta),\mathbf{n}\big),\mathbf{k}(\beta)\Big) = \tilde{w}(\mathbf{F},\mathbf{n})\quad \forall\beta. \tag{5.2.6}$$

Therefore,

$$\begin{aligned}\frac{d}{d\beta}\tilde{w}\Big(\mathbf{F}\tilde{\mathbf{Q}}\big(\mathbf{k}(\beta),\mathbf{n}\big),\mathbf{k}(\beta)\Big) &= \frac{d}{d\beta}\tilde{w}(\mathbf{F},\mathbf{n})\\ &= 0.\end{aligned}$$

Thus, by the definition of $D_{\mathbf{n}}\tilde{w}$ given by Equation (4.9),

$$D_{\mathbf{n}}\tilde{w} = D_{\mathbf{n}}\breve{w} = 0.$$

Attention is next turned to the representation of interface fields in terms of the scalar invariants of the surface deformation gradient. A *superficial, isotropic, scalar function*, ϕ, is characterized by the property that

$$\begin{aligned}\phi(\hat{\mathbf{Q}}^T\hat{\mathbf{U}}\hat{\mathbf{Q}},\mathbf{n}) =&\phi(\hat{\mathbf{U}},\mathbf{n})\\ &\forall\hat{\mathbf{U}}\in \mathrm{Sym}^+(\mathbf{n}^\perp),\quad \forall\hat{\mathbf{Q}}\in \mathrm{Orth}_+(\mathbf{n}^\perp,\mathbf{n}^\perp).\end{aligned}\tag{5.2.7}$$

Such functions admit an equivalent representation in terms of the two fundamental scalar invariants of their first argument—a property expressed in the following

Representation Theorem for Superficial, Isotropic, Scalar Functions:

If ϕ is a superficial, isotropic, scalar function, then there exists a function, $\hat{\phi}:\hat{\mathcal{I}}\times \mathrm{Unit}(\mathbb{E}^3)\mapsto \mathbb{R}$ such that

$$\begin{aligned}\phi(\hat{\mathbf{U}},\mathbf{n}) =&\hat{\phi}(i(\hat{\mathbf{U}}),j(\hat{\mathbf{U}}),\mathbf{n})\\ &\forall\hat{\mathbf{U}}\in \mathrm{Sym}^+(\mathbf{n}^\perp),\quad \forall\mathbf{n}\in \mathrm{Unit}(\mathbb{E}^3),\end{aligned}\tag{5.2.8}$$

where

$$\hat{\mathcal{I}} := \left\{(\zeta_1,\zeta_2)\,\middle|\,(\zeta_1,\zeta_2)\in\mathbb{R}^2_+,\quad (4\zeta_2-\zeta_1^2)<0\right\}\tag{5.2.9}$$

and

$$\begin{aligned}i(\hat{\mathbf{U}}) :=&\mathrm{Trace}(\hat{\mathbf{U}})\\ j(\hat{\mathbf{U}}) :=&\mathrm{Det}(\hat{\mathbf{U}}).\end{aligned}\tag{5.2.10}$$

This is proved in Appendix C and is used to establish a key result presented as the

Interface Representation Theorem:

Hyperelastic materials whose bulk is characterized by Equation (5.2.2) are isotropic if and only if the interface energy can be represented by a function $\hat{w}:\hat{\mathcal{I}}\mapsto\mathbb{R}$, such that

$$\begin{aligned}\breve{w}(\mathbb{F},\mathbf{n}) =&\hat{w}\big(i(\hat{\mathbf{U}}),j(\hat{\mathbf{U}})\big)\\ &\forall\mathbb{F}\in \mathrm{Lin}^{NS}(\mathbf{n}^\perp,\mathbb{E}^3),\quad \forall\mathbf{n}\in \mathrm{Unit}(\mathbb{E}^3),\end{aligned}\tag{5.2.11}$$

where

$$\hat{\mathbf{U}} := \sqrt{\mathbb{F}^T \mathbb{F}} = \sqrt{\hat{\mathbf{F}}^T \hat{\mathbf{F}}}. \tag{5.2.12}$$

Proved in Appendix C, this theorem, in conjunction with its counterpart from classical elasticity theory, imply that a necessary and sufficient condition for a hyperelastic material to be isotropic is that Equations $(5.2.2)_1$ and (5.2.11) be satisfied. Note that the interfaces of such bodies are completely characterized by the two scalar invariants of the surface-deformation gradient *without regard* for interface orientation.

Equation $(4.17)_2$ gives the referential deformational surface stress, $\hat{\mathbf{S}}$, as a function of $\breve{w}$ so the above result can be used to express $\hat{\mathbf{S}}$ in terms of $\hat{w}$. This is accomplished in Appendix C, with the result that

$$\hat{\mathbf{S}} = \bar{\mathbf{I}}\{\partial_1 \hat{w}(i,j)\hat{\mathbf{F}}\hat{\mathbf{U}}^{-1} + j\partial_2 \hat{w}(i,j)\hat{\mathbf{F}}^{-T}\}, \tag{5.2.13}$$

where the arguments of i and j are $\hat{\mathbf{U}}$, which have been suppressed for the sake of clarity. Proposition 5.1, the Interface Representation Theorem, and Equation $(4.1.17)_3$ then allow $\hat{\mathbf{C}}$ to be expressed as

$$\hat{\mathbf{C}} = \mathbf{I}\{-\partial_1 \hat{w}(i,j)\hat{\mathbf{U}} + [\hat{w}(i,j) - j\partial_2 \hat{w}(i,j)]\mathbf{1}_s\}, \tag{5.2.14}$$

where, again, the arguments of i and j are $\hat{\mathbf{U}}$ and have been supressed for the sake of clarity.

The following is a summary of the interfacial characterization of isotropic, hyperelastic materials:

$$\begin{aligned} w &= \hat{w}(i,j) \\ \hat{\mathbf{S}} &= \bar{\mathbf{I}}\{(\partial_1 \hat{w})\hat{\mathbf{F}}\hat{\mathbf{U}}^{-1} + (j\partial_2 \hat{w})\hat{\mathbf{F}}^{-T}\} \\ \hat{\mathbf{T}} &= \frac{1}{j}(\partial_1 \hat{w})\hat{\mathbf{V}} + (\partial_2 \hat{w})\mathbf{1}_{\bar{s}} \\ \hat{\mathbf{C}} &= \mathbf{I}\{-(\partial_1 \hat{w})\hat{\mathbf{U}} + (\hat{w} - j\partial_2 \hat{w})\mathbf{1}_s\}, \end{aligned} \tag{5.2.15}$$

where

$$\begin{aligned} i &:= i(\hat{\mathbf{U}}) = i(\hat{\mathbf{V}}), \qquad j := j(\hat{\mathbf{U}}) = j(\hat{\mathbf{U}}) \\ \hat{\mathbf{U}} &:= \sqrt{\mathbb{F}^T \mathbb{F}} = \sqrt{\hat{\mathbf{F}}^T \hat{\mathbf{F}}}, \qquad \hat{\mathbf{V}} := \sqrt{\hat{\mathbf{F}}\hat{\mathbf{F}}^T}. \end{aligned} \tag{5.2.16}$$

5.3 Further Insights Regarding $\hat{\mathbf{C}}$. Proposition 5.1 gives additional insight into the role of the accretive stress. Recalling the comments of Section 4.2, it may be concluded that any work performed by $\hat{\mathbf{C}}$ to reorient the interface must be due to material anisotropy, since this work is always zero for isotropic bodies. LEO & SEKERKA[1989] conclude that such a work term should be present for anisotropic hyperelastic materials and the idea is also in line with the earlier work of CAHN & HOFFMAN[1972] and HOFFMAN & CAHN[1974] who espoused the utility of adopting a capillary traction vector to account for anisotropic effects in non-deformable media. In fact, consideration of such a work term can be traced back to HERRING[1951a,b].

The tangential component of $\hat{\mathbf{C}}$ has a physically meaningful relation with the symmetry exhibited by the interface and is embodied in the following

Fluid-Surface Theorem:

(A) For a hyperelastic material with unimodular mechanical symmetry:

(a) $\bar{w} = \bar{\sigma}$, a constant;

(b) $\hat{\mathbf{C}} = \mathbf{0}$; and

(c) $\hat{\mathbf{T}} = \bar{\sigma}\mathbf{1}_{\bar{\mathcal{S}}}$.

(B) For a hyperelastic material with a constitution such that $\hat{\mathbf{C}} = \mathbf{0}$:

(a) $\bar{w} = \bar{\sigma}$, a constant; and

(b) $\hat{\mathbf{T}} = \bar{\sigma}\mathbf{1}_{\bar{\mathcal{S}}}$.

(C) For a hyperelastic material with a constitution such that $\bar{w} = \bar{\sigma}$, a constant:

(a) $\hat{\mathbf{C}} = \mathbf{0}$; and

(b) $\hat{\mathbf{T}} = \bar{\sigma}\mathbf{1}_{\bar{\mathcal{S}}}$.

Part **(A)** is due to GURTIN & STRUTHERS[1990], while Parts **(B)** and **(C)** are new and are proved in Appendix D. In conjunction with the Tension-Energy

Theorem, they imply that an interface exhibits a *fluid nature*—that is, surface energy and surface tension characterized by the same scalar constant—if and only if $\hat{\mathbf{C}} = \mathbf{0}$. Thus, $\hat{\mathbf{C}}$ accounts for special properties of solid-solid interfaces not associated with their fluid counterparts. Its tangential component is non-zero for all *solid-like* interfaces, and its normal component is non-zero only for anisotropic interfaces.

6. SLOW, DILATIVE PHASE TRANSiTIONS

6.1 Dilatation in Martensitic Phase Transitions. Chapters three through five present a continuum mechanical model of coherent phase growth for hyperelastic materials. For the remainder of this work attention is restricted to phase transitions that evolve at such a slow rate that inertial effects may be considered negligible. These are referred to as *slow processes*. Under this restriction, the theory is applied to study the dilatational aspects of martensitic phase transitions. Of particular interest is the affect of surface properties on these processes, so a class of isotropic materials is considered that can also sustain slow phase transitions without interfacial structure being taken into account.

Though it is common to idealize martensitic phase changes as occurring in response to shear,[6.1] this imposes severe restrictions on the interface properties that may be modeled because of the requirement that any traction jump, $-\nabla_s \cdot \hat{\mathbf{S}}$, that is generated be in the direction of the shear. Otherwise, the surface fields would result in an unbalanced force. However, there is also a volume change associated with martensitic phenomena that, in fact, dominates the material response in certain settings.[6.2] Since the traction jump condition for pure dilatation allows a number of reasonable interface constitutions to be considered, the dilatant aspects of martensitic phase transitions are focused on in lieu of embracing more generalized kinematics. This simplified setting still admits an investigation of the relationship between surface properties and surface effects. The results may then be used to draw conclusions about what happens under more complex deformations and may be applied directly to better understand those transitions where dilatation dominates.

6.1 ABEYARATNE[1980, 1981]; JAMES[1981]; TRUSKINOVSKII[1987]; FOSDICK & MacSITHIGH [1983]; GURTIN[1983]; ABEYARATNE & KNOWLES[1987a]; SILLING[1988b]; JIANG[1989]; FRIED[1991a,b,c]; ROSAKIS[1991].

6.2 See, for instance, BUDIANSKY, HUTCHINSON & LAMBROPOULOS[1983]; LAMBROPOULOS[1983]; SILLING[1987]; ABEYARATNE & JIANG[1988a,b].

6.2 Loss of Ellipticity Under Pure Dilatation. For hyperelastic materials without interfacial structure, a necessary condition for a body to support slow phase transitions is that the bulk linear momentum balance,

$$\nabla \cdot [\partial \tilde{W}(\mathbf{F})] = 0, \tag{6.2.1}$$

lose ellipticity for some deformations. For isotropic materials, (strong) ellipticity is lost under a pure dilation if and only if

$$\{\partial^2 \tilde{W}(\lambda \mathbf{1})[\mathbf{a} \otimes \mathbf{b}]\} \cdot [\mathbf{a} \otimes \mathbf{b}] \quad \forall \mathbf{a}, \mathbf{b} \in \mathrm{Unit}(\mathbb{E}^3), \tag{6.2.2}$$

where λ is the isotropic stretch associated with the deformation. Using the results of HOGER & CARLSON[1984] to facilitate evaluation of $\partial^2 \tilde{W}(\lambda \mathbf{1})$, it may be shown that Equation (6.2.2) is equivalent to

$$\begin{aligned} \partial_{11}\breve{W} - \frac{1}{2\lambda}\partial_1 \breve{W} + 4\lambda^2 \partial_{22}\breve{W} - \frac{1}{2}\partial_2 \breve{W} + \lambda^4 \partial_{33}\breve{W} > 0 \\ \frac{1}{\lambda}\partial_1 \breve{W} + \partial_2 \breve{W} > 0, \end{aligned} \tag{6.2.3}$$

where

$$\breve{W} = \breve{W}(3\lambda, 3\lambda^2, \lambda^3).$$

If either of these equalities is violated for some interval of stretches, λ, then Equation (6.2.1) loses ellipticity under the associated pure dilatations.

6.3 Two-phase, Dilative Solids. Consider a particular class of isotropic, hyperelastic materials whose bulk is characterized by

$$\breve{W}(I_1, I_2, I_3) = 2\mu \left[I_1 - 3 + \int_1^{I_3} h(J)\, dJ \right], \quad \mu > 0, \tag{6.3.1}$$

where the constant μ is the shear modulus at infinitesimal deformations, and h is a smooth, constitutive function satisfying

$$h(1) = -1, \quad h'(1) > \frac{2}{3}. \tag{6.3.2}$$

Equation $(6.3.2)_1$ ensures that the reference configuration is stress-free, while the inequality of $(6.3.2)_2$ guarantees that the (infinitesimal deformation) Poisson's ratio is in the range $(-1, \frac{1}{2})$. The stored energy response function of Equation (6.3.1) was considered by HAUGHTON[1987] but not within the context of discontinuous deformation gradients.

For such materials, Equation (6.2.3) reduces to the strong ellipticity conditions of

$$\mu > 0, \qquad h'(J) > 0. \tag{6.3.3}$$

The first of these is satisfied by construction, and so a necessary and sufficient condition for Haughton materials to lose ellipticity in pure dilation is that h lose monotonicity over a portion of its domain. A subclass of the Haughton materials that is of particular interest is the *Two-phase, Dilative (2-PD) Solids*, for which h loses monotonicity over a single,intermediate interval of dilations as shown in Figure 3 and summarized by

$$\begin{aligned} &h : I\!R \mapsto I\!R_- \\ &h'(J) > 0, \quad J \in (0, J_L) \\ &h'(J) < 0, \quad J \in (J_L, J_U) \\ &h'(J) > 0, \quad J > J_U \end{aligned} \tag{6.3.4}$$

and

$$\begin{aligned} &h'(J_L) = h'(J_U) = 0 \\ &h(J_L) \in (-1, 0) \\ &h(J_U) < -1 \\ &\lim_{J \searrow 0} h(J) = -\infty. \end{aligned} \tag{6.3.5}$$

Such materials have a monotonic response to shear, a non-monotonic response to dilatation, and the shear and dilatation components of a deformation are uncoupled in the sense that the shear response is independent of h. If it were not for the I_1 dependence of $\breve{W}$, the bulk material would exhibit unimodular symmetry and be a generalization of the classical Van der Waals fluid. The low and high

intervals of J for which h is monotone-increasing delineate the *low* and *high dilatation phases* of such materials. Of particular interest in this work are settings wherein a single interface separates these low and high dilatation phases.

For 2-PD Solids, Equation (5.2.13) allows the stress to be expressed as

$$\begin{aligned} \mathbf{S} &= 2\mu\big[\mathbf{F}\mathbf{U}^{-1} + Jh(J)\mathbf{F}^{-T}\big] \\ \mathbf{T} &= 2\mu\big[\frac{1}{J}\mathbf{V} + h(J)\mathbf{1}\big], \end{aligned} \tag{6.3.6}$$

where

$$J = \mathrm{Det}(\mathbf{F}) = I_3(\mathbf{U}).$$

Since $h(J_U) < -1$, it follows from Equation (6.3.5) that these materials can sustain *permanent deformations* since there exist non-trivial deformations for which the associated stress is zero.

6.4 A Reduced Form for the Driving Traction.

For hyperelastic materials involved in slow processes, the driving traction, f, defined by Equation (3.5.4), may be expressed as

$$\begin{aligned} f &= \mathbf{n}\cdot[\![I\!P]\!]\mathbf{n} + (\nabla_s\cdot\hat{\mathbf{C}})\cdot\mathbf{n} \\ &= \mathbf{n}\cdot[\![I\!P]\!]\mathbf{n} + 2H\tilde{w} - I\!F^T\hat{\mathbf{S}}\cdot\mathbf{L} - \nabla_s\cdot(D_{\mathbf{n}}\tilde{w}), \end{aligned} \tag{6.4.1}$$

where $\mathbf{L}$ and H are the referential curvature tensor and mean curvature, respectively, and

$$I\!P(\mathbf{F}) := \tilde{W}(\mathbf{F})\mathbf{1} - \mathbf{F}^T\partial\tilde{W}(\mathbf{F}), \quad \forall\mathbf{F}\in\mathrm{Lin}_+(I\!E^3, I\!E^3) \tag{6.4.2}$$

is the Eshelby Energy-Momentum Tensor.[6.3] Note that the interface deformational stress, $\hat{\mathbf{S}}$, does not affect the form of (6.4.1), while the accretive stress, $\hat{\mathbf{C}}$, does. This result is relevant to subsequent discussions of the role of interface properties in determining phase equilibria. When restricted to isotropic, hyperelastic materials, Proposition 5.1 and Equation (5.2.15) give that

$$f = \mathbf{n}\cdot[\![I\!P]\!]\mathbf{n} + 2H\hat{w} - \big[(\partial_1\hat{w})\hat{\mathbf{U}} + j(\partial_2\hat{w})\mathbf{1}_s\big]\cdot\mathbf{L}. \tag{6.4.3}$$

[6.3] Eshelby[1956, 1970].

By virtue of Equations (6.4.1) and (6.4.3), the driving traction for 2-PD Solids is given by

$$f = 2\mu\left[\!\!\left[\int_1^J h(\zeta)\,d\zeta - Jh(J)\right]\!\!\right] + 2\mu\big[I_1 - (\mathbf{Un})\cdot\mathbf{n}\big] + 2H[\hat{w} - j\partial_2\hat{w}] - (\partial_1\hat{w})\hat{\mathbf{U}}\cdot\mathbf{L}. \tag{6.4.4}$$

6.5 Two-phase, Linearly Dilative Solids. An important subclass of 2-PD Solids are those characterized by a piecewise linear response function, h:

$$\begin{aligned} h(J) &= \beta(J-1) - 1, && J \in [J_{min}, J_L] \\ h(J) &= \beta'(J - J_U) + \beta(J_{min} - 1) - 1, && J \in [J_L, J_U] \\ h(J) &= \beta(J - J_{max}), && J \in [J_U, J_{max}] \end{aligned} \tag{6.5.1}$$

with

$$\begin{aligned} J_{max} &:= J_U - J_{min} + 1 + \frac{1}{\beta}, \\ \beta' &:= -\beta\left(\frac{J_L - J_{min}}{J_U - J_L}\right) \end{aligned} \tag{6.5.2}$$

and

$$\beta \in \left(\frac{2}{3}, \frac{1}{J_L - 1}\right). \tag{6.5.3}$$

This is illustrated in Figure 4, where the commonly occurring quantity,

$$\Gamma := J_U - J_{min},$$

is also shown. Equation (6.5.3) ensures both that Poisson's ratio is within the proper interval for infinitesimal deformations and that h takes on only negative values. Such materials are referred to as *Two-phase, Linearly Dilative (2-PLD) Solids.*

The associated form of the driving traction from Equation (6.4.4) is

$$f = -\beta\mu\{J_+^2 - J_-^2 + \Gamma(J_U + J_L)\} + 2\mu\big[I_1 - (\mathbf{Un})\cdot\mathbf{n}\big] + 2H[\hat{w} - j\partial_2\hat{w}] - (\partial_1\hat{w})\hat{\mathbf{U}}\cdot\mathbf{L} \tag{6.5.4}$$

for $J_+ \in [J_{min}, J_L]$, $J_- \in [J_U, J_{max})$,

and

$$f = \beta\mu\{J_+^2 - J_-^2 + \Gamma(J_U + J_L)\} + 2\mu[\![I_1 - (\mathbf{Un})\cdot\mathbf{n}]\!] + 2H[\hat{w} - j\partial_2\hat{w}] - (\partial_1\hat{w})\hat{\mathbf{U}}\cdot\mathbf{L} \tag{6.5.5}$$

for $J_+ \in [J_U, J_{max}]$, $J_- \in [J_{min}, J_L]$.

Here J_+ and J_- refer to the local values of $\det(\mathbf{F})$ on either side of the phase interface. Under the conditions of Equation (6.5.4), $f > 0$ implies that locally, any transition favors the high dilatation phase. $f > 0$ in Equation (6.5.5) implies the converse.

7. THE CYLINDER PROBLEM FOR 2-PLD SOLIDS

7.1 Temporal Shocks. Interest is now focused on the consideration of a *nucleation event*—that is, the onset of a martensitic phase transition during which the bulk deformation loses spatial smoothness across some surface. Within the context of slow processes, such nucleation events are considered to occur over very small intervals of time.

A standard approach in modeling phenomena wherein relevant fields vary greatly over some small dimension is to approximate the transition region as a discontinuity. Such an idealization is used in the present work with time as the dimension of interest. The nucleation event is treated as a discontinuity or shock, global in spatial extent, in relevant field quantities across a *nucleation instant.*

Two issues arise as costs of embracing such an idealized theory of phase nucleation. The first is that the Mechanical Dissipation Imbalance does not apply at nucleation instants, since it is a rate relation. The second issue concerns the absence of *nucleation conditions* linking pre- and post-nucleation stages and from which the onset time of a phase transition may be determined. Thus, within the context of this simplified theory there exist axiomatic deficiencies directly attributable to the treatment of the formation of a nucleus as occurring at a single instant. As an alternative to developing a more elaborate set of postulates, a constitutive remedy is suggested using a *nucleation criterion* as a means of accounting for these deficiencies.

7.2 Problem Setting. An ideal setting to explore many of the features of the mechanical theory of nucleation and growth is that of a cylindrical nucleus forming within a solid cylinder under axially and radially symmetric loading conditions. Here the problem is essentially one-dimensional, yet there exists a meaningful notion of interface curvature, and this admits a number of nontrivial manifestations of the interfacial structure. The Cylinder Problem is used to consider an idealized transition process that occurs in response to *extensional*

boundary loading. This is accomplished by first considering the slow motion of a cylinder composed of a 2-PLD Solid without any interface—that is, in a configuration such that either the high- or low-dilatation phase is present, but not both. Attention is then focused on the analogous situation for two-phase motions involving a single interface, first without any surface effects and then under a variety of surface constitutions. In each case an analysis is presented which exhibits all the possible states in which the body can exist. This turns out to be a convenient way of considering the effect of various cylinder loading programs on the nucleation and growth of new phases. A key element here is the *phase segregation constraints*, referring to the requirement that at every point in a low-dilatation phase, $J \in (J_{min}, J_L)$, and everywhere in a high-dilatation phase, $J \in (J_U, J_{max})$. After each process has been investigated independently, the single- and two-phase motions are linked via a nucleation event, and it is here that the nucleation criterion put forth is investigated.

Throughout this application, the reference configuration is taken to be a cylinder with positions given by radius $q \in [0, Q]$. The map $\tilde{r}:[0,Q] \times \mathcal{T} \to \mathbb{R}_+$ describes the cylinder motion over time interval $\mathcal{T}$. When an interface exists, it is described by either its referential location, $q = s(t)$, or its actual location at $\bar{s}(t) := \tilde{r}\big(s(t),t\big)$. Figure 5 illustrates this problem geometry. The normal interface velocity is given by $V_n = \dot{s}$, and the following expressions can be derived:

$$\begin{aligned} &2H = -\frac{1}{s}, \qquad 2\bar{H} = -\frac{1}{\bar{s}} \\ &J(q,t) = \frac{\tilde{r}(q,t)\tilde{r}'(q,t)}{q}, \qquad j(t) = \frac{\tilde{r}\big(s(t),t\big)}{s(t)} = \frac{\bar{s}(t)}{s(t)}. \end{aligned} \tag{7.2.1}$$

Under the cylinder motion prescribed, the bulk linear momentum localization, Equation (6.2.1), can be simplified using Equation $(6.3.6)_1$:

$$\begin{aligned} \nabla\cdot\mathbf{S} =& 2\mu\nabla\cdot\left[\mathbf{F}\mathbf{U}^{-1} + Jh(J)\mathbf{F}^{-T}\right] \\ =& 2\mu\big[h(J)\nabla\cdot(J\mathbf{F}^{-1}) + J\mathbf{F}^{-1}\nabla\big(h(J)\big)\big]. \end{aligned} \tag{7.2.2}$$

But $\nabla\cdot(J\mathbf{F}^{-1}) = \mathbf{0}$ for such cylindrical motions, so that Equation (6.2.1) becomes

$$2\mu J\mathbf{F}^{-1}\nabla\big(h(J)\big) = \mathbf{0}. \tag{7.2.3}$$

Since $\mu > 0$, $J > 0$, and $\mathbf{F}$ is invertible, this is equivalent to

$$h\big(J(q,t)\big) = \tilde{h}(t), \tag{7.2.4}$$

where $\tilde{h}$ is some scalar function of time on $\mathcal{T}$.

Now consider the linear momentum jump condition, Equation $(3.3.4)_2$. For slow processes, this reduces to

$$[\![\mathbf{Sn}]\!] = -\nabla_s \cdot \hat{\mathbf{S}}. \tag{7.2.5}$$

Under cylindrical motions, with $\hat{\mathbf{S}}$ given by Equation $(5.2.15)_2$,

$$\nabla_s \cdot \hat{\mathbf{S}} = 2H\big[\partial_1 \hat{w} + \partial_2 \hat{w}\big]\mathbf{n}. \tag{7.2.6}$$

With $\mathbf{S}$ given by Equation $(6.3.6)_1$ the jump in traction can be expressed as

$$[\![\mathbf{Sn}]\!] = 2\mu j [\![h(J)]\!]\mathbf{n}. \tag{7.2.7}$$

Thus, the linear momentum jump condition reduces to the scalar equation

$$2\mu j [\![h(J)]\!] = \hat{\gamma}_1, \tag{7.2.8}$$

where

$$\begin{aligned} \hat{\gamma}_1 &:= -\,(\nabla_s \cdot \hat{\mathbf{S}}) \cdot \mathbf{n} \\ &= -\,2H\big[\partial_1 \hat{w} + \partial_2 \hat{w}\big]. \end{aligned} \tag{7.2.9}$$

Finally, consider the driving traction given by Equation (6.4.4). Under the cylinder motions

$$[\![I_1 - \mathbf{U}\mathbf{n} \cdot \mathbf{n}]\!] = 0$$

and

$$\hat{\mathbf{U}} \cdot \mathbf{L} = 2Hj.$$

The driving traction can therefore be expressed as

$$f = 2\mu \left[\!\!\left[\int_1^J h(\zeta)\, d\zeta - Jh(J) \right]\!\!\right] + \hat{\gamma}_2, \tag{7.2.10}$$

where

$$\begin{aligned}\hat{\gamma}_2 :=& (\nabla_s \cdot \hat{\mathbf{C}}) \cdot \mathbf{n} \\ =& 2H\left[\hat{w} - j(\partial_1 \hat{w} + \partial_2 \hat{w})\right].\end{aligned} \tag{7.2.11}$$

$\hat{\gamma}_1$ and $\hat{\gamma}_2$ embody the surface effects produced by the deformational and accretive interface stresses, respectively. Equations (7.2.4), (7.2.8), and (7.2.10), along with Equation (4.3.1) and the kinematic stipulation that all deformations be continuous, give the following system summary for slow, two-phase cylindrical motion of a 2-PD Solid:

$$\begin{aligned}&\frac{\tilde{r}(q,t)\tilde{r}'(q,t)}{q} = J_i(t), \quad q \in [0, s(t)) \\ &\frac{\tilde{r}(q,t)\tilde{r}'(q,t)}{q} = J_m(t), \quad q \in [s(t), Q) \\ &[\![h(J)]\!] = \frac{\hat{\gamma}_1}{2\mu j} \\ &[\![\tilde{r}]\!] = 0, \qquad \tilde{r}(0,t) = 0 \\ &\dot{s} = \hat{V}(f), \qquad \hat{V}(f) f \geq 0 \\ &f = 2\mu \left[\!\!\left[\int_1^J h(\zeta)\, d\zeta - J h(J) \right]\!\!\right] + \hat{\gamma}_2,\end{aligned} \tag{7.2.12}$$

where J_i and J_m are functions of time to be determined by the loading conditions, and $\hat{\gamma}_1$ and $\hat{\gamma}_2$ are defined in Equations (7.2.9) and (7.2.11). Here the subscripts i and m refer to the *inclusion* and *matrix*, respectively.

For 2-PLD Solids with a *high* dilatation inclusion, this system reduces to

$$\begin{aligned}&\frac{\tilde{r}(q,t)\tilde{r}'(q,t)}{q} = J_i(t) \in [J_U, J_{max}), \quad q \in [0, s(t)) \\ &\frac{\tilde{r}(q,t)\tilde{r}'(q,t)}{q} = J_m(t) \in [J_{min}, J_L], \quad q \in [s(t), Q) \\ &J_m - J_i = -\Gamma + \frac{\hat{\gamma}_1}{2\mu\beta j} \\ &[\![\tilde{r}]\!] = 0, \qquad \tilde{r}(0,t) = 0 \\ &\dot{s} = \hat{V}(f), \qquad \hat{V}(f) f \geq 0 \\ &f = -\beta\mu\left[J_m^2 - J_i^2 + \Gamma(J_U + J_L)\right] + \hat{\gamma}_2.\end{aligned} \tag{7.2.13}$$

Likewise, for 2-PLD Solids with a *low* dilatation inclusion, Equation (7.2.12) is expressible as

$$\begin{aligned}
&\frac{\tilde{r}(q,t)\tilde{r}'(q,t)}{q} = J_i(t) \in [J_{min}, J_L), \quad q \in [0, s(t)) \\
&\frac{\tilde{r}(q,t)\tilde{r}'(q,t)}{q} = J_m(t) \in [J_U, J_{max}], \quad q \in [s(t), Q) \\
&J_m - J_i = \Gamma + \frac{\hat{\gamma}_1}{2\mu\beta j} \\
&[\![\tilde{r}]\!] = 0, \qquad \tilde{r}(0,t) = 0 \\
&\dot{s} = \hat{V}(f), \qquad \hat{V}(f)f \geq 0 \\
&f = \beta\mu\left[J_m^2 - J_i^2 + \Gamma(J_U + J_L)\right] + \hat{\gamma}_2
\end{aligned} \tag{7.2.14}$$

7.3 Single-phase Solutions. Consider the cylinder problem wherein only one phase is present. For clarity, take time to be fixed and suppress temporal arguments. Then the relevant system is just

$$\frac{\tilde{r}(q)\tilde{r}'(q)}{q} = J_0, \qquad \tilde{r}(0) = 0, \tag{7.3.1}$$

with J_0 the constant dilatation of the cylinder to be determined from the boundary data, and this equation can be solved to give

$$\tilde{r}(q) = qJ_0^{\frac{1}{2}}. \tag{7.3.2}$$

Since interest is focused on the system response to various loading programs, the radial stress component, τ, is evaluated:

$$\begin{aligned}
\tau :=& \mathbf{T}\big(\tilde{r}(1)\big)\bar{\mathbf{n}} \cdot \bar{\mathbf{n}} \\
=& 2\mu\left[\frac{Q}{R} + h\big(J(1)\big)\right],
\end{aligned} \tag{7.3.3}$$

where $R := \tilde{r}(1)$ gives the position of the outer radius of the cylinder and $h(J)$ is given by Equation (6.4.1). Since $J_0 = (R/Q)^2$, the cylinder deformation can be re-expressed with respect to R:

$$\tilde{r}(q) = \frac{qR}{Q} \quad \forall q \in [0, Q], \tag{7.3.4}$$

so that given R, there exists a unique deformation defined by Equation (7.3.4). Moreover,

$$\tau = 2\mu\left[\frac{Q}{R} + h\left(\frac{R^2}{Q^2}\right)\right], \tag{7.3.5}$$

so that under the extensional loading of interest, there exists an invertible relationship between radial stress, τ, and the cylinder boundary, R. These results are summarized by the system *macroscopic response*[7.1] of Figure 6, where the set of all possible low- and high-dilatation solutions are plotted on the R, τ-plane. As is clear from the picture, if the material phase is prescribed and either R or τ is given, then any solution that exists is necessarily unique. Note that the phase segregation constraints determine the range of boundary data over which each phase can exist.

7.4 Two-phase Solutions: No Surface Fields. Now consider the analogous situation but with a single interface at $q=s$ and no surface fields. For definiteness, suppose that the inner region is in the *high-dilatation* phase. Again, interest is focused on extensional loading at a fixed time. Under these conditions, Equation (7.2.13) implies that

$$\begin{aligned}
&\tilde{r}(q) = qJ_i^{\frac{1}{2}}, \qquad q \in [0, s] \\
&\tilde{r}(q) = [s^2 J_i + (q^2 - s^2)J_m]^{\frac{1}{2}}, \quad q \in [s, Q] \\
&J_i = J_m + \Gamma \\
&f = \beta\mu\Gamma\left[2J_m - J_L - J_{min}\right] \\
&\dot{s} = \hat{V}(f), \qquad \hat{V}(f)f \geq 0 \\
&J_i \in [J_{min}, J_L], \qquad J_m \in [J_U, J_{max}], \qquad s \in [0, Q].
\end{aligned} \tag{7.4.1}$$

Then there exist (J_m, s) parameterizations of all the possible (R, τ) pairs that the cylinder can support:

$$\begin{aligned}
&\tilde{R}(s, J_m) := \left[Q^2 J_m + \Gamma s^2\right]^{\frac{1}{2}} \\
&\tilde{\tau}(s, J_m) := 2\mu\left[\frac{Q}{\tilde{R}(s, J_m)} + h(J_m)\right], \qquad \forall (s, J_m) \in \tilde{\Pi}
\end{aligned} \tag{7.4.2}$$

7.1 ABEYARATNE & KNOWLES[1988].

where

$$\tilde{\Pi} := \left\{ (s, J_m) \middle| s \in [0, Q], \quad J_m \in [J_{min}, J_L], R \geq 1 \right\} \tag{7.4.3}$$

and is shown in Figure 7.

As for the single-phase case, the system macroscopic response for two-phase solutions provides a means of characterizing the system behavior under all possible conditions of loading. In the two-phase setting, the response plot is constructed by mapping $\tilde{\Pi}$ into the R, τ-plane via the functions $\tilde{R}$ and $\tilde{\tau}$. It can be shown that

$$\begin{aligned}
\partial_1 \tilde{R}(s, J_m) &= \frac{\Gamma s}{\tilde{R}(s, J_m)} \quad > 0 \\
\partial_2 \tilde{R}(s, J_m) &= \frac{Q^2}{2\tilde{R}(s, J_m)} \quad > 0 \\
\partial_1 \tilde{\tau}(s, J_m) &= -2\mu \left[\frac{\Gamma s Q}{\tilde{R}^3(s, J_m)} \right] \quad < 0 \\
\partial_2 \tilde{\tau}(s, J_m) &= 2\mu \left[-\frac{Q^3}{2\tilde{R}^3(s, J_m)} + \beta \right] \quad > 0.
\end{aligned} \tag{7.4.4}$$

This map of $\tilde{\Pi}$ is invertible, since

$$\text{Det} \begin{pmatrix} \partial_1 \tilde{R} & \partial_2 \tilde{R} \\ \partial_1 \tilde{\tau} & \partial_2 \tilde{\tau} \end{pmatrix} = \frac{2\mu \Gamma s \beta}{\tilde{R}(s, J_m)} > 0, \tag{7.4.5}$$

and its image is shown in Figure 8, where the monotonicity of all curves shown in the figure hold in general. Note that on this macroscopic response, curves of constant s are monotone-increasing, while curves of constant J_m are monotone-decreasing. Significantly, the left and right borders, L_4' and L_2', of the macroscopic response region are composed of portions of the single-phase responses.

The set of parameters used to generate Figure 8 is listed next to the plot and gives a transition dilatation of 5%. This is approximately the amount of volume expansion experimentally measured by PORTER, EVANS & HEUER[1979] for the unconstrained transition of partially stabilized zirconia.

A key element of the analysis of phase nucleation and growth turns out to be how the sign of the interface driving traction varies over the macroscopic response region. It may be shown that the region is partitioned by a single curve into one

area, where $f > 0$ and another, where $f < 0$. Since a state is called Maxwell if its associated driving traction is zero, a condition that holds at every point on the partition, it is referred to as the *Maxwell curve.*[7.2]

Since $f = 0$ implies that J_m is fixed at

$$J_m = \frac{1}{2}(J_L + J_{min}), \tag{7.4.6}$$

Equations $(7.4.4)_1$ and $(7.4.4)_2$ give that the curve is monotone-decreasing, as shown in Figure 9, and it may be shown that all curves of constant driving traction have this feature.

Now consider a slow, two-phase motion for the system. At each instant the associated state must be within the macroscopic response region, so that any motion may be associated with a curve through this region. For a given loading history, the actual curve traced out is determined by the kinetic relation of the material, Equation $(7.2.14)_6$, with the set of admissible curves restricted by Equation $(7.2.14)_7$. Specifically, this inequality stipulates that a phase embryo cannot shrink in the region where $f > 0$ and cannot grow in region where $f < 0$. This is summarized in Figure 10, where an admissible two-phase motion is illustrated. Note that while the kinetic relation controls the rate of phase growth in response to loading, the dissipation inequality implies that hysterisis is involved in any cyclic process of the type depicted. The area enclosed by the hysteresis curve represents the net work that must be performed on the cylinder during the course of one such loading cycle.

7.5 Nucleation Events. Both single- and two-phase solutions have been analyzed in the absence of surface fields, and a nucleation criterion linking the two solution sets is now presented. A time-position diagram of the transition process is given in Figure 11 where, as shown, a nucleation event may produce an embryo of finite size. Some information must be identified, however, which serves to link

[7.2] ABEYARATNE & KNOWLES[1988].

the states before and after a nucleation event. Characterization of the boundary conditions of the system during nucleation is one means of providing such linking data. The region exterior to the cylinder is referred to as the *loading device*, and interest is focused on devices endowed with an energy, $E_{LD}(t)$, such that

$$E_{LD}(t) = \tilde{E}_{LD}\big(R(t), \lambda(t)\big) \quad \forall t \in \mathcal{T}, \tag{7.5.1}$$

with λ continuous and $\tilde{E}_{LD}$ smooth. Such loading devices are called *conservative* if they store all energy expended in deforming their boundaries. Thus, for λ fixed, the rate at which work is done by the cylinder is equal to the rate at which energy is absorbed by such a loading device. Use of Equation (4.1.17) then gives that

$$\frac{d}{dt}\Big\{E(t) + \tilde{E}_{LD}\big(R(t), \lambda_0\big)\Big\} = -2\pi s f \dot{s} \tag{7.5.2}$$

for all slow processes, so that interfacial accretion or a change in the loading parameter, λ, are the only ways in which the total system energy can change for conservative loading devices. Here E is the sum of the bulk and surface energies associated with the body. Conservative loading devices provide information linking pre- and post-nucleation states because any discontinuous change in total energy will neccessarily be associated with the formation of an interface.

Define the *nucleation energy* associated with the cylinder under conservative loading as

$$\mathbf{B}(t) := \big\{E(t^{(+)}) + E_{LD}(t^{(+)})\big\} - \big\{E(t^{(-)}) + E_{LD}(t^{(-)})\big\}, \tag{7.5.3}$$

where, at $t = t^{(-)}$, the cylinder exists in a single-phase state, and at $t = t^{(+)}$ the cylinder exists in a two-phase state with a single, closed interface at $\bar{s}(t^{(+)})$. B is a generalization of the classical thermostatics notion of *availability* associated with fluids under soft and hard loading.[7.3]

For a given state at $t = t^{(-)}$, $\mathbf{B}(t)$ may be computed over the space, Γ, of all possible two-phase states compatible with the loading conditions. A given

[7.3] See, for instance, ADKINS[1968] Ch.10.

two-phase state is called *critical* if the associated value of $\mathbf{B}$ is a local extremum with respect to variations in interface position consistent with any constraints imposed by the loading device. If the extremum is a maximum, the critical state is referred to as *maximizing*, whereas *minimizing* critical states are associated with local minima in the nucleation energy.

7.6 A Nucleation Criterion. The following criterion is offered as a means of determining when and how a nucleation event occurs for hyperelastic materials and conservative loading devices involved in slow processes:

> A nucleation event will occur at $t = t_*$ if and only if there exists a maximizing critical state such that
>
> (i) $\mathbf{B}(t_*) \leq \mathbf{B}_0$, $\mathbf{B}_0 \geq 0$, a material constant; and
>
> (ii) there exist no smaller maximizing critical nuclei.
>
> When these conditions are both satisfied, the critical state will be achieved at $t = t_*^{(+)}$.

The energy, $\mathbf{B}$, associated with the formation of such a critical state is referred to as the *nucleation barrier*. As a result of embryo production, the total energy of body plus loading device increases by this amount. This suggests that for $\mathbf{B}(t_*) > 0$, the physical process modeled as a nucleation shock produces rather than dissipates energy. The nucleation criterion allows energy barriers below a prescribed magnitude to be overcome, implying that it is physically reasonable for the total energy to have to undergo (small) excursions—that is, to fluxuate—in order to conceive a phase embryo. $\mathbf{B}_0$ may be interpreted as the maximum magnitude of such fluxuations and in this way is related to the thermal activation of the system.[7.4] This simple model of nucleation therefore accounts for a system energy that rapidly fluxuates by a prescribed constant, and this could be easily

[7.4] See the relevant comments of MULLER[1985] p.21 and PIPPARD[1981] pp.98–99. Statistical mechanics considerations of martensitic nucleation are undertaken by THADHANI & MEYERS[1986] and ROITBURD[1990].

generalized. Suppose, for instance, that the bulk and surface energy response functions had a very small stochastic element. Then nucleation events—that is, system fluxuations to critical states—would be probablistic. Here, however, emphasis is placed on modeling the conditions under which nucleation occurs and not on the probability that these conditions are realized. As the subsequent investigation shows, a number of important surface effects are captured by this simple system.

7.7 The Nucleation Problem: No Surface Fields. The proposed nucleation criterion provides a means of modeling the onset of a phase transition in The Cylinder Problem. This is illustrated for three types of loading devices that differ in the quantities that are temporally continuous accross a nucleation shock:

$(\mathcal{SL})$	Soft Loading:	$[\![\tau]\!]^{t_*} = 0;$
$(\mathcal{HL})$	Hard Loading:	$[\![R]\!]^{t_*} = 0;$
$(\mathcal{ML})$	Specialized, Mixed Loading:	$[\![\lambda]\!]^{t_*} = 0,$

where

$$E_{LD} = \tfrac{\pi c}{2}(\lambda^2 - R^2)^2, \quad \tau = c(\lambda^2 - R^2), \quad c = \text{constant}.$$

Here

$$[\![\phi]\!]^{t_*} := \lim_{h \searrow 0} \{\phi(t_* + h) - \phi(t_* - h)\}, \tag{7.7.1}$$

with ϕ the temporally continuous quantity and $t = t_*$ the *nucleation instant.*

The mixed loading device may be interpreted as a hyperelastic, unit volume annulus with inner and outer radii of R and λ, respectively, characterized by the stored-energy function

$$\mathcal{W}(\mathcal{J}) = \frac{c}{2}\mathcal{J}^2. \tag{7.7.2}$$

Here $\mathcal{J}$ is the determinant of the annulus deformation. This is shown in Figure 12 and serves to illustrate that the nucleation model is not restricted only to soft and hard loading.

Under a given loading condition and prenucleation dilatation, the set, Γ, of two-phase states to which the cylinder can nucleate represents a curve on the macroscopic response plot. This is shown in Figure 13(a,b,c) with soft and hard loading associated with horizontal and vertical lines, respectively, and mixed loading given by monotone-decreasing curves of slope $= -2cR$. Since the curves of constant interface position, s, are monotone-increasing, (Equations $(7.4.4)_{2,4}$ and Figure 8), any given set, Γ, may be parameterized by s. Thus, there exists a function, $\tilde{B}(s, J_0)$, that delivers the nucleation energy as a function of prenucleation dilatation, J_0, and postnucleation interface position, s. By Equation (7.5.2),

$$\partial_1 \tilde{B}(s, J_0) = -2\pi s f, \tag{7.7.3}$$

and, since $\tilde{B}(0, J_0) = 0$ by construction, the nucleation energy increases from zero as s increases from $s = 0$, is maximized at the first intersection of Γ with the Maxwell curve, then decreases with increasing s until the next Maxwell curve intersection is reached, and so on. This is illustrated in Figure 14 for the case of soft loading. Equation (7.7.3) also implies that *all critical states are Maxwell* so that, in particular, two-phase states associated with nucleation are always Maxwell.

As shown in Appendix E,

$$\partial_2 \tilde{B}(s, J_0) < 0 \tag{7.7.4}$$

under all three types of loading conditions. The nucleation energy therefore *decreases* for fixed s as the prenucleation dilatation, J_0, is increased. Profiles of B are provided in Figure 15 for soft and hard loading. Note that under soft loading B always has an extremum at the origin and at most one other extremum, which is always a maximum. For sufficiently large prenucleation dilatation, the two extrema coincide at $s = 0$. Hard loading also has an extremum at the origin and at most one other extremum—which is always a minimum. Again, the two coincide at $s = 0$ for sufficiently large prenucleation dilatation. The mixed loading case

may take on the qualitative features of either hard or soft loading depending upon the magnitude of c—the load parameter.

With the nucleation energy completely characterized, it is straightforward to apply the criterion of the previous section to model a nucleation event. Suppose, for example, that the cylinder is initially in its single-phase, stress-free state and then a soft-loading program is intitiated so that the cylinder begins to expand (Figure 16(a,b,c)). As it does, a maximizing critical state develops and eventually reaches a point where the nucleation barrier is equal to B_0. A nucleation event then occurs. At $J_0 = \frac{1}{2}(J_L + J_{min})$, (Equation (7.4.6)), the nucleation barrier is zero so that this is the largest prenucleation dilatation that can be achieved under soft loading.

Now consider the analogous case with hard loading as shown in Figure 17(a,b,c). As the outer radius is extended from $R = Q$, there is initially no maximizing critical state. At $J_0 = \frac{1}{2}(J_L + J_{min})$, however, $s = 0$ becomes a maximizing critical state, and since the associated nucleation barrier is zero, a nucleation event occurs. The case of nucleation under hard loading is thus somewhat degenerate in that independent of the magnitude of B_0, a temporally smooth, $(s = 0)$, nucleation event occurs at $J_0 = \frac{1}{2}(J_L + J_{min})$. This result is significantly altered by the inclusion of interfacial properties as illucidated in subsequent chapters.

7.8 Embryo Stability. Consider the embryo nucleated under soft-loading conditions. If the nucleus size is perturbed out at constant load, then the driving traction becomes positive. Since $f\dot{s} \geq 0$ by Equation $(7.4.1)_6$, the embryo cannot decrease in size. Likewise, any perturbation to a smaller nucleus cannot be followed by growth. Since perturbations of the embryo have permanent repercussions, the soft-loaded embryo is *unstable*. In a completely analogous manner, it may be shown that embryos formed via hard loading are *stable*. In terms of the nucleation energy, maximizing critical states are always unstable while minimizing critical states are always stable. Subsequent results demonstrate that certain interface properties affect both the number and type of such equilibrium

states—one of the primary surface effects that the model is designed to capture.

8. THE CYLINDER PROBLEM: INTERFACES WITH BONDING ENERGY

8.1 Two-phase Solutions: Interfaces with Bonding Energy.

Suppose that the interface is endowed with a constant value of surface energy per unit *referential area.* Then the total interface energy can be varied only through accretion. This characterization has the atomistic interpretation that surface energy is a function of only the number of bonds that exist across the interface between atoms on either side. An illustration of this *bonding energy* interpretation is shown in Figure 18.

For a bonding energy constitution, Equation (4.1.17) gives that

$$\hat{\mathbf{C}} = \sigma \mathbf{I}, \qquad \hat{\mathbf{T}} = 0 \tag{8.1.1}$$

Here $\sigma = \hat{w}(i,j)$ is the constant value of referential interface energy. Surface properties modeled by bonding energy therefore cause no traction jump at the interface since $\nabla_s \cdot \hat{\mathbf{S}} = 0$. These properties have a purely energetic manifestation, and this is fundamentally different from the classical case wherein surface energy generates a deformational surface tension of equal magnitude.[8.1] Here the bonding energy generates an accretive surface tension of equal magnitude and is thus an ideal constitution for investigating the effect of accretive stress on the phase transformation process in isotropic materials.

The macroscopic response is now constructed with such an interface under the kinematic and bulk constitutive assumptions of the previous chapter. The relevant system is summarized by Equation (7.2.13), where now Equations (7.2.9) and (7.2.11) give that

$$\hat{\gamma}_1 = 0, \qquad \hat{\gamma}_2 = 2H\sigma = -\frac{\sigma}{s}. \tag{8.1.2}$$

[8.1] Such an interface constitution is considered in Chapter nine.

Equation (7.2.13) then reduces to

$$\begin{aligned}
&\tilde{r}(q) = qJ_i^{\frac{1}{2}}, \qquad q \in [0,s] \\
&\tilde{r}(q) = [s^2 J_i + (q^2 - s^2)J_m]^{\frac{1}{2}}, \quad q \in [s,Q] \\
&J_i = J_m + \Gamma \\
&f = \beta\mu\Gamma\left[2J_m - J_L - J_{min}\right] - \frac{\sigma}{s} \\
&\dot{s} = \hat{V}(f), \qquad \hat{V}(f)f \geq 0 \\
&J_i \in [J_{min}, J_L], \qquad J_m \in [J_U, J_{max}], \qquad s \in [0,q].
\end{aligned} \tag{8.1.3}$$

This implies that $\tilde{R}$, $\tilde{\tau}$, and $\tilde{\Pi}$, defined in Chapter seven, are unaffected by such an interfacial constitution, so that the macroscopic response region is unaffected as well.

The Maxwell curve, however, is significantly altered by the presence of interface bonding energy. The slope of the Maxwell curve may be expressed as a function of s and it is found that

$$\begin{aligned}
&\text{Slope}_{MW} < 0, \quad s^3 > \frac{\sigma Q^2}{4\beta\mu\Gamma^2} \\
&\text{Slope}_{MW} > 0, \quad s^3 < \frac{\sigma Q^2}{4\beta\mu\Gamma^2}.
\end{aligned} \tag{8.1.4}$$

Moreover, the Maxwell curve now intersects the top border of the response region rather than its left border, as is the case where no surface effects are present. The value of interface position, s, associated with this left end of the Maxwell curve is given by

$$s_{min}^{(mw)} := \frac{\sigma}{\beta\mu\Gamma(J_L - J_{min})}. \tag{8.1.5}$$

The presence of interface bonding energy therefore *precludes* the existence of a Maxwell state with interface position equal to zero. Moreover, embryos that are sufficiently small are unable to grow because of the dissipation inequality restriction on the sign of the growth rate. These results are illustrated in Figure 19. Equations (8.1.4) and (8.1.5) imply that a necessary and sufficient condition

for the Maxwell curve slope to change sign is that

$$\sigma < \frac{Q\beta\mu}{2}\Gamma^{\frac{1}{2}}(J_L - J_{min})^{\frac{3}{2}}. \tag{8.1.6}$$

Reference is often made to the *Gibbs free energy* in association with phase transitions. Within a purely mechanical context, the bulk stored energy, $\tilde{W}(\mathbf{F})$, coincides with the Helmholtz free energy of the material at a fixed temperature. The Gibbs function is then taken to be the Legendre transform,[8.2] G, of $\tilde{W}$ so that

$$G(\mathbf{F}) := \tilde{W}(\mathbf{F}) - \partial\tilde{W}(\mathbf{F}) \cdot \mathbf{F}. \tag{8.1.7}$$

Without surface fields, Equations $(3.3.4)_2$ and (3.5.4) imply that for hyperelastic materials involved in slow processes, a given state is Maxwell if and only if

$$[\![G]\!] = 0. \tag{8.1.8}$$

This is commonly referred to as the *Maxwell Rule* and is, in many cases, a necessary condition for the existence of two-phase equilibria.[8.3] Within the context of The Cylinder Problem, though, Maxwell states satisfy

$$\begin{aligned} [\![G]\!] &= -\left(\nabla_s \cdot \hat{\mathbf{C}}\right) \cdot \mathbf{n} \\ &= -\hat{\gamma}_2. \end{aligned} \tag{8.1.9}$$

For $\hat{\gamma}_2 \neq 0$, the Gibbs function must suffer a jump across phase interfaces under conditions of equilibrium—that is, under circumstances where the driving traction vanishes.[8.4] Maxwell states in the cylinder problem with bonding energy satisfy

$$[\![G]\!] = \frac{\sigma}{s}. \tag{8.1.10}$$

This result has a graphical interpretation on a plot of the stress response function, h. With no surface fields, the driving traction vanishes if and only if the areas,

---

8.2 SEWELL[1969].

8.3 See for instance, CALLEN[1960]; PIPPARD[1981]; JAMES[1981]; GURTIN[1983].

8.4 For related work regarding interfacial energy and the Maxwell Rule, see FONSECA[1989].

A_1 and A_2, of Figure 20(a) are equal, which occurs for $J_m = \frac{1}{2}(J_L + J_{min})$. With constant referential energy, however, the driving traction is a function of embryo size and

$$[A_1(s) - A_2(s)] = -\frac{\sigma}{2\mu s}. \tag{8.1.11}$$

This result is shown in Figure 20(b).

8.2 Nucleation with Bonding Energy. The nucleation criterion of Section 7.6 is now applied to link single- and two-phase states for the cylinder problem with interface bonding energy. Analogous to the case with no interfacial structure, it may be shown that the set, Γ, of two-phase states to which the cylinder can nucleate from a given single-phase dilatation is parameterizable by s. Therefore, there exists a function, $\tilde{B}(s, J_0)$, giving the nucleation energy with interfacial structure taken into account. By construction, $\tilde{B}(0, J_0) = 0$ and by Equation (7.5.2),

$$\partial_1 \tilde{B}(s, J_0) = -2\pi s f, \tag{8.2.1}$$

with f given by Equation $(8.1.3)_4$. As is the case with no surface fields,

$$\partial_2 \tilde{B}(s, J_0) < 0 \tag{8.2.2}$$

under all three types of loading, and this is proved in Appendix E. Finally, the surface energy increases B by $2\pi\sigma s$ over the case with no surface effects taken into account. Profiles of B are provided in Figure 21 for soft and hard loading. Note that for soft loading the surface energy forces the maximizing extremum to be associated with non-zero values of s. A manifestation of surface energy under hard loading is the presence of a new maximizing extremum associated with non-zero values of s. The mixed loading case may take on the qualitative features of either hard or soft loading, depending upon the magnitude of c—the loading parameter.

Consider how bonding energy affects the nucleation process under soft loading as shown in Figure 22. Under increasing boundary traction, the nucleation

barrier decreases, and a dilatation *may* eventually be reached for which the nucleation barrier is equal to B_0. If so, then a nucleation event occurs. Since the surface energy increases B by $2\pi\sigma s$, a higher value of dilatation is now required to initiate a nucleation event as compared to the case without surface effects. This is the mechanical analogue of the more classical supersaturating and supercooling phenomena attributed to surface properties in association with concentration- and temperature-induced transformations, respectively. This type of supercritical surface effect is therefore referred to as *superstraining* and is illustrated in Figures 22(c) and 23(c).

The effect of constant, referential surface energy on nucleation is even more interesting under hard loading as illustrated in Figure 23. As the cylinder boundary is extended, a maximizing and minimizing critical state pair develop. Through further extension, the associated nucleation barrier drops and *may* eventually decrease to B_0. If the nucleation energy associated with the larger minimizing critical state is non-dissipative, a nucleation event will occur. Otherwise, the cylinder extension must continue until both conditions are met. (This special case is illustrated in Figure 24.) Under such hard loading, nucleation events always require superstraining and are associated with embryos of finite size.

8.3 Embryo Stability. In Section 7.8 the stability of embryos was examined in the absence of surface effects, and the effect of bonding energy on this stability analysis is now considered. As may be seen by inspection of Figure 22(c), all embryos formed under soft loading are unstable, as was the case with no surface properties taken into account. Hard- and mixed-loaded embryos, however, are now unstable as well, as shown in Figure 23(d). Such nuclei either shrink and disappear, or grow out to the larger, stable, critical state. This is a key surface effect associated with the transformation process. The existence of such unstable nuclei has in fact been discussed by a number of authors.[8.5] Here the result is extended to continuum models of martensitic phase transformations, and unlike

[8.5] ULBRICHT, SCHMELZER, MAHNKE & SCHWEITZER[1988]; PIPPARD[1981].

the previous investigations, the current analysis is not restricted to only hard and soft loading.

9. THE CYLINDER PROBLEM: INTERFACES WITH A FLUID NATURE

9.1 Two-phase Solutions: Fluid-like Interfaces. Suppose that the interface is endowed with a constant value of surface energy, $\bar{\sigma}$, per unit *actual area.* By Part (C) of the Fluid-Surface Theorem of Chapter five,

$$\hat{\mathbf{C}} = 0, \qquad \hat{\mathbf{T}} = \bar{\sigma}\mathbf{1}_{\bar{s}}, \tag{9.1.1}$$

and the interface is said to have a fluid nature. This is an appropriate billing from two different perpectives. Taken alone, the surface displays unimodular symmetry and thus, as discussed in Chapter five, meets the interfacial-symmetry demands of a fluid. Secondly, this constitution implies the existence of a deformational surface tension equal in magnitude to the surface energy, which is a measured classical result for the surface of fluids. The interface properties modeled by a fluid-like interface induce a traction jump of magnitude $2H\bar{\sigma}$ in a direction normal to the interface, thus capturing the fluid surface effect focused on by the Gibbs-Thomson relation of Chapter one. Despite is fluid pedigree, this interface is often used in continuum models of martensitic phenomena.[9.1]

The macroscopic response is now constructed for such an interface constitution under the kinematic conditions and bulk constitution of The Cylinder Problem. The relevant system is summarized by Equation (7.2.13), where now Equations (7.2.9) and (7.2.11) give that

$$\hat{\gamma}_1 = -2H\bar{\sigma} = \frac{\bar{\sigma}}{s}, \qquad \hat{\gamma}_2 = 0. \tag{9.1.2}$$

[9.1] See, for instance, PORTER & EASTERLING[1981, Chapter 6]; THADHANI & MEYERS[1986]. Exceptions are ROITBURD[1990] and MULLER & XU[1991].

Equation (7.2.13) thus reduces to

$$\begin{aligned}
&\tilde{r}(q) = q J_i^{\frac{1}{2}}, \qquad q \in [0, s] \\
&\tilde{r}(q) = [s^2 J_i + (q^2 - s^2) J_m]^{\frac{1}{2}}, \quad q \in [s, Q] \\
&J_i = J_m + \Gamma - \frac{\bar{\sigma}}{2\mu\beta J_i^{\frac{1}{2}} s} \\
&f = -\beta\mu\left[J_m^2 - J_i^2 + \Gamma(J_U + J_L)\right] \\
&\dot{s} = \hat{V}(f), \qquad \hat{V}(f) f \geq 0 \\
&J_i \in [J_{min}, J_L], \qquad J_m \in [J_U, J_{max}], \qquad s \in [0, q].
\end{aligned} \tag{9.1.3}$$

Unlike the case of interface bonding energy, the presence of a constant, actual interface energy significantly affects the macroscopic response region. Equation (9.1.3) implies that there exist (J_m, s) parameterizations of all the possible (R, τ) pairs that the cylinder can support. The set of all (J_m, s) pairs consistent with the phase segregation constraints is denoted by $\breve{\Pi}$ and is constructed using

$$\breve{s}(J_i, J_m) := \frac{\bar{\sigma}}{2\mu\beta J_i^{\frac{1}{2}}(J_m - J_i + \Gamma)} \quad \forall \quad J_i \in [J_U, J_{max}], \; J_m \in [J_{min}, J_L] \tag{9.1.4}$$

and

$$\breve{J}_m(s) := J_{min} + \frac{\bar{\sigma}}{2\mu\beta J_U^{\frac{1}{2}} s} \qquad \forall s \in \left[\breve{s}(J_U, J_L), Q\right]. \tag{9.1.5}$$

Then

$$\breve{\Pi} := \left\{ (J_m, s) \middle| J_m \in \left(\breve{J}_m(s), J_L\right), \quad \forall s \in \left[\breve{s}(J_U, J_L), Q\right], \quad R \geq 1 \right\}. \tag{9.1.6}$$

This set of (J_m, s) pairs is exhibited in Figure 25, and its image under the following maps is the macroscopic response region sought:

$$\begin{aligned}
&\breve{R}(s, J_m) := \left[J_m(Q^2 - s^2) + s^2 \breve{J}_i(s, J_m)\right]^{\frac{1}{2}} \\
&\breve{\tau}(s, J_m) := 2\mu\left[\frac{Q}{\breve{R}(s, J_m)} + h(J_m)\right]
\end{aligned} \qquad \forall (s, J_m) \in \breve{\Pi}, \tag{9.1.7}$$

where $\breve{J}_i$ is defined on $\breve{\Pi}$ by

$$\breve{J}_i(\cdot, J_m) = \breve{s}^{-1}(\cdot, J_m).$$

It can be shown that

$$\begin{aligned} &\partial_1 \breve{R}(s, J_m) > 0 \\ &\partial_2 \breve{R}(s, J_m) > 0 \qquad \forall (s, J_m) \in \breve{\Pi}. \\ &\partial_1 \breve{\tau}(s, J_m) < 0 \end{aligned}$$

Moreover, provided that either

$$\bar{\sigma}^2 \leq (2\mu\beta Q)^2 J_U (J_L - J_{min})(2J_U - J_L + J_{min})(2\beta J_L - 1) \tag{9.1.9}$$

or

$$\beta \geq \frac{J_U}{J_L(2J_U - J_L + J_{min})} \tag{9.1.10}$$

is satisfied, then

$$\partial_2 \breve{\tau}(s, J_m) > 0, \quad \forall (s, J_m) \in \breve{\Pi}. \tag{9.1.11}$$

Thus, Equation (9.1.11) is met for sufficiently small values of surface energy, or independent of the surface energy magnitude, for materials with a stress response function, h, that has a sufficiently steep slope. Restricting attention to materials for which Equation (9.1.9) is satisfied is physically reasonable, since surface energy should generally represent a very small contribution to the system. However, Equation (9.1.10) is satisfied in most situations anyway, since $\beta \geq \frac{2}{3}$ by construction, and the righthand side of Equation (9.1.10) is always less than one. Attention is therefore restricted to constitutions for which Equation (9.1.11) is satisified.

The map of $\breve{\Pi}$ into the R, τ-plane is invertible, and its image, the macroscopic response region, is shown in Figure 26. The monotonicity of all curves depicted in the figure hold in general. A key surface effect associated with fluid-like interfaces is that the sets of single-phase solutions, also given in Figure 26, are disjoint from those involving two phases. This is due to the effect of a finite traction-jump on the phase segregation constraints and implies that the cylinder simply cannot support embryos that are too small. Such restrictions on nucleus size imposed by

the phase segregation constraints are an important feature of continuum models that characterize materials via a single, constitutive law. [9.2]

The Maxwell curve is affected in a manner similar to that associated with interface bonding energy, though here the construction is more complicated. Like the case of interface bonding energy, the slope of the Maxwell curve may change sign once at most and is guaranteed to do so for $\bar{\sigma}$ sufficiently small. Moreover, the Maxwell curve now intersects the top border of the response region rather than its left/bottom corner, as is the case when no surface effects are present. Figure 26 illustrates these results.

In Chapter eight it was shown that without surface fields a Maxwell state exists if and only if the Gibbs function is continuous across phase boundaries. From Equation (8.1.9) it is clear that this condition is also satisfied whenever $\hat{\gamma}_2 = 0$—a characteristic of interfaces that do not support an accretive stress. Since this is the case for fluid-like interfaces, $[\![G]\!] = 0$ for such systems. It is interesting to note that some classical thermodynamics texts take this to be a general result, independent of the interface constitution.[9.3] Here it is shown that $[\![G]\!] = 0$ for fluid-like interfaces only because they support no accretive stress. It is worth emphasizing that the existence of jumps in traction and jumps in the Gibbs function are unrelated—the former being associated with interface deformational stress, while the latter is a manifestation of interface accretive stress. The traction jump, though, does affect the slope of the Maxwell line connecting $\big(J_m, h(J_m)\big)$ with $\big(J_i, h(J_i)\big)$ at $f = 0$ with

$$\text{Maxwell Line Slope} = \frac{-\bar{\sigma}}{2\mu\Gamma\bar{s} - \bar{\sigma}} \quad < \quad 0. \tag{9.1.12}$$

This is illustrated in Figure 27.

9.2 Nucleation with Fluid-like Interfaces.

The nucleation criterion of Section 7.6 is now applied to the cylinder problem with a fluid-like interface. Once again it may be shown that there exists a function, $\tilde{B}(s, J_0)$, giving

[9.2] Rosakis[1991].

[9.3] Adkins[1968] p.213.

the nucleation energy, but now with the new type of surface structure taken into account. The following results, proved in Appendix E, hold for all three types of loading devices:

$$\begin{aligned} &\partial_1 \tilde{B}(s, J_0) = -2\pi s f \\ &\partial_2 \tilde{B}(s, J_0) < 0 \\ &\left.\frac{\partial B}{\partial \bar{\sigma}}\right|_{s, J_0} = 2\pi \bar{s}, \end{aligned} \tag{9.2.1}$$

for all (s, J_0) pairs where $\tilde{B}$ is defined.

Profiles of B are provided in Figure 28 for soft and hard loading. Though similar to those associated with constant bonding energy, these plots exhibit a non-zero lower bound on the size of embryo that may be nucleated. For materials with fluid-like interfaces, the nucleation process proceeds in the same manner as for materials with constant, referential surface energy despite the inability of the system to support a range of embryo sizes. The nucleation criterion suggested is thus robust enough to account for such phenomena. This is shown for soft and hard loading in Figures 29 and 30, respectively. By comparison of these plots with those of Figures 22(c) and 23(c), it is clear that fluid-like interfaces result in superstraining.

9.3 Embryo Stability. The stability of any embryo formed can be analyzed by the method developed in Chapter eight. As is clear by inspection of Figures 29 and 30, all embryos that form are unstable with growth either unbounded or tending towards an identifiable, larger, stable embryo configuration. Shrinkage, on the other hand, continues only to a finite nuclei size beyond which the embryo must collapse. This admits the interpretation that the final embryo demise occurs on a time scale much faster than the model is intended to capture.

10. THE CYLINDER PROBLEM: INTERFACES WITH A MEMBRANE NATURE

10.1 A Membrane-like Interface. The interface constitutions considered in Chapters eight and nine represent extremes. The interface with bonding energy generates only an accretive stress, while a deformational stress alone is supported by fluid-like interfaces. The stresses, moreover, are surface tensions in both cases. A final constitution is introduced in this chapter to illustrate a more complete set of surface properties that seem physically reasonable for solid-solid interfaces. Consider a hyperelastic interface characterized by the surface energy response function,

$$\hat{w}(i,j) = \hat{\mu}(i-1)^2 + \frac{1}{2}\hat{\nu}j^2, \qquad \hat{\mu},\hat{\nu} > 0, \tag{10.1.1}$$

with $\hat{w}$, i, and j as defined in Equations $(5.2.15)_1$ and (5.2.16). In the absence of interface deformation, $w = \hat{\mu} + \hat{\nu}/2 =: \hat{\eta}/2$, so that there is energy stored in the surface solely because it represents an interface between two dissimilar phases. It may be shown that $\hat{\mu}$ is the shear modulus associated with infinitesimal deformations of the interface, and that the interface bulk modulus is equal to $\hat{\mu} + \hat{\nu}$. The interface is thus capable of generating both shear and dilatational stresses, and with $\hat{\mu}, \hat{\nu} > 0$, satisfies physical intuition regarding its response to small deformations. It is reasonable to consider such a surface constitution, since interface fields are intended to account for the local interaction of bulk phases that themselves support both shear and dilatation. The restriction of Equations $(5.2.15)_{3,4}$ to the cylinder problem kinematics gives

$$\begin{aligned}
\hat{\mathbf{T}} &= \frac{1}{j}(\partial_1\hat{w})\hat{\mathbf{F}} + (\partial_2\hat{w})\mathbf{1}_{\bar{s}} \\
\hat{\mathbf{C}} &= \mathbf{I}\{(\partial_1\hat{w})\hat{\mathbf{F}} + (\hat{w} - j(\partial_2\hat{w})\mathbf{1}_s\} \\
\hat{\bar{\mathbf{C}}} &= \frac{1}{2j}\bar{\mathbf{I}}\{(\partial_1\hat{w})\hat{\mathbf{F}} + (\hat{w} - j(\partial_2\hat{w})\mathbf{1}_s\},
\end{aligned} \tag{10.1.2}$$

so that the interfacial stresses are not tensions for $\partial_1\hat{w} \neq 0$. For the membrane-like

interface, Equations (10.1.1) and (10.1.2) imply that

$$\begin{aligned}\hat{\mathbf{T}} =& 2\hat{\mu}(i-1)\hat{\mathbf{F}} + \hat{\nu} j \mathbf{1}_{\bar{s}} \\ \hat{\mathbf{C}} =& \mathbf{I}\left\{-2\hat{\mu}(i-1)\hat{\mathbf{F}} + \left[\hat{\mu}(i-1)^2 - \frac{\hat{\nu} j^2}{2}\right]\mathbf{1}_s\right\} \\ \hat{\tilde{\mathbf{C}}} =& \frac{1}{2j}\hat{\mathbf{C}},\end{aligned} \tag{10.1.3}$$

so that both interfacial stress fields are present, and even in this simple setting, are not in the form of surface tensions.

10.2 Macroscopic Response: Membrane-like Interfaces. The macroscopic response for the cylinder problem is now constructed for the membrane-like interface. The relevant system is summarized by Equation (7.2.13), where now Equations (7.2.9) and (7.2.11) give that

$$\hat{\gamma}_1 = \frac{\hat{\eta} J_i^{\frac{1}{2}}}{s}, \quad \hat{\gamma}_2 = \frac{\hat{\eta} J_i}{s}, \tag{10.2.1}$$

where the facts have been used that $i = j + 1$ and $J_i = j^2$ for this problem. Equation (7.2.13) thus reduces to

$$\begin{aligned}&\frac{\tilde{r}(q,t)\tilde{r}'(q,t)}{q} = J_i(t) \in [J_U, J_{max}), \quad q \in [0, s(t)) \\ &\frac{\tilde{r}(q,t)\tilde{r}'(q,t)}{q} = J_m(t) \in [J_{min}, J_L], \quad q \in [s(t), Q) \\ &J_i = J_m + \Gamma - \frac{\hat{\eta}}{2\mu\beta s} \\ &[\![\tilde{r}]\!] = 0, \qquad \tilde{r}(0,t) = 0 \\ &f = -\beta\mu\left[J_m^2 - J_i^2 + \Gamma(J_U + J_L)\right] + \frac{\hat{\eta} J_i}{2s} \\ &\dot{s} = \hat{V}(f), \qquad \hat{V}(f) f \geq 0 \\ &J_i \in [J_{min}, J_L], \qquad J_m \in [J_U, J_{max}], \qquad s \in [0, Q].\end{aligned} \tag{10.2.2}$$

This system is much easier to analyze than that associated with fluid interfaces because of the simple relation that exists among J_i, J_m, and s. This simplicity may be interpreted as being due to the endowment of the interface with solid

rather than fluid properties so that the surface deformation is more compatible with that of the bulk on either side. Equation $(10.2.2)_3$ manifests this result.

As was the case for fluid-like interfaces, the traction jump across the phase boundary significantly affects the macroscopic response of the cylinder. The construction of this response characterization is accomplished via the now familiar route of making (J_m, s) parameterizations of all the possible (R, τ) pairs that the cylinder can support. The set of all (J_m, s) pairs consistent with the phase segregation constraints, Equation $(10.2.1)_{7,8}$, is denoted by $\check{\Pi}$ and is constructed using

$$s_{min} := \frac{\hat{\eta}}{2\mu\beta(J_L - J_{min})} \tag{10.2.3}$$

and

$$\check{J}_m(s) := J_{min} + \frac{\hat{\eta}}{2\mu\beta s} \quad \forall s \in [s_{min}, 1]. \tag{10.2.4}$$

Then

$$\check{\Pi} := \left\{ (J_m, s) \middle| J_m \in \left(\check{J}_m(s), J_L\right), \quad \forall s \in [s_{min}, Q], \quad R \geq Q \right\}. \tag{10.2.5}$$

This set is qualitatively the same as its fluid interface counterpart, exhibited in Figure 25. Its image under the following maps is the macroscopic response region sought:

$$\begin{aligned} \check{R}(s, J_m) &:= \left[J_m(Q^2 - s^2) + s^2 \check{J}_i(s, J_m)\right]^{\frac{1}{2}} \\ \check{\tau}(s, J_m) &:= 2\mu\left[\frac{Q}{\check{R}(s, J_m)} + h(J_m)\right] \end{aligned} \qquad \forall (s, J_m) \in \check{\Pi}, \tag{10.2.6}$$

where

$$\check{J}_i(s, J_m) := J_m + \Gamma - \frac{\hat{\eta}}{2\mu\beta s}. \tag{10.2.7}$$

It can be shown that

$$\begin{aligned} &\partial_1 \check{R}(s, J_m) > 0 \\ &\partial_2 \check{R}(s, J_m) > 0 \\ &\partial_1 \check{\tau}(s, J_m) < 0 \\ &\partial_2 \check{\tau}(s, J_m) > 0 \end{aligned} \qquad \forall (s, J_m) \in \check{\Pi}. \tag{10.2.8}$$

Note that unlike the fluid interface case, no restrictions need be placed on the surface energy magnitude in order to guarantee these inequalities.

The map of $\check{\Pi}$ into the R, τ-plane is invertible, and its image is qualitatively the same as that of the fluid-like interface. It is straightforward to show that the Maxwell curve changes slope once at most and is guaranteed to do so for $\hat{\eta}$ sufficiently small. Thus, the macroscopic response associated with the fluid-like and membrane-like interfaces are qualitatively the same with the exception of the restrictions mentioned above. Superstraining, nucleation, and embryo stability are therefore similar.

11. CONCLUDING REMARKS

A model for martensitic phase transformations has been presented that captures a number of important surface effects. A set of physically reasonable postulates laid the groundwork for this theory from which field equations and jump conditions were derived. Attention was then restricted to hyperelastic materials, and an Interface Representation Theorem was developed in association with isotropic bodies. This result was used to characterize a number of physically meaningful interfaces. An energy barrier nucleation criterion was suggested, which models martensitic nucleation events as temporal shocks that are global in spatial extent.

A major objective of the investigation was to examine the relationship between interface properties and surface effects, and this was accomplished via special examples. Four interface constitutions were examined in conjunction with Two-phase, Linearly Dilative materials: interfaces with no surface fields; interfaces with bonding energy; fluid-like interfaces; and membrane-like interfaces. The interface with bonding energy manifests itself in a purely accretive surface tension, while the fluid-like interface generates the opposite extreme—a purely deformational surface tension. The interface with membrane-like features is the most general of the four since it supports both accretive and deformational stresses, with neither in the form of a simple, surface tension. This interface reacts under infinitesimal surface deformations as would a two-dimensional, linear, elastic solid.

It was found that all three non-trivial interface constitutions cause the surface effect of superstraining, whereas a traction jump exists only for the fluid-like and membrane-like interfaces. The Maxwell Rule (continuity of the Gibbs function) is violated for interfaces with bonding energy and membrane-like surfaces. All three types of interfaces imply that any nuclei that form must be of finite size and it was found that sufficiently small nuclei cannot be supported by fluid-like and membrane-like interfaces. This last result is due to the phase segregation constraints. Finally, it was determined that materials with any of the three

non-trivial, interface constitutions support a new, unstable, critical nucleus in association with both hard and mixed loading.

In order to facilitate the investigation of surface effects, a concept of nucleation energy was introduced. All cases considered were found to allow this energy to be described as a function of prenucleation dilatation and referential embryo size. Significantly, the nucleation energy decreases with increasing dilatation, and its extrema, with respect to variations in embryo size, identify the system Maxwell states. For all interface constitutions considered, the nucleation energy increases with the magnitude of surface energy.

Future investigations in this area should proceed on two fronts, with the first being a consideration of surface fields in transformations induced by a combination of both shear and dilatation. This is a more realistic model of most martensitic phenomena. As a first step towards this, it would be helpful to study the effect of interface bonding energy on an anti-plane shear idealization of martensitic phase transformations. Because bonding energy does not induce a traction jump, the anti-plane shear kinematics does not pose an unbalanced force problem.

The second major front on which the present research could be extended is numerical implementations of the model, where less idealized problem settings could be considered. This would allow for direct comparison with experimental data as a means of developing practical characterizations of the interface between martensitic phases. Areas of particular interest are: heterogeneous nucleation; the effect of surface properties on nucleation shape and not just size; and the competition between new embryo nucleation and existing embryo growth.

APPENDIX A. GALILEAN OBJECTIVITY

Consider the admissible, two-phase motions, $\mathcal{X}_{\mathcal{T}}$ and $\mathcal{X}^*_{\mathcal{T}}$, of a latticed body, $\{\mathcal{B},\mathcal{L}\}$, with

$$\mathcal{X}^*(t) = \mathbf{Q}\mathcal{X}(t) + \mathbf{d}t + \mathbf{e} \quad \forall t \in \mathcal{T}, \tag{A.1}$$

where

$$\mathbf{Q} \in \mathrm{Orth}_+(\mathbb{E}^3,\mathbb{E}^3), \qquad \mathbf{d},\mathbf{e} \in \mathbb{E}^3.$$

Let

$$\begin{aligned}
\phi:&\quad (\bar{\mathcal{R}}_{\mathcal{T}} \setminus \bar{\mathcal{S}}_{\mathcal{T}}) \to \mathbb{R}_+\\
\mathbf{A}:&\quad (\bar{\mathcal{R}}_{\mathcal{T}} \setminus \bar{\mathcal{S}}_{\mathcal{T}}) \to \mathrm{Lin}(\mathbb{E}^3,\mathbb{E}^3)\\
\hat{\phi}:&\quad \bar{\mathcal{S}}_{\mathcal{T}} \to \mathbb{R}_+\\
\hat{\mathbf{A}}:&\quad (\mathbf{y},t) \in \bar{\mathcal{S}}_{\mathcal{T}} \mapsto \hat{\mathbf{A}}(\mathbf{y},t) \in \mathrm{Lin}\big(\bar{\mathbf{n}}^{\perp}(\mathbf{y},t),\mathbb{E}^3\big)
\end{aligned} \tag{A.2}$$

be fields associated with $\{\mathcal{B},\mathcal{L}\}$ during motion $\mathcal{X}_{\mathcal{T}}$, with $\bar{\mathcal{R}}_{\mathcal{T}}$ and $\bar{\mathcal{S}}_{\mathcal{T}}$ as defined in Section 3.1. Let

$$\begin{aligned}
\phi^*:&\quad (\bar{\mathcal{R}}^*_{\mathcal{T}} \setminus \bar{\mathcal{S}}^*_{\mathcal{T}}) \to \mathbb{R}_+\\
\mathbf{A}^*:&\quad (\bar{\mathcal{R}}^*_{\mathcal{T}} \setminus \bar{\mathcal{S}}^*_{\mathcal{T}}) \to \mathrm{Lin}(\mathbb{E}^3,\mathbb{E}^3)\\
\hat{\phi}^*:&\quad \bar{\mathcal{S}}^*_{\mathcal{T}} \to \mathbb{R}_+\\
\hat{\mathbf{A}}^*:&\quad (\mathbf{y},t) \in \bar{\mathcal{S}}^*_{\mathcal{T}} \mapsto \hat{\mathbf{A}}^*(\mathbf{y},t) \in \mathrm{Lin}\big(\bar{\mathbf{n}}^{\perp}(\mathbf{y},t),\mathbb{E}^3\big)
\end{aligned} \tag{A.3}$$

be the analogous fields of $\{\mathcal{B},\mathcal{L}\}$ during motion $\mathcal{X}^*_{\mathcal{T}}$.

The fields associated with $\{\mathcal{B},\mathcal{L}\}$ are said to exhibit *Galilean Objectivity* if

$$\begin{aligned}
\hat{\phi}^*\big(\mathbf{z}^*(\mathbf{y},t),t\big) &= \hat{\phi}(\mathbf{y},t)\\
\hat{\mathbf{A}}^*\big(\mathbf{z}^*(\mathbf{y},t),t\big) &= \mathbf{Q}\hat{\mathbf{A}}(\mathbf{y},t)\mathbf{Q}^T
\end{aligned} \qquad \forall (\mathbf{y},t) \in \bar{\mathcal{R}}_{\mathcal{T}} \setminus \bar{\mathcal{S}}_{\mathcal{T}} \tag{A.4}$$

and

$$\begin{aligned}
\phi^*\big(\mathbf{z}^*(\mathbf{y},t),t\big) &= \phi(\mathbf{y},t)\\
\mathbf{A}^*\big(\mathbf{z}^*(\mathbf{y},t),t\big) &= \mathbf{Q}\mathbf{A}(\mathbf{y},t)\mathbf{Q}^T
\end{aligned} \qquad \forall (\mathbf{y},t) \in \bar{\mathcal{S}}_{\mathcal{T}}, \tag{A.5}$$

where

$$\mathbf{z}^*(\mathbf{y},t) := \mathbf{Q}\mathbf{y} + \mathbf{d}t + \mathbf{e} \quad \forall (\mathbf{y},t) \in \bar{\mathcal{R}}_{\mathcal{T}}. \tag{A.6}$$

APPENDIX B. INVARIANCE LEMMA

Let

$$e: \quad (\mathcal{R}_T \setminus \mathcal{S}_T) \to \mathbb{R}$$

$$f: \quad \mathcal{S}_T \to \mathbb{R}$$

$$g: \quad \mathcal{S}_T \to \mathbb{R},$$

and suppose that

$$\int_{\mathcal{P}} e\, dV + \int_{\mathcal{Q}(t)} f\, dA + \int_{\partial\mathcal{Q}(t)} g V_m\, dL \leq 0 \quad \forall \mathcal{P} \subset \mathcal{R}, \quad \forall t \in \mathcal{T}.$$

Then $g = 0$ on $\mathcal{S}_T$.

This is proved in GURTIN & STRUTHERS[1990].

APPENDIX C. INTERFACE REPRESENTATION FOR ISOTROPIC, HYPERELASTIC MATERIALS

C.1 Proof of the Representation Theorem for Superficial, Isotropic, Scalar Functions.

Lemma 1:

$(\zeta_1, \zeta_2) \in I\!R^2_+$ coincide, respectively, with $i(\hat{\mathbf{A}}), j(\hat{\mathbf{A}})$ of $\hat{\mathbf{A}} \in \mathrm{Sym}^+(\mathbf{n}^\perp)$ if and only if $(\zeta_1, \zeta_2) \in \hat{\mathcal{I}}$, with $\hat{\mathcal{I}}$ as defined in Equation (5.2.9).

Proof: (Neccessity)

Suppose $\hat{\mathbf{A}} \in \mathrm{Sym}^+(\mathbf{n}^\perp)$. Then $\hat{\mathbf{A}}$ has two real positive eigenvalues, $\hat{\lambda}$, satisfying the characteristic equation

$$p(\hat{\lambda}) = -\hat{\lambda}^2 + i(\hat{\mathbf{A}})\hat{\lambda} - j(\hat{\mathbf{A}}) = 0.$$

Application of the quadratic formula then reveals that $(i(\hat{\mathbf{A}}), j(\hat{\mathbf{A}})) \in \hat{\mathcal{I}}$.

Proof: (Sufficiency)

Suppose $(\zeta_1, \zeta_2) \in \hat{\mathcal{I}}$. Then

$$-\hat{\lambda}^2 + \zeta_1\hat{\lambda} - \zeta_2 = 0$$

has two positive roots, λ_1, λ_2, such that $\zeta_1 = \lambda_1 + \lambda_2$ and $\zeta_2 = \lambda_1\lambda_2$. The component representation of $\hat{\mathbf{A}}$ in its principal, rectilinear, Cartesian coordinate basis is thus given by

$$[\hat{\mathbf{A}}] = \begin{bmatrix} \lambda_1 & 0 \\ 0 & \lambda_2 \end{bmatrix}.$$

Clearly, $i(\hat{\mathbf{A}}) = \zeta_1$ and $j(\hat{\mathbf{A}}) = \zeta_2$.

Lemma 2:

Let $\hat{\mathbf{A}}, \hat{\mathbf{B}} \in \mathrm{Sym}^+(\mathbf{n}^\perp)$. Then $i(\hat{\mathbf{A}}) = i(\hat{\mathbf{B}})$, $j(\hat{\mathbf{A}}) = j(\hat{\mathbf{B}})$ if and only if there exists a $\hat{\mathbf{Q}} \in \mathrm{Orth}_+(\mathbf{n}^\perp, \mathbf{n}^\perp)$, such that $\hat{\mathbf{B}} = \hat{\mathbf{Q}}^T\hat{\mathbf{A}}\hat{\mathbf{Q}}$.

Proof: (Sufficiency)

Suppose $\hat{\mathbf{B}} = \hat{\mathbf{Q}}^T\hat{\mathbf{A}}\hat{\mathbf{Q}}$, $\hat{\mathbf{Q}} \in \mathrm{Orth}_+(\mathbf{n}^\perp, \mathbf{n}^\perp)$. Then

$$\begin{aligned} i(\hat{\mathbf{B}}) &= \langle \hat{\mathbf{B}}, \mathbf{1}_s \rangle = \langle \hat{\mathbf{Q}}^T\hat{\mathbf{A}}\hat{\mathbf{Q}}, \mathbf{1}_s \rangle \\ &= \langle \hat{\mathbf{A}}, \hat{\mathbf{Q}}\hat{\mathbf{Q}}^T \rangle = \langle \hat{\mathbf{A}}, \mathbf{1}_s \rangle = i(\hat{\mathbf{A}}). \end{aligned}$$

Also,

$$j(\hat{\mathbf{B}}) = j(\hat{\mathbf{Q}}^T\hat{\mathbf{A}}\hat{\mathbf{Q}}) = j(\hat{\mathbf{Q}}^T)j(\hat{\mathbf{A}})j(\hat{\mathbf{Q}}) = j(\hat{\mathbf{A}}).$$

Proof: (Necessity)

Suppose $i(\hat{\mathbf{A}}) = i(\hat{\mathbf{B}})$ and $j(\hat{\mathbf{A}}) = j(\hat{\mathbf{B}})$. Then the eigenvalues of $\hat{\mathbf{A}}$ and $\hat{\mathbf{B}}$ coincide since they are both given by the characteristic polynomial

$$-\hat{\lambda}^2 + i\hat{\lambda} - j = 0.$$

Let $\{\mathbf{e}_1, \mathbf{e}_2\}$ and $\{\mathbf{e}'_1, \mathbf{e}'_2\}$ be the associated principal bases for $\hat{\mathbf{A}}$ and $\hat{\mathbf{B}}$, respectively. Then there exists a $\hat{\mathbf{Q}} \in \mathrm{Orth}_+(\mathbf{n}^\perp, \mathbf{n}^\perp)$, such that $\hat{\mathbf{Q}}\mathbf{e}'_\alpha = \mathbf{e}_\alpha, \quad \alpha = 1, 2.$ Thus ,

$$\hat{\mathbf{B}}\mathbf{e}'_\alpha = \lambda_\alpha \mathbf{e}'_\alpha = \lambda_\alpha \hat{\mathbf{Q}}^T\mathbf{e}_\alpha = \hat{\mathbf{Q}}^T\hat{\mathbf{A}}\mathbf{e}_\alpha = \hat{\mathbf{Q}}^T\hat{\mathbf{A}}\hat{\mathbf{Q}}\mathbf{e}'_\alpha, \quad \alpha = 1, 2,$$

implying that $\hat{\mathbf{B}} = \hat{\mathbf{Q}}^T\hat{\mathbf{A}}\hat{\mathbf{Q}}$.

Proof of the Theorem: (Sufficiency)

Suppose there exists a function $\tilde{\phi} : \hat{\mathcal{I}} \times \mathrm{Unit}(\mathbb{E}^3) \to \mathbb{R}$ such that

$$\phi(\hat{\mathbf{U}}, \mathbf{n}) = \tilde{\phi}\big(i(\hat{\mathbf{U}}), j(\hat{\mathbf{U}}), \mathbf{n}\big) \quad \forall\, \hat{\mathbf{U}} \in \mathrm{Sym}^+(\mathbf{n}^\perp), \quad \forall\, \mathbf{n} \in \mathrm{Unit}(\mathbb{E}^3).$$

Then by Lemma 2,

$$\begin{aligned} \phi(\hat{\mathbf{U}}, \mathbf{n}) &= \tilde{\phi}\big(i(\hat{\mathbf{Q}}^T\hat{\mathbf{U}}\hat{\mathbf{Q}}), j(\hat{\mathbf{Q}}^T\hat{\mathbf{U}}\hat{\mathbf{Q}}), \mathbf{n}\big) \\ &= \phi(\hat{\mathbf{Q}}^T\hat{\mathbf{U}}\hat{\mathbf{Q}}, \mathbf{n}) \quad \forall\, \hat{\mathbf{Q}} \in \mathrm{Orth}_+(\mathbf{n}^\perp, \mathbf{n}^\perp). \end{aligned}$$

Therefore, ϕ is a superficial, isotropic, scalar function.

Proof of the Theorem: (Necessity)

Suppose ϕ is a superficial, isotropic, scalar function. Then by Lemmas 1 and 2 there exists a single-valued function, $\tilde{\phi} : \hat{\mathcal{I}} \times \text{Unit}(\mathbb{E}^3) \to \mathbb{R}$, such that

$$\phi(\hat{\mathbf{U}}, \mathbf{n}) = \tilde{\phi}(i(\hat{\mathbf{U}}), j(\hat{\mathbf{U}}), \mathbf{n}) \quad \forall \hat{\mathbf{U}} \in \text{Sym}^+(\mathbf{n}^\perp), \quad \forall \mathbf{n} \in \text{Unit}(\mathbb{E}^3).$$

C.2 Characterization of Interface Energy via a Superficial, Isotropic, Scalar Function for Isotropic, Hyperelastic Materials.

Claim 2.1:

With $\breve{w}$ as defined by Equation $(4.1.17)_1$, Galilean objectivity implies that

$$\breve{w}(\mathbf{FI}, \mathbf{n}) = \breve{w}(\mathbf{I}\hat{\mathbf{U}}, \mathbf{n}) \quad \forall \mathbf{F} \in \text{Lin}_+(\mathbb{E}^3, \mathbb{E}^3), \quad \forall \mathbf{n} \in \text{Unit}(\mathbb{E}^3),$$

with $\mathbf{I}$ the inclusion map associated with $\mathbf{n}^\perp$.

Here

$$\hat{\mathbf{U}} = (\mathbb{F}^T \mathbb{F})^{1/2} = (\hat{\mathbf{F}}^T \hat{\mathbf{F}})^{1/2},$$

with $\mathbb{F}$ and $\hat{\mathbf{F}}$ defined as in Section 2.5.

Proof:

Galilean objectivity implies that

$$\breve{w}(\mathbf{QFI}, \mathbf{n}) = \breve{w}(\mathbf{FI}, \mathbf{n}) \quad \forall \mathbf{Q} \in \text{Orth}_+(\mathbb{E}^3, \mathbb{E}^3), \quad \forall \mathbf{F} \in \text{Lin}_+(\mathbb{E}^3, \mathbb{E}^3),$$
$$\forall \mathbf{n} \in \text{Unit}(\mathbb{E}^3).$$

By the Polar Decomposition Theorem, there exists unique

$$\hat{\mathbf{U}} \in \text{Sym}^+(\mathbf{n}^\perp), \quad \hat{\mathbf{Q}} \in \text{Orth}_+(\mathbf{n}^\perp, \mathbf{n}^\perp),$$

such that $\hat{\mathbf{F}} = \hat{\mathbf{Q}}\hat{\mathbf{U}}$ for every $\hat{\mathbf{F}} \in \text{Lin}_+(\mathbf{n}^\perp, \bar{\mathbf{n}}^\perp)$.

Consider a particular linear transformation

$$\mathbf{Q} = \mathbf{I}\hat{\mathbf{Q}}^T\bar{\mathbf{P}} + \mathbf{n} \otimes \bar{\mathbf{n}}.$$

Note that this $\mathbf{Q}$ is in $\mathrm{Orth}_+(\mathbb{E}^3, \mathbb{E}^3)$ since

$$\begin{aligned}\mathbf{Q}\mathbf{Q}^T &= (\mathbf{I}\hat{\mathbf{Q}}^T\bar{\mathbf{P}} + \mathbf{n}\otimes\bar{\mathbf{n}})(\bar{\mathbf{I}}\hat{\mathbf{Q}}\mathbf{P} + \bar{\mathbf{n}}\otimes\mathbf{n})\\ &= \mathbf{I}\hat{\mathbf{Q}}^T\bar{\mathbf{P}}\bar{\mathbf{I}}\hat{\mathbf{Q}}\mathbf{P} + \mathbf{I}\hat{\mathbf{Q}}^T\bar{\mathbf{P}}\bar{\mathbf{n}}\otimes\mathbf{n} + (\mathbf{n}\otimes\bar{\mathbf{n}})\bar{\mathbf{I}}\hat{\mathbf{Q}}\mathbf{P} + (\mathbf{n}\otimes\bar{\mathbf{n}})(\bar{\mathbf{n}}\otimes\mathbf{n})\\ &= \mathbf{I}\hat{\mathbf{Q}}^T\mathbf{1}_{\bar{s}}\hat{\mathbf{Q}}\mathbf{P} + \mathbf{n}\otimes\mathbf{n}\\ &= \mathbf{I}\hat{\mathbf{Q}}^T\hat{\mathbf{Q}}\mathbf{P} + \mathbf{n}\otimes\mathbf{n} = \mathbf{I}\mathbf{P} + \mathbf{n}\otimes\mathbf{n} = \mathbf{1}.\end{aligned}$$

For this choice of $\mathbf{Q}$,

$$\begin{aligned}\mathbf{Q}\mathbf{F}\mathbf{I} = \mathbf{Q}\bar{\mathbf{I}}\hat{\mathbf{F}} = \mathbf{Q}\bar{\mathbf{I}}\hat{\mathbf{Q}}\hat{\mathbf{U}} &= (\mathbf{I}\hat{\mathbf{Q}}^T\bar{\mathbf{P}} + \mathbf{n}\otimes\bar{\mathbf{n}})\bar{\mathbf{I}}\hat{\mathbf{Q}}\hat{\mathbf{U}}\\ &= \mathbf{I}\hat{\mathbf{Q}}^T\bar{\mathbf{P}}\bar{\mathbf{I}}\hat{\mathbf{Q}}\hat{\mathbf{U}} + (\mathbf{n}\otimes\bar{\mathbf{n}})\bar{\mathbf{I}}\hat{\mathbf{Q}}\hat{\mathbf{U}} = \mathbf{I}\hat{\mathbf{Q}}^T\mathbf{1}_{\bar{s}}\hat{\mathbf{Q}}\hat{\mathbf{U}} = \mathbf{I}\hat{\mathbf{U}}.\end{aligned}$$

Thus, Galilean objectivity implies that $\breve{w}(\mathbf{F}\mathbf{I}, \mathbf{n}) = \breve{w}(\mathbf{I}\hat{\mathbf{U}}, \mathbf{n})$ as claimed.

Claim 2.2:

Galilean objectivity implies that

$$\breve{w}(\mathbf{I}\hat{\mathbf{Q}}\hat{\mathbf{U}}, \mathbf{n}) = \breve{w}(\mathbf{I}\hat{\mathbf{U}}, \mathbf{n}) \quad \forall\,\mathbf{n}\in\mathrm{Unit}(\mathbb{E}^3), \quad \forall\,\hat{\mathbf{U}}\in\mathrm{Sym}^+(\mathbf{n}^\perp) \quad \forall\,\hat{\mathbf{Q}}\in\mathrm{Orth}_+(\mathbf{n}^\perp, \mathbf{n}^\perp).$$

Proof:

By definition, Galilean objectivity implies that $\tilde{w}(\mathbf{Q}\mathbf{F}, \mathbf{n}) = \tilde{w}(\mathbf{F}, \mathbf{n})$. Thus,

$$\breve{w}(\mathbf{F}\mathbf{I}, \mathbf{n}) = \breve{w}(\mathbf{Q}\mathbf{F}\mathbf{I}, \mathbf{n}). \tag{C.2.1}$$

Now suppose that $\mathbf{Q} := \mathbf{I}\hat{\mathbf{Q}}\mathbf{P} + \mathbf{n}\otimes\mathbf{n}$ with $\hat{\mathbf{Q}}\in\mathrm{Orth}_+(\mathbf{n}^\perp, \mathbf{n}^\perp)$. Then $\mathbf{Q}^T\mathbf{Q} = 1$ and $\hat{\mathbf{Q}} = \mathbf{P}\mathbf{Q}\mathbf{I}$. From Claim 2.1 and Equation (C.2.1),

$$\breve{w}(\mathbf{F}\mathbf{I}, \mathbf{n}) = \breve{w}(\mathbf{I}\hat{\mathbf{U}}, \mathbf{n}) = \breve{w}(\mathbf{Q}\mathbf{I}\hat{\mathbf{U}}, \mathbf{n}). \tag{C.2.2}$$

But for the $\mathbf{Q}$ chosen,

$$\mathbf{Q}\mathbf{I}\hat{\mathbf{U}} = (\mathbf{I}\hat{\mathbf{Q}}\mathbf{P} + \mathbf{n}\otimes\mathbf{n})\mathbf{I}\hat{\mathbf{U}} = \mathbf{I}\hat{\mathbf{Q}}\mathbf{P}\mathbf{I}\hat{\mathbf{U}} = \mathbf{I}\hat{\mathbf{Q}}\hat{\mathbf{U}}. \tag{C.2.3}$$

Equations (C.2.2) and (C.2.3) together imply that

$$\breve{w}(\mathbf{I}\hat{\mathbf{Q}}\hat{\mathbf{U}}, \mathbf{n}) = \breve{w}(\mathbf{I}\hat{\mathbf{U}}, \mathbf{n}) \quad \forall\,\mathbf{n}\in\mathrm{Unit}(\mathbb{E}^3), \quad \forall\,\hat{\mathbf{U}}\in\mathrm{Sym}^+(\mathbf{n}^\perp) \quad \forall\,\hat{\mathbf{Q}}\in\mathrm{Orth}_+(\mathbf{n}^\perp, \mathbf{n}^\perp).$$

Claim 2.3: Material isotropy implies that

$$\breve{w}(\mathbf{I}\hat{\mathbf{U}}, \mathbf{n}) = \breve{w}(\mathbf{I}\hat{\mathbf{U}}\hat{\mathbf{Q}}, \mathbf{n}) \quad \forall \mathbf{n} \in \mathrm{Unit}(\mathbb{E}^3), \quad \forall \hat{\mathbf{U}} \in \mathrm{Sym}^+(\mathbf{n}^\perp), \quad \forall \hat{\mathbf{Q}} \in \mathrm{Orth}_+(\mathbf{n}^\perp, \mathbf{n}^\perp).$$

Proof:

By definition, material isotropy implies that

$$\tilde{w}(\mathbf{FQ}, \mathbf{Q}^T\mathbf{n}) = \tilde{w}(\mathbf{F}, \mathbf{n}) \quad \forall \mathbf{F} \in \mathrm{Lin}_+(\mathbb{E}^3, \mathbb{E}^3), \quad \forall \mathbf{n} \in \mathrm{Unit}(\mathbb{E}^3), \quad \forall \mathbf{Q} \in \mathrm{Orth}_+(\mathbb{E}^3, \mathbb{E}^3). \tag{C.2.4}$$

Choose $\mathbf{Q} := \mathbf{I}\hat{\mathbf{Q}}\mathbf{P} + \mathbf{n} \otimes \mathbf{n}$, as in the previous claim, and note that

$$\mathbf{Q}^T\mathbf{n} = (\mathbf{I}\hat{\mathbf{Q}}^T\mathbf{P} + \mathbf{n} \otimes \mathbf{n})\mathbf{n} = \mathbf{n}.$$

Thus, isotropy implies that $\tilde{w}(\mathbf{FQ}, \mathbf{n}) = \tilde{w}(\mathbf{F}, \mathbf{n})$ for such a $\mathbf{Q}$ which, by the construction of $\breve{w}$ in Equation (4.1.7), gives that

$$\breve{w}(\mathbf{FI}, \mathbf{n}) = \breve{w}(\mathbf{FQI}, \mathbf{n}). \tag{C.2.5}$$

But

$$\mathbf{FQI} = \mathbf{F}(\mathbf{I}\hat{\mathbf{Q}}\mathbf{P} + \mathbf{n} \otimes \mathbf{n})\mathbf{I} = \mathbf{FI}\hat{\mathbf{Q}}\mathbf{PI} = \mathbf{FI}\hat{\mathbf{Q}}.$$

Equation (C.2.5) can thus be written as

$$\breve{w}(\mathbb{F}, \mathbf{n}) = \breve{w}(\mathbb{F}\hat{\mathbf{Q}}, \mathbf{n}), \tag{C.2.6}$$

and this holds for every $\mathbb{F} \in \mathrm{Lin}^{NS}(\mathbf{n}^\perp, \mathbb{E}^3)$, $\mathbf{n} \in \mathrm{Unit}(\mathbb{E}^3)$, $\hat{\mathbf{Q}} \in \mathrm{Orth}_+(\mathbf{n}^\perp, \mathbf{n}^\perp)$. Since $\mathbf{I}\hat{\mathbf{U}} \in \mathrm{Lin}^{NS}(\mathbf{n}^\perp, \mathbb{E}^3)$, Equation (C.2.6) implies that

$$\breve{w}(\mathbf{I}\hat{\mathbf{U}}, \mathbf{n}) = \breve{w}(\mathbf{I}\hat{\mathbf{U}}\hat{\mathbf{Q}}, \mathbf{n}) \quad \forall \mathbf{n} \in \mathrm{Unit}(\mathbb{E}^3), \quad \forall \hat{\mathbf{U}} \in \mathrm{Sym}^+(\mathbf{n}^\perp), \quad \forall \hat{\mathbf{Q}} \in \mathrm{Orth}_+(\mathbf{n}^\perp, \mathbf{n}^\perp).$$

Claim 2.4:

For isotropic, hyperelastic materials the referential interface energy can be represented by a superficial isotropic response function,

$$\check{w}(\cdot, \mathbf{n}) : \mathrm{Sym}^+(\mathbf{n}^\perp) \to I\!R, \quad \forall \mathbf{n} \in \mathrm{Unit}(I\!E^3).$$

Proof:

Claim 2.1 and the fact that the inclusion map, $\mathbf{I}$, is determined solely by the unit normal, $\mathbf{n}$, admits construction of a function

$$\check{w}(\cdot, \mathbf{n}) : \mathrm{Sym}^+(\mathbf{n}^\perp) \to I\!R, \quad \forall \mathbf{n} \in \mathrm{Unit}(I\!E^3),$$

such that $\check{w}(\mathbf{I}\hat{\mathbf{U}}, \mathbf{n}) = \check{w}(\hat{\mathbf{U}}, \mathbf{n})$. Then Claims 2.2 and 2.3 combine to imply that $\check{w}$ is a superficial, isotropic, scalar function.

C.3 Proof of the Interface Representation Theorem.

Claim 3.1:

For isotropic, hyperelastic materials the referential interface energy can be represented by a function

$$\hat{w} : \hat{\mathcal{I}} \times \mathrm{Unit}(I\!E^3) \to I\!R,$$

such that

$$\hat{w}\big(i(\hat{\mathbf{U}}), j(\hat{\mathbf{U}}), \mathbf{n}\big) = \check{w}(\hat{\mathbf{U}}, \mathbf{n}) \quad \forall \hat{\mathbf{U}} \in \mathrm{Sym}^+(\mathbf{n}^\perp), \quad \forall \mathbf{n} \in \mathrm{Unit}(I\!E^3).$$

This is immediate from the Representation Theorem for Superficial, Isotropic, Scalar Functions and Claim 2.4.

Claim 3.2:

Let $\mathbf{F}^* = \mathbf{F}\mathbf{Q}$, $\mathbf{n}^* = \mathbf{Q}^T\mathbf{n}$, and $\mathbf{I}^* = \mathbf{Q}^T\mathbf{I}\mathbf{Q}$, with $\mathbf{F} \in \mathrm{Lin}_+(I\!E^3, I\!E^3)$, $\mathbf{n} \in \mathrm{Unit}(I\!E^3)$, $\mathbf{Q} \in \mathrm{Orth}_+(I\!E^3, I\!E^3)$, and $\mathbf{I}$ the inclusion map for $\mathbf{n}^\perp$. Let

$$\hat{\mathbf{U}} = \left[(\mathbf{F}^*\mathbf{I}^*)^T(\mathbf{F}^*\mathbf{I}^*)\right]^{1/2}$$
$$\hat{\mathbf{U}}^* = \left[(\mathbf{F}\mathbf{I})^T(\mathbf{F}\mathbf{I})\right]^{1/2}.$$

Then $\hat{\mathbf{U}}$ and $\hat{\mathbf{U}}^*$ have the same trace and determinant.

Proof: (Determinant)

$$\begin{aligned} j^2(\hat{\mathbf{U}}^*) &= j\big(\mathbf{P}^*(\mathbf{F}^{*T}\mathbf{F}^*\mathbf{I}^*\big) = j(\mathbf{Q}^T\mathbf{P}\mathbf{F}^T\mathbf{F}\mathbf{I}\mathbf{Q}) \\ &= j^2(\hat{\mathbf{U}}). \end{aligned}$$

Since both determinants must be positive, this expression implies that they are equal as well.

Proof: (Trace)

$$\begin{aligned} i(\hat{\mathbf{U}}^{*2}) &= \big\langle \mathbf{P}^*\mathbf{F}^{*T}\mathbf{F}^*\mathbf{I}^*, \mathbf{1}_{\bar{s}} \big\rangle = \big\langle \mathbf{Q}^T\mathbf{P}\mathbf{F}^T\mathbf{F}\mathbf{I}\mathbf{Q}, \mathbf{1}_{\bar{s}} \big\rangle \\ &= \big\langle \mathbf{P}\mathbf{F}^T\mathbf{F}\mathbf{I}, \mathbf{1}_{\bar{s}} \big\rangle = i(\hat{\mathbf{U}}^2). \end{aligned}$$

But

$$i(\hat{\mathbf{U}}) = \big[i(\hat{\mathbf{U}}^2) + 2j^2(\hat{\mathbf{U}})\big]^{1/2}.$$

Therefore, $\hat{\mathbf{U}}$ and $\hat{\mathbf{U}}^*$ must have the same trace.

Claim 3.3:

For isotropic, hyperelastic materials

$$\partial_3 \hat{w}(i, j, \mathbf{n}) = 0 \quad \forall \{i, j, \mathbf{n}\} \in \hat{\mathcal{I}} \times \mathrm{Unit}(\mathbb{E}^3).$$

Proof:

Define $\mathbf{F}^*$, $\hat{\mathbf{U}}^*$, $\mathbf{n}^*$, and $\mathbf{I}^*$ as in the previous claim. Then material isotropy implies that $\tilde{w}(\mathbf{F}, \mathbf{n}) = \tilde{w}(\mathbf{F}^*, \mathbf{n}^*)$, and in terms of $\hat{w}$ this means that

$$\hat{w}\big(i(\hat{\mathbf{U}}), j(\hat{\mathbf{U}}), \mathbf{n}\big) = \hat{w}\big(i(\hat{\mathbf{U}}^*), j(\hat{\mathbf{U}}^*), \mathbf{n}^*\big).$$

But by Claim 3.2 this is equivalent to

$$\hat{w}(i, j, \mathbf{n}) = \hat{w}(i, j, \mathbf{n}^*) \quad \forall \{i, j\} \in \hat{\mathcal{I}}, \quad \forall \mathbf{n}, \mathbf{n}^* \in \mathrm{Unit}(\mathbb{E}^3).$$

Therefore,

$$\partial_3 \hat{w}(i, j, \mathbf{n}) = 0 \quad \forall \{i, j, \mathbf{n}\} \in \hat{\mathcal{I}} \times \mathrm{Unit}(\mathbb{E}^3).$$

Because of this result, the orientation dependence of $\hat{w}$ may be dropped and $\hat{w}$ considered a function $\hat{w} : \hat{\mathcal{I}} \to I\!R$.

Proof of the Representation Theorem: (Necessity)

Necessity is immediate from Claims 3.1 and 3.3.

Proof of the Representation Theorem: (Sufficiency)

By Equation (5.1.5), a sufficient condition to guarantee isotropy for materials whose bulk is characterized by Equation (5.2.2) is that

$$\tilde{w}(\mathbf{F}\mathbf{Q}, \mathbf{Q}^T\mathbf{n}) = \tilde{w}(\mathbf{F}, \mathbf{n}) \quad \forall \mathbf{F} \in \mathrm{Lin}_+(I\!E^3, I\!E^3), \quad \forall \mathbf{n} \in \mathrm{Unit}(I\!E^3),$$
$$\forall \mathbf{Q} \in \mathrm{Orth}_+(I\!E^3, I\!E^3).$$

In terms of $\hat{w}$ this is equivalent to

$$\hat{w}\big(i(\hat{\mathbf{U}}), j(\hat{\mathbf{U}})\big) = \hat{w}\big(i(\hat{\mathbf{U}}^*), j(\hat{\mathbf{U}}^*)\big) \quad \forall \mathbf{F} \in \mathrm{Lin}_+(I\!E^3, I\!E^3), \quad \forall \mathbf{n} \in \mathrm{Unit}(I\!E^3),$$
$$\forall \mathbf{Q} \in \mathrm{Orth}_+(I\!E^3, I\!E^3),$$

where $\hat{\mathbf{U}}$ and $\hat{\mathbf{U}}^*$ are as defined in Claim 3.2. But this equality is guaranteed by Claim 3.2.

C.4 A Characterization of Interfacial Stresses for Isotropic, Hyperelastic Materials.

For the remainder of this appendix, a prime indicates the directional derivative of a function. Also, it is convenient to introduce the two-dimensional Right Cauchy-Green Tensor, $\hat{\mathbf{C}} := \hat{\mathbf{U}}^2$. The directional derivative of $\check{w}$ with respect to its first argument is then given by

$$\big\langle \hat{\mathbf{S}}, I\!B \big\rangle = \check{w}'(I\!F, \mathbf{n})I\!B = \big[\partial_1\hat{w}(i,j)i'(\hat{\mathbf{U}}) + \partial_2\hat{w}(i,j)j'(\hat{\mathbf{U}})\big]\Phi'(\hat{\mathbf{C}})\Gamma'(I\!F)I\!B$$
$$\forall I\!B \in \mathrm{Lin}^{NS}(\mathbf{n}^\perp, I\!E^3), \tag{C.4.1}$$

where

$$\Phi(\hat{\mathbf{C}}) := \hat{\mathbf{C}}^{1/2} \quad \forall \hat{\mathbf{C}} \in \mathrm{Sym}^+(\mathbf{n}^\perp)$$
$$\Gamma(I\!F) := I\!F^T I\!F \quad \forall I\!F \in \mathrm{Lin}^{NS}(\mathbf{n}^\perp, I\!E^3). \tag{C.4.2}$$

A standard mathematical result* is that

$$\begin{aligned} i'(\hat{\mathbf{U}})\hat{\mathbf{D}} &= i(\hat{\mathbf{D}}) \quad \forall \hat{\mathbf{U}}, \hat{\mathbf{D}} \in \mathrm{Sym}^+(\mathbf{n}^\perp) \\ j'(\hat{\mathbf{U}})\hat{\mathbf{D}} &= j(\hat{\mathbf{U}})i(\hat{\mathbf{U}}^{-1}\hat{\mathbf{D}}) \quad \forall \hat{\mathbf{U}}, \hat{\mathbf{D}} \in \mathrm{Sym}^+(\mathbf{n}^\perp). \end{aligned} \tag{C.4.3}$$

Also,

$$\begin{aligned} \Gamma'(\mathbb{F})\mathbb{B} &= \mathbb{B}^T\mathbb{F} + \mathbb{F}^T\mathbb{B} \quad \forall \mathbb{F}, \mathbb{B} \in \mathrm{Lin}^{NS}(\mathbf{n}^\perp, \mathbb{E}^3), \\ \Phi'(\hat{\mathbf{C}})\hat{\mathbf{D}} &= \frac{1}{2}\hat{\mathbf{C}}^{-1/2}\hat{\mathbf{D}} \quad \hat{\mathbf{C}}, \hat{\mathbf{D}} \in \mathrm{Sym}^+(\mathbf{n}^\perp). \end{aligned} \tag{C.4.4}$$

Equation (C.4.4) implies that

$$\Phi'(\hat{\mathbf{C}})\big[\Gamma'(\mathbb{F})\mathbb{B}\big] = \frac{1}{2}\hat{\mathbf{U}}^{-1}(\mathbb{B}^T\mathbb{F} + \mathbb{F}^T\mathbb{B}), \tag{C.4.5}$$

and this result can be used with Equation $(C.4.3)_1$ to obtain

$$\begin{aligned} i'(\hat{\mathbf{U}})\Phi'(\hat{\mathbf{C}})\Gamma'(\mathbb{F})\mathbb{B} &= \frac{1}{2}i\big[\hat{\mathbf{U}}^{-1}(\mathbb{B}^T\mathbb{F} + \mathbb{F}^T\mathbb{B})\big] \\ &= \big\langle \mathbb{F}\hat{\mathbf{U}}^{-1}, \mathbb{B}\big\rangle. \end{aligned} \tag{C.4.6}$$

Likewise, Equations $(C.4.3)_2$ and (C.4.5) imply that

$$\begin{aligned} j'(\hat{\mathbf{U}})\Phi'(\hat{\mathbf{C}})\Gamma'(\mathbb{F})\mathbb{B} &= \frac{1}{2}j(\hat{\mathbf{U}})\big\langle \hat{\mathbf{U}}^{-2}, \mathbb{B}^T\mathbb{F} + \mathbb{F}^T\mathbb{B}\big\rangle \\ &= j(\hat{\mathbf{U}})\big\langle \mathbb{F}\hat{\mathbf{U}}^{-2}, \mathbb{B}\big\rangle. \end{aligned} \tag{C.4.7}$$

Equations (C.4.6) and (C.4.7) can then be applied to Equation (C.4.1) to obtain

$$\begin{aligned} \big\langle \hat{\mathbf{S}}, \mathbb{B}\big\rangle =& \partial_1\hat{w}(i,j)\big\langle \mathbb{F}\hat{\mathbf{U}}^{-1}, \mathbb{B}\big\rangle + \partial_2\hat{w}(i,j)j(\hat{\mathbf{U}})\big\langle \mathbb{F}\hat{\mathbf{U}}^{-2}, \mathbb{B}\big\rangle \\ & \forall \mathbb{B} \in \mathrm{Lin}^{NS}(\mathbf{n}^\perp, \mathbb{E}^3). \end{aligned} \tag{C.4.8}$$

Therefore ,

$$\hat{\mathbf{S}} = \partial_1\hat{w}(i,j)\mathbb{F}\hat{\mathbf{U}}^{-1} + \partial_2\hat{w}(i,j)j(\hat{\mathbf{U}})\mathbb{F}\hat{\mathbf{U}}^{-2} \tag{C.4.9}$$

and

$$\hat{\mathbf{T}} = \frac{1}{j}\partial_1\hat{w}(i,j)\bar{\mathbf{P}}\mathbb{F}\hat{\mathbf{U}}^{-1}\hat{\mathbf{F}}^T + \partial_2\hat{w}(i,j)\bar{\mathbf{P}}\mathbb{F}\hat{\mathbf{U}}^{-2}\hat{\mathbf{F}}^T. \tag{C.4.10}$$

These representations can be simplified by using the left polar decomposition of the surface-deformation gradient. Given $\hat{\mathbf{F}} = \hat{\mathbf{Q}}\hat{\mathbf{U}} = \hat{\mathbf{V}}\hat{\mathbf{Q}}$, then $\hat{\mathbf{V}} = \hat{\mathbf{F}}\hat{\mathbf{U}}^{-1}\hat{\mathbf{F}}^T$. Therefore,

$$\bar{\mathbf{P}}\mathbb{F}\hat{\mathbf{U}}^{-1}\hat{\mathbf{F}}^T = \hat{\mathbf{V}}. \tag{C.4.11}$$

---

* CIARLET[1988] p11.

A simplification is also possible by noting that

$$\bar{\mathbf{P}}\mathbb{F}\hat{\mathbf{U}}^{-2}\hat{\mathbf{F}}^{T} = \mathbf{1}_{\bar{s}}. \tag{C.4.12}$$

Thus, the interface deformational stresses for isotropic, hyperelastic materials can be represented as

$$\hat{\mathbf{S}} = \bar{\mathbf{I}}\big[\partial_1\hat{w}(i,j)\hat{\mathbf{F}}\hat{\mathbf{U}}^{-1} + j(\hat{\mathbf{U}})\partial_2\hat{w}(i,j)\hat{\mathbf{F}}^{-T} \tag{C.4.13}$$

and

$$\hat{\mathbf{T}} = \frac{1}{j}\partial_1\hat{w}(i,j)\hat{\mathbf{V}} + \partial_2\hat{w}(i,j)\mathbf{1}_{\bar{s}}. \tag{C.4.14}$$

These are the representations provided in Equation (5.2.15) with the expression for accretive stress, $\hat{\mathbf{C}}$, obtained using Equation $(4.1.17)_3$.

APPENDIX D. FLUID-SURFACE THEOREM

(B) For a hyperelastic material with constitution such that $\hat{\mathbf{C}} = \mathbf{0}$:

(a) $\bar{w} = \bar{\sigma}$, a constant; and

(b) $\hat{\mathbf{T}} = \bar{\sigma}\mathbf{1}_{\bar{s}}$.

Proof: (b)

For $\hat{\mathbf{C}} = \mathbf{0}$, the Tension-Energy Theorem of Section 3.4 implies that

$$\mathbb{F}^T\hat{\mathbf{S}} = w\mathbf{1}_s.$$

In terms of $\hat{\mathbf{T}}$, this is equivalent to

$$w\mathbf{1}_s = j\mathbb{F}^T\bar{\mathbf{I}}\hat{\mathbf{T}}\hat{\mathbf{F}}^{-T} = j\hat{\mathbf{F}}^T\hat{\mathbf{T}}\hat{\mathbf{F}}^{-T}.$$

Therefore,

$$\hat{\mathbf{T}} = \frac{w}{j}\hat{\mathbf{F}}^{-T}\mathbf{1}_s\hat{\mathbf{F}}^T = \bar{w}\mathbf{1}_{\bar{s}}.$$

(b) is therefore proved once (a) is proved.

Proof: (a)

As shown, $\hat{\mathbf{C}} = \mathbf{0}$ implies that $\hat{\mathbf{T}} = \bar{w}\mathbf{1}_{\bar{s}}$ and in terms of $\hat{\mathbf{S}}$ this is equivalent to

$$\hat{\mathbf{S}} = w\bar{\mathbf{I}}\hat{\mathbf{F}}^{-T}. \tag{D.1}$$

But for hyperelastic materials,

$$\hat{\mathbf{S}} = \partial_1\breve{w}(\mathbb{F}, \mathbf{n}) \tag{D.2}$$

from Equation $(4.1.17)_2$. Let

$$\bar{\sigma}(\mathbb{F}, \mathbf{n}) := \frac{1}{j}\breve{w}(\mathbb{F}, \mathbf{n})$$

so that

$$\partial_1\breve{w}(\mathbb{F}, \mathbf{n}) = j\bar{\mathbf{I}}\hat{\mathbf{F}}^{-T}\bar{\sigma}(\mathbb{F}, \mathbf{n}) + j\partial_1\bar{\sigma}(\mathbb{F}, \mathbf{n}). \tag{D.3}$$

Here use has been made of the identity,

$$\partial_1 \tilde{j}(I\!F, \mathbf{n}) = j\bar{\mathbf{I}}\hat{\mathbf{F}}^{-T} \tag{D.4}$$

from GURTIN & STRUTHERS[1990], (Equation 3.19), with

$$\tilde{j}(I\!F, \mathbf{n}) = j.$$

Equations $(D.1)$–$(D.3)$ then imply that

$$\breve{w}(I\!F, \mathbf{n})\bar{\mathbf{I}}\hat{\mathbf{F}}^{-T} = j\bar{\sigma}(I\!F, \mathbf{n})\bar{\mathbf{I}}\hat{\mathbf{F}}^{-T} + j\partial_1\bar{\sigma}(I\!F, \mathbf{n}).$$

Therefore,

$$\partial_1\bar{\sigma}(I\!F, \mathbf{n}) = \mathbf{0}. \tag{D.5}$$

$\hat{\mathbf{C}} = \mathbf{0}$ also implies that $\hat{\mathbf{C}}^T\mathbf{n} = \mathbf{0}$ which, by Equation $(4.1.17)_3$, gives that

$$\mathbf{0} = D_{\mathbf{n}}\breve{w}(I\!F, \mathbf{n}) = \big[D_{\mathbf{n}}j(\mathbf{F}, \mathbf{n})\big]\bar{\sigma}(I\!F, \mathbf{n}) + j(\mathbf{F}, \mathbf{n})\big[D_{\mathbf{n}}\bar{\sigma}(I\!F, \mathbf{n})\big], \tag{D.6}$$

where

$$\breve{j}(\mathbf{F}, \mathbf{n}) := \frac{\mathrm{Det}(\mathbf{F})}{\|\mathbf{F}^{-T}\mathbf{n}\|}$$

from Equation $(2.5.6)_2$. But following the definition of $D_{\mathbf{n}}(\cdot)$ given by Equation (4.1.11),

$$\begin{aligned} D_{\mathbf{n}}\breve{j}(\mathbf{F}, \mathbf{n}) &= \frac{d}{d\beta}\left\{\frac{\mathrm{Det}\big[\mathbf{F}\tilde{\mathbf{Q}}(\mathbf{k}(\beta), \mathbf{n})\big]}{\big\|\big[\mathbf{F}\tilde{\mathbf{Q}}(\mathbf{k}(\beta), \mathbf{n})\big]^{-T}\mathbf{k}(\beta)\big\|}\right\}\Bigg|_{\beta=0} \\ &= \frac{d}{d\beta}\left\{\frac{\mathrm{Det}(\mathbf{F})}{\big\|\mathbf{F}^{-T}\tilde{\mathbf{Q}}(\mathbf{k}(\beta), \mathbf{n})\mathbf{k}(\beta)\big\|}\right\}\Bigg|_{\beta=0} \\ &= \frac{d}{d\beta}\left\{\frac{\mathrm{Det}(\mathbf{F})}{\|\mathbf{F}^{-T}\mathbf{n}\|}\right\}\Bigg|_{\beta=0} \\ &= 0. \end{aligned} \tag{D.7}$$

Since

$$D_{\mathbf{n}}\tilde{j}(I\!F, \mathbf{n}) = D_{\mathbf{n}}\breve{j}(I\!F\mathbf{P} + \mathbf{f}\otimes\mathbf{n}, \mathbf{n})$$

by construction, Equations $(D.6)$ and $(D.7)$ imply that

$$D_{\mathbf{n}}\bar{\sigma}(I\!F, \mathbf{n}) = \mathbf{0}. \tag{D.8}$$

Use of Equations (4.1.7), (4.1.8), and (4.1.12) with $\bar{\sigma}$ in place of w then gives that $\bar{\sigma}$ must be a constant-valued function. Thus, $\bar{w} = \bar{\sigma}$, a constant, and the proof of **(B)** is complete.

(C) For a hyperelastic material with constitution such that $\bar{w} = \bar{\sigma}$, a constant:

(a) $\hat{\mathbf{C}} = \mathbf{0}$; and

(b) $\hat{\mathbf{T}} = \bar{\sigma}\mathbf{1}_{\bar{\mathcal{S}}}$.

Proof: (b)

$\bar{w} = \bar{\sigma}$ is equivalent to $w = j\bar{\sigma}$ so that $\hat{\mathbf{S}} = j\bar{\sigma}\bar{\mathbf{I}}\hat{\mathbf{F}}^{-T}$. Expression of this result in terms of $\hat{\mathbf{T}}$ gives that $\hat{\mathbf{T}} = \bar{\sigma}\mathbf{1}_{\bar{\mathcal{S}}}$.

Proof: (a)

The above expression for $\hat{\mathbf{S}}$ implies that

$$\mathbf{I}\mathbb{F}^T\hat{\mathbf{S}} = j\bar{\sigma}\mathbf{I} = w\mathbf{I}. \tag{D.9}$$

From $(D.6)$ and the fact that $w = j\bar{\sigma}$,

$$D_{\mathbf{n}}\breve{w}(\mathbb{F}, \mathbf{n}) = \mathbf{0}. \tag{D.10}$$

Substitution of this result and Equation $(D.9)$ into Equation $(4.1.17)_3$ yields

$$\hat{\mathbf{C}} = w\mathbf{I} - w\mathbf{I} - \mathbf{n} \otimes \mathbf{0} = \mathbf{0}. \tag{D.11}$$

This completes the proof of **(C)**.

APPENDIX E. STRAIN DEPENDENCE OF THE NUCLEATION ENERGY

E.1 Nucleation Energy. As discussed in Chapters seven through ten, there exists a representation for the nucleation energy, B, as a function of embryo size, s, and prenucleation dilatation, J_0. This function is now constructed and shown to have a monotonically decreasing response to dilatation for fixed s. This will be accomplished for hard, soft, and specialized mixed loading with the following interface constitutions: no surface fields; bonding energy interfaces; fluid-like interfaces; and membrane-like interfaces.

The nucleation energy is defined by Equation (7.5.3) which, using Equation (7.7.1), can be written

$$B = [\![E]\!]^{t_*} + [\![E_{LD}]\!]^{t_*}. \tag{E.1.1}$$

The second term in this expression obviously depends upon the type of loading device, but a general expression can be derived for the first term, and this will now be done. Let $E_{(-)}$ and $E_{(+)}$ denote the total energy stored in the cylinder just before and just after a nucleation event, respectively. Then Equation (6.3.1) gives that

$$\begin{aligned} E_{(-)} &= 2\mu\pi Q\left\{2(J_0^{1/2}-1) + \int_1^{J_0} h(J)\,dJ\right\} \\ E_{(+)} &= 4\mu\pi \int_0^{Q} [I_1(q)-3]\,dq + 2\mu\pi s^2 \int_1^{J_i} h(J)\,dJ \\ &\qquad + 2\mu\pi(Q^2-s^2)\int_1^{J_m} h(J)\,dJ + 2\pi s w \end{aligned} \tag{E.1.2}$$

where

$$\begin{aligned} I_1(q) - 3 &= 2(J_i^{1/2}-1), && q \in (0,s) \\ &= \frac{s^2(J_i - J_m) + 2q^2 J_m}{\tilde{r}(q)q} - 2, && q \in (s,Q). \end{aligned} \tag{E.1.3}$$

Explicit evaluation of these expressions results in

$$\begin{aligned}[\![E]\!]^{t_*} =& 4\mu\pi Q[\![R]\!]^{t_*} \\ &+ 2\mu\pi s^2\left[\frac{\beta\Gamma}{2}(J_U + J_L) - \frac{\beta}{2}(J_m^2 - J_i^2) + (\beta+1)J_m - \beta J_{max} J_i\right] \\ &+ 2\mu\pi Q^2\left[\frac{\beta}{2}(J_m^2 - J_0^2) - (\beta+1)(J_m - J_0)\right] + 2\pi sw.\end{aligned} \tag{E.1.4}$$

Under hard loading

$$[\![E_{LD}]\!]^{t_*} = 0, \tag{E.1.5}$$

and this continuity condition for nucleation implies that

$$J_0 = J_m + \frac{s^2}{Q^2}(J_i - J_m). \tag{E.1.6}$$

The analogous results for soft loading are that

$$[\![E_{LD}]\!]^{t_*} = -\pi\tau(J_0)[\![R^2]\!]^{t_*}, \tag{E.1.7}$$

with $\tau(J_0)$ given by Equations (7.3.5) and (7.3.2), and

$$\left[\!\left[\frac{Q}{R}\right]\!\right]^{t_*} = \beta(J_0 - J_m). \tag{E.1.8}$$

For specialized, mixed loading,

$$[\![E_{LD}]\!]^{t_*} = \frac{\pi c}{2}[\![(\lambda^2 - R^2)^2]\!]^{t_*} \tag{E.1.9}$$

and

$$\left(Q^2 - \frac{2\mu\beta}{c}\right)(J_0 - J_m) = s^2(J_i - J_m) + \frac{2\mu\beta}{c}\left[\!\left[\frac{Q}{R}\right]\!\right]^{t_*}. \tag{E.1.10}$$

Equations $(E.1.4)$–$(E.1.10)$ can be used to construct the desired nucleation-energy functions and to analyze their response to variations in prenucleation dilatation.

E.2 Interfaces with Bonding Energy.*

With an interface characterized by bonding energy, Equation $(8.1.3)_3$ is used to relate J_i and J_m. In conjunction with the above results, this allows the nucleation energy to be expressed as a function of s and J_0.

Hard Loading

Under hard loading, Equations $(8.1.3)_3$ and $(E.1.4)$–$(E.1.6)$ allow B to be respresented by

$$B_{HL}(s, J_0) := -\beta\Gamma\mu\pi s^2\left[2J_0 - \frac{s^2}{Q^2}\Gamma - (J_L + J_{min})\right] + 2\pi s\sigma. \qquad (E.1.11)$$

Therefore,

$$\partial_2 B_{HL}(s, J_0) = -2\beta\Gamma\mu\pi s^2 < 0. \qquad (E.1.12)$$

Soft Loading

With a loading device characterized as *soft*, Equations $(8.1.3)_3$ and $(E.1.8)$ together imply the existence of a representation, $\tilde{J}_m(s, J_0)$, for J_m. Then Equations $(7.4.2)_1$, $(E.1.7)$, and $(E.1.4)$ allow the nucleation energy to be represented as a function of s and J_0 only such that

$$\begin{aligned}\partial_2 B_{SL}(s, J_0) =& 2\mu\pi Q^2\beta[J_m\partial_2\tilde{J}_m(s, J_0) - J_0] - 2\mu\pi Q^2(\beta+1)[\partial_2\tilde{J}_m(s, J_0) - 1] \\ &+ 4\mu\pi Q^3\left[\frac{\partial_2\tilde{J}_m(s, J_0)}{2R_{(+)}} - \frac{1}{2R_{(-)}}\right] - 2\mu\pi\left(\frac{-Q^3}{2R_{(-)}^3} + \beta\right)(R_{(+)}^2 - R_{(-)}^2) \\ &- \pi Q^2\tau[\partial_2\tilde{J}_m(s, J_0) - 1] \\ \\ =& -2\mu\pi\left(\frac{-Q^3}{2R_{(-)}^3} + \beta\right)(R_{(+)}^2 - R_{(-)}^2) \\ <& \ 0.\end{aligned}$$

---

* The result obtained here covers the claim for no surface fields as a special case.

Specialized, Mixed Loading

Analogous to the case for soft-loading devices, Equations $(8.1.3)_3$ and $(E.1.10)$ together imply the existence of a representation, $\tilde{J}_m(s, J_0)$, for J_m in systems controlled by specialized, mixed loading. Equations $(E.1.4)$ and $(E.1.9)$ therefore allow the nucleation energy to be expressed as a function of s and J_0, as desired, such that

$$\begin{aligned}\partial_2 B_{ML}(s, J_0) =& 2\mu\pi Q^2\beta[J_m\partial_2\tilde{J}_m(s, J_0) - J_0] - 2\mu\pi Q^2(\beta+1)[\partial_2\tilde{J}_m(s, J_0) - 1] \\ &+ 2\mu\pi Q^3\left[\frac{\partial_2\tilde{J}_m(s, J_0)}{R_{(+)}} - \frac{1}{R_{(-)}}\right] - \pi c(\lambda^2 - R_{(-)}^2)[2\lambda\lambda'(J_0) - Q^2] \\ &+ \pi c(\lambda^2 - R_{(+)}^2)[2\lambda\lambda'(J_0) - \partial_2\tilde{J}_m(s, J_0)] \\ \\ =& \pi(\tau_{(+)} - \tau_{(-)})\left[Q^2 + \frac{2\mu}{c}\left(\beta - \frac{Q^3}{2R_{(-)}^3}\right)\right] \\ <& 0.\end{aligned}$$

E.3 Fluid-like Interfaces.

Equation $(9.1.3)_3$ is used to express J_i via a function, $\breve{J}_i(s, J_m)$, for fluid-like interfaces. In conjunction with Equations $(E.1.4)$–$(E.1.10)$, this allows the nucleation energy to be expressed as a function of s and J_0.

Hard Loading

Under hard loading, Equations $(9.1.3)_3$ and $(E.1.4)$–$(E.1.6)$ together imply the existence of a representation, $\tilde{J}_m(s, J_0)$, for J_m with

$$\partial_2\tilde{J}_m(s, J_0) = \frac{Q^2}{Q^2 - s^2 + s^2\partial_2\breve{J}_i(s, J_m)}. \qquad (E.2.1)$$

Then Equations $(9.1.7)_1$, $(E.1.5)$, and $(E.1.4)$ allow the nucleation energy to be represented as a function of s and J_0 only such that

$$\partial_2 B_{HL}(s, J_0) = \frac{\tau_{(+)}}{2}[Q^2 - s^2 + s^2\partial_2\breve{J}_i(s, J_m)]\partial_2\tilde{J}_m(s, J_0) - \frac{Q^2\tau_{(-)}}{2}.$$

Use of Equation $(E.2.1)$ then yields

$$\partial_2 B_{HL}(s, J_0) = \pi Q^2(\tau_{(+)} - \tau_{(-)}) \quad < \quad 0.$$

Soft Loading

With a loading device characterized as *soft*, Equations $(9.1.3)_3$ and $(E.1.8)$ together imply the existence of a representation, $\tilde{J}_m(s, J_0)$, for J_m. Then Equations $(9.1.7)_1$, $(E.1.7)$, and $(E.1.4)$ allow the nucleation energy to be represented as a function of s and J_0 only such that

$$\begin{aligned}\partial_2 B_{SL}(s, J_0) =& \pi \partial_2 \tilde{J}_m(s, J_0)\tau_{(+)}[Q^2 - s^2 + s^2 \partial_2 \breve{J}_i(s, J_m)] - \pi \tau'_{(-)}(J_0)(R^2_{(+)} - R^2_{(-)}) \\ & - \pi \partial_2 \tilde{J}_m(s, J_0)\tau_{(+)}[Q^2 - s^2 + s^2 \partial_2 \breve{J}_i(s, J_m)] + \pi Q^2 \tau_{(+)} - \pi Q^2 \tau_{(+)} \\ = & \quad - \pi \tau'_{(-)}(J_0)(R^2_{(+)} - R^2_{(-)}) \\ < & \quad 0.\end{aligned}$$

Here Equation (7.3.5) has been used to obtain

$$\tau_{(-)}(J_0) = 2\mu \left[\frac{Q}{J_0^{1/2}} + \beta(J_0 - 1) - 1 \right],$$

and it is easy to show that this function is monotone-increasing.

Specialized, Mixed Loading

Again it is straightforward to establish the existence of a representation, $\tilde{J}_m(s, J_0)$, for J_m in systems controlled by specialized, mixed loading. Equations $(E.1.4)$ and $(E.1.9)$ therefore allow the nucleation energy to be expressed as a function of s and J_0. Then a series of alegebraic manipulations lead to

$$\partial_2 B_{ML}(s, J_0) = \pi \left[\lambda^2(J_0)\right]'(\tau_{(+)} - \tau_{(-)}) \quad < \quad 0,$$

where

$$\lambda^2(J_0) := Q^2 J_0 + \frac{\tau_{(-)}(J_0)}{c}$$

is a representation for λ obtained from Equation $(E.1.10)$.

E.4 Membrane-like Interfaces.

Equation $(10.2.2)_3$ is used to express J_i via a function, $\check{J}_i(s, J_m)$, for fluid-like interfaces. In conjunction with Equations $(E.1.4)$–$(E.1.10)$, this allows the nucleation energy to be expressed as a function of s and J_0.

Hard Loading

Under hard loading, Equations $(10.2.2)_3$ and $(E.1.4)$–$(E.1.6)$ together imply the existence of a representation, $\tilde{J}_m(s, J_0)$, for J_m such that

$$\begin{aligned}\partial_2 B_{HL}(s, J_0) = &-2\mu\beta\pi s^2(J_m - J_i)\partial_2\tilde{J}_m(s, J_0) + 2\mu\pi s^2(\beta+1)\partial_2\tilde{J}_m(s, J_0)\\ &-2\mu\pi s^2\beta J_{max}\partial_2\tilde{J}_m(s, J_0) + 2\mu\pi Q^2\beta[J_m\partial_2\tilde{J}_m(s, J_0) - J_0]\\ &-2\mu\pi Q^2(\beta+1)[\partial_2\tilde{J}_m(s, J_0) - 1] + 2\pi s\hat{\eta}\partial_2\tilde{J}_m(s, J_0)\\ = &\ \pi Q^2(\tau_{(+)} - \tau_{(-)}) \quad < \quad 0.\end{aligned}$$

Soft Loading

With a loading device characterized as *soft*, Equations $(10.2.2)_3$ and $(E.1.8)$ together imply the existence of a representation, $\tilde{J}_m(s, J_0)$, for J_m. Then Equations $(10.2.6)_1$, $(E.1.7)$ and $(E.1.4)$ allow the nucleation energy to be represented as a function of s and J_0 only. A series of algrabraic manipulations then lead to

$$\partial_2 B_{SL}(s, J_0) = -\tau'_{(-)}(J_0)(R^2_{(+)} - R^2_{(-)}) \quad < \quad 0.$$

Specialized, Mixed Loading

Once again it is straightforward to establish the existence of a representation, $\tilde{J}_m(s, J_0)$, for J_m in systems controlled by specialized, mixed loading. Equations $(E.1.4)$ and $(E.1.9)$ therefore allow the nucleation energy to be expressed as a function of s and J_0. In a manner analogous to that in cases previously considered, it is found that

$$\partial_2 B_{ML}(s, J_0) = \pi\left[\lambda^2(J_0)\right]'(\tau_{(+)} - \tau_{(-)}) \quad < \quad 0.$$

REFERENCES

[1888] THOMSON, J.J., *Applications of Dynamics to Physics and Chemistry*, Macmillan, London.

[1928] GIBBS, J.W., *Collected Works I*, Longsmans, Green, & Co, Inc., New York.

[1941] ADAM, N., *The Physics and Chemistry of Surfaces*, Oxford, London.

[1950] SHUTTLEWORTH, R., The surface tension of solids, *The Proceedings of the Physical Society*, **A63**, 444–457.

[1951a] HERRING, C., Surface tension as a motivation for sintering, *The Physics of Powder Metallurgy* (ed. W. Kingston), McGraw Hill, New York.

[1951b] HERRING, C., Some theorems on the free energies of crystal surfaces, *Physical Review*, **82**, 87–93.

[1952] CHANG, L., On diffusionless transformation in Au-Cd single crystals containing 47.5 atomic weight percent Cadmium: characteristics of single interface transformation, *Journal of Applied Physics*, **23**, 725–728.

[1952] HERRING, C., The use of classical macroscopic concepts in surface-energy problems, *Structure and Properties of Solid Surfaces* (eds. R. Gomer & C.S. Smith), University of Chicago, Chicago.

[1953] BURKART, M.W. & T.A. READ, Diffusionless phase transformation in the Indium-Thallium system, *Journal of Metals*, **4**, 1516–1524.

[1956] CECH, R.E. & E. TURNBULL, Heterogeneous nucleation of the martensite transformation, *Transactions of the Metallurgical Society of the A.I.M.E.*, **206**, 124–132.

[1956] ESHELBY, J.D., Continuum theory of lattice defects, *Solid State Physics*, **3** (eds. F. Seitz & D. Turnbull), Academic Press, New York.

[1959] COLEMAN, B.D. & W. NOLL, On the thermostatics of continuous media, *Archive for Rational Mechanics and Analysis* **4**, 97–128.

[1960] CALLEN, H.B., *Thermodynamics*, John Wiley & Sons, London.

[1960] SCRIVEN, L.E., Dynamics of a fluid interface, *Chemical Engineering Science*, **12**, 98–108.

[1961] ESHELBY, J.D., Elastic inclusions and inhomogeneities, *Progress in Solid Mechanics, II* (eds. I.N. Sneddon & R. Hill), North-Holland, New York.

[1962] ARIS, R., *Vectors, Tensors, and the Basic Equations of Fluid Mechanics*, Prentice-Hall, New Jersey.

[1963] MULLINS, W.W. & R.F. SEKERKA, Morphological stability of a particle growing by diffusion or heat flow, *Journal of Applied Physics*, **34**, 323–329.

[1964] CAHN, J.W., W.B. HILLIG & G.W. SEARS, The molecular mechanism of solidification, *Acta Metallurgica*, **12**, 1421–1439.

[1964] CHALMERS, B., *Principles of Solidification*, Wiley, New York.

[1964] MULLINS, W.W. & R.F. SEKERKA, Stability of a planar interface during solidification of a dilute, binary alloy, *Journal of Applied Physics*, **35**, 444–451.

[1965] VORONKOV, V.V., Conditions for formation of mosaic structure on a crytallization front, *Soviet Physics–Solid State*, **6**, 2378–2381.

[1966] CORIELL, S.R. & R.L. PARKER, Interface kinetics and the stability of a solid sphere growing from a melt, *Proceedings of the International Conference on Crystal Growth*, 20–24.

[1967] ADAMSON, A.W., *Physical Chemistry of Surfaces*, Interscience Publishers, New York.

[1968] ADKINS, C.J., *Equilibrium Thermodynamics*, McGraw-Hill, London.

[1969] DUNNING, W.J., General and theoretical introduction, *Nucleation* (ed. A.C. Zettlemoyer), Marcel Dekker, Inc, New York.

[1969] SEWELL, M.J., On dual approximation principles and optimization in continuum mechanics, *Royal Society of London Proceedings*, **265**, 319–335.

[1970] ESHELBY, J.D., Energy relations and the energy-momentum tensor in continuum mechanics, *Inelastic Behavior of Solids* (eds. M.F. Kanninen, et al.), McGraw-Hill, New York.

[1971] RICE, J.R., Inelastic constitutive relations for solids: An internal variable theory and its application to metal plasticity, *Journal of the Mechanics and Physics of Solids*, **19**, 433–455.

[1971] RUBENSTEIN, L.I., *The Stefan Problem*, The American Mathematical Society, Providence.

[1972] CAHN, J.W. & D.W. HOFFMAN, A vector thermodynamics for anisotropic surfaces. 1. Fundamentals and application to plane surface junctions, *Surface Science*, **31**, 368–388.

[1973] KRISHNAN, R.V. & L.C. BROWN, Martensitic transformations in β Ag-Cd alloys, *Metallurgical Transactions*, **4**, 1017–1022.

[1973] OTSUKA, K., M. TAKAHASHI & K. SHIMIZU, Single interface martensitic transformation in Cu-Al-Ni alloy, *Metallurgical Transactions*, **4**, 2003–2006.

[1974a] DELAEY, L., R.V. KRISHNAN, H. TAS & H. WARLIMONT, Thermoelasticity, pseudoelasticity and the memory effects associated with martensitic transformations, Part1: Structural and microstructural changes associated with the transformations, *Journal of Materials Science*, **9**, 1521–1535.

[1974b] DELAEY, L., R.V. KRISHNAN, H. TAS & H. WARLIMONT, Thermoelasticity, pseudoelasticity and the memory effects associated with martensitic transformations, Part 2: The macroscopic mechanical behavior, *Journal of Materials Science*, **9**, 1536–1544.

[1974c] DELAEY, L., R.V. KRISHNAN, H. TAS & H. WARLIMONT, Thermoelasticity, pseudoelasticity and the memory effects associated with martensitic transformations, Part 3: Thermodynamics and kinetics, *Journal of Materials Science*, **9**, 1544–1555.

[1974] DELVES, R.T., Theory of interface stability, 40–103, *Crystal Growth* (ed. B.R. Pamplin), Pergamon Press, New York.

[1974] GUILLEMIN, V. & A. POLLACK, *Differential Topology*, Prentice-Hall, New Jersey.

[1974] HOFFMAN, D.W. & J.W. CAHN, A vector thermodynamics for anisotropic surfaces. 2. Curved and faceted surfaces, *Acta Metallurgica*, **22**, 1205–1214.

[1974] ROBIN, P.F., Thermodynamic equilibrium across a coherent interface in a stressed crystal, *American Mineralogist*, **59**, 1286–1298.

[1975] ERICKSEN, J.L., Equilibrium of bars, *Journal of Elasticity*, **5**, 191–201.

[1975] GURTIN, M.E. & A.I. MURDOCH, A continuum theory of elastic material surfaces, *Archive for Rational Mechanics and Analysis*, **57**, 291–323.

[1975] KNOWLES, J.K. & E. STERNBERG, On the ellipticity of the equations of nonlinear elastostatics for a special material, *Journal of Elasticity*, **5**, 341–361.

[1975] MOECKEL, G.P., Thermodynamics of an interface, *Archive for Rational Mechanics and Analysis*, **57**, 255–280.

[1975] RICE, J.R., Continuum mechanics and thermodynamics of plasticity in relation to microscale deformation mechanisms, *Constitutive Equations in Plasticity* (ed. A.S. Argon), MIT Press, Cambridge, Massachusetts.

[1976] GURTIN, M.E. & A.I. MURDOCH, Surface stress in solids, *International Journal of Solids and Structures*, **14**, 431–440.

[1976] MURDOCH, A.I., A thermodynamical theory of elastic material interfaces, *Quarterly Journal of Mechanics and Applied Mathematics*, **29**, 245–275.

[1977] KNOWLES, J.K. & E. STERNBERG, On the failure of ellipticity of the equations for finite elastostatic plane strain, *Archive for Rational Mechanics and Analysis*, **63**, 321–336.

[1977] PORTER, D.L. & A.H. HEUER, Mechanisms of toughening in partially stabilized zirconia, *Journal of the American Ceramics Society*, **60**, 183–184.

[1978] KNOWLES, J.K. & E. STERNBERG, On the failure of ellipticity and the emergence of discontinuous deformation gradients in plane finite elastostatics, *Journal of Elasticity*, **8**, 329–379.

[1978] NISHIYAMA, Z., *Martensitic Transformation*, Academic Press, New York.

[1979] FERNANDEZ-DIAZ, J. & W.O. WILLIAMS, A generalized Stefan condition, *Journal of Applied Mathematics and Physics (ZAMP)*, **30**, 749–755.

[1979] JAMES, R.D., Co-existent phases in the one-dimensional static theory of elastic bars, *Archive for Rational Mechanics and Analysis*, **72**, 99–140.

[1979] KNOWLES, J.K., On the dissipation associated with equilibrium shocks in finite elasticity, *Journal of Elasticity*, **9**, 131–158.

[1979] PORTER, D.L., A.G. EVANS & A.H. HEUER, Transformation toughening in partially stabilized zirconia (PSZ), *Acta Metallurgica*, **27**, 1649–1654.

[1980] ABEYARATNE, R., Discontinuous deformation gradients in plane finite elastostatics of incompressible materials, *Journal of Elasticity*, **10**, 255–293.

[1980] CAHN, J.W., Surface stress and the chemical equilibrium of small crystals. 1. The case of the isotropic surface, *Acta Metallurgica*, **28**, 1333–1338.

[1980] DUNN, J.E. & R.L. FOSDICK, The morphology and stability of material phases, *Archive for Rational Mechanics and Analysis*, **74**, 1–99.

[1980] JAMES, R.D., The propagation of phase boundaries in elastic bars, *Archive for Rational Mechanics and Analysis*, **73**, 125–158.

[1980] PARRY, G.P., Twinning in nonlinearly elastic monatomic crystals, *International Journal of Solids and Structures*, **16**, 275–281.

[1980] SABURI, T., C.M. WAYMAN, K. TAKATA & S. NENNO, The shape memory mechanism in 18R martensitic alloys, *Acta Metallurgica*, **28**, 15–32.

[1981] ABEYARATNE, R., Discontinuous deformation gradients in finite twisting of an incompressible elastic tube, *Journal of Elasticity*, **11**, 43–80.

[1981] JAMES, R.D., Finite deformation by mechanical twinning, *Archive for Rational Mechanics and Analysis*, **77**, 143–176.

[1981] PIPPARD, A.B., *The Elements of Classical Thermodynamics*, Cambridge University Press.

[1981] PORTER, D.A. & K.E. EASTERLING, *Phase Transformations in Metals and Alloys*, Van Nostrand, Berkshire, England.

[1982] CAHN, J.W. & F.C. LARCHE, Surface stress and the chemical equilibrium of small crystals. 2. Solid particles embedded in a solid matrix, *Acta Metallurgica*, **30**, 51–56.

[1983] BUDIANSKY, B., J.W. HUTCHINSON & J.C. LAMBROPOULOS, Continuum theory of dilatant transformation toughening in ceramics, *International Journal of Solids and Structures*, **19**, 337–355.

[1983] FOSDICK, R.L. & G. MACSITHIGH, Helical shear of an elastic, circular tube with a non-convex stored energy, *Archive for Rational Mechanics and Analysis*, **84**, 31–53.

[1983] GURTIN, M.E., Two-phase deformations of elastic solids, *Archive for Rational Mechanics and Analysis*, **84**, 1–29.

[1983] LAMBROPOULOS, J.C., Shear, shape and orientation effects in transformation toughening, *International Journal of Solids and Structures*, **22**, 1083–1106.

[1983] RUF, H. & A.G. EVANS, Toughening by monoclinic zirconia, *Journal of the American Ceramics Society*, **66**, 328–332.

[1983] YATOMI, C., & N. NISHIMURA, On the dissipation inequality in equilibrium shocks, *Journal of Elasticity*, **13**, 311–316.

[1984] HOGER, A. & D. CARLSON, On the derivative of the square root of a tensor and Guo's rate theorems, *Journal of Elasticity*, **14**, 329–336.

[1984] KINDERLEHRER, D. Twinning of crystals, II, *IMA Preprint Series 106*, University of Minnesota, Minneapolis, Minnesota.

[1985] ALEXANDER, J.I.D. & W.C. JOHNSON, Thermomechanical equilibrium in solid-fluid systems with curved interfaces, *Journal of Applied Physics*, **58**, 816–824.

[1985a] GRUGICIC, M., G.B. OLSON, & W.S. OWEN, Mobility of the $\beta_1 - \gamma_1'$ martensitic interface, Part I. experimental measurements, *Metallurgical Transactions*, **16A**, 1723–1734.

[1985b] GRUGICIC, M., G.B. OLSON, & W.S. OWEN, Mobility of the $\beta_1 - \gamma_1'$ martensitic interface, Part II. model calculations, *Metallurgical Transactions*, **16A**, 1734–1744.

[1985] MULLER, I., *Thermodynamics*, Pitman, Boston.

[1986] AHLERS, M., Martensite and equilibrium phases in Cu-Zn and Cu-Zn-Al alloys, *Progress in Materials Science*, **30**, 135–186.

[1986] ALEXANDER, J.I.D. & W.C. JOHNSON, Interfacial conditions for thermomechanical equilibrium in two-phase crystals, *Journal of Applied Physics*, **59**, 2735–2746.

[1986] FOSDICK, R.L., Structure and dynamical stability of Gibbsian states, *New Perspectives in Thermodynamics* (ed. J. Serrin), Springer-Verlag, New York.

[1986] GURTIN, M.E., On the two-phase stefan problem with interfacial energy and entropy, *Archive for Rational Mechanics and Analysis*, **96**, 200–241.

[1986a] JAMES, R.D., Displacive phase transformations in solids, *Journal of the Mechanics and Physics of Solids*, **34**, 359–394.

[1986b] JAMES, R.D., Phase transformations and non-elliptic free energy, *New Perspectives in Thermodynamics* (ed. J. Serrin), Springer-Verlag, New York.

[1986] THADHANI, N.N. & M.A. MEYERS, Kinetics of isothermal martensitic transformation, *Progress in Materials Science*, **30**, 1–37.

[1987a] ABEYARATNE, R. & J.K. KNOWLES, Non-elliptic elastic materials and the modeling of dissipative mechanical behavior: An example, *Journal of Elasticity*, **18**, 227–278.

[1987b] ABEYARATNE, R. & J.K. KNOWLES, Non-elliptic elastic materials and the modeling of elastic-plastic behavior for finite deformation, *Journal of the Mechanics and Physics of Solids*, **35**, 343–365.

[1987] BALL, J.M. & R.D. JAMES, Fine phase mixtures as minimizers of energy, *Archive for Rational Mechanics and Analysis*, **100**, 13–52.

[1987] HAUGHTON, D.M., Inflation and bifurcation of thick-walled, compressible, elastic, spherical shells, *IMA Journal of Applied Mathematics*, **39**, 259–272.

[1987] SILLING, S.A., The effect of supercritical dilatational transformation on crack tip singularities, *Brown University Technical Report*, Rhode Island.

[1987] TRUSKINOVSKII, L.M., Dynamics of non-equilibrium phase boundaries in a heat conducting non-linearly elastic medium, *Journal of Applied Mathematics and Mechanics (PMM USSR)*, **51**, 777–784.

[1987] VISINTIN, A., Stefan problem with a kinetic condition at the free boundary, *Annali Di Matematica Pura Ed Applicata*, **146**, 97–122.

[1988a] ABEYARATNE, R. & G. JIANG, Dilatationally nonlinear elastic materials: (I) Some theory, *Technical Report 5, ONR Grant N00014-87-k-0117.*

[1988b] ABEYARATNE, R. & G. JIANG, Dilatationally nonlinear elastic materials: (II) An example illustrating stress concentration reduction, *Technical Report 6, ONR Grant N00014-87-k-0117.*

[1988] ABEYARATNE, R. & J.K. KNOWLES, On the dissipative response due to discontinuous strains in bars of unstable elastic materials, *International Journal of Solids and Structures* **24**, 1021–1044.

[1988a] ALTS, T. & K. HUTTER, Continuum description of the dynamics and thermodynamics of phase boundaries between ice and water. I. Surface balance laws and their interpretation in terms of three-dimensional balance laws averaged over the phase change boundary layer, *Journal of Non-equilibrium Thermodynamics*, **13**, 221–257.

[1988b] ALTS, T. & K. HUTTER, Continuum description of the dynamics and thermodynamics of phase boundaries between ice and water. II. Thermodynamics, *Journal of Non-equilibrium Thermodynamics*, **13**, 259–280.

[1988c] ALTS, T. & K. HUTTER, Continuum description of the dynamics and thermodynamics of phase boundaries between ice and water. III. Thermostatics and its consequences, *Journal of Non-equilibrium Thermodynamics*, **13**, 301–329.

[1988] CIARLET, P.G., *Mathematical Elasticity Volume I: Three-dimensional Elasticity*, North-Holland, New York.

[1988a] GURTIN, M.E., Toward a nonequilibrium thermodynamics of two-phase materials, *Archive for Rational Mechanics and Analysis*, **100**, 275–312.

[1988b] GURTIN, M.E., Multiphase thermomechanics with interfacial structure. 1. Heat conduction and the capillary balance law, *Archive for Rational Mechanics and Analysis*, **104**, 185–221.

[1988] KINDERLEHRER, D., Equilibrium configurations of crystals, *Archive for Rational Mechanics and Analysis*, **103**, 237–277.

[1988a] SILLING, S.A., Numerical studies of loss of ellipticity near singularities in an elastic material, *Journal of Elasticity*, **19**, 213–239.

[1988b] SILLING, S.A., Consequences of the Maxwell relation for anti-plane shear deformations of an elastic solid, *Journal of Elasticity*, **19**, 241–284.

[1988c] SILLING, S.A., Dynamic growth of martensitic plates in an elastic material, *Brown University Technical Report*, Rhode Island.

[1988] STRAIN, J., Linear stability of planar solidification fronts, *Physica D*, **30**, 277–320.

[1988] ULBRICHT, H., J. SCHMELZER, R. MAHNKE & F. SCHWEITZER, *Thermodynamics of Finite Systems and the Kinetics of First-Order Phase Transitions*, Teuber-Text Zur Physik, Leipzig.

[1988] VISINTIN, A., Surface tension effects in phase transition, *Material Instabilities in Continuum Mechanics and Related Mathematical Problems* (ed. J.M. Ball), Oxford, New York.

[1989] ABEYARATNE, R. & J.K. KNOWLES, Kinetic relations and the propagation of phase boundaries in solids, *Technical Report 10, ONR Grant N00014-87-K-0117.*

[1989] ANGENENT, S. & M.E. GURTIN, Multiphase thermomechanics with interfacial structure 2. Evolution of an isothermal interface, *Archive for Rational Mechanics and Analysis*, **108**, 323–391.

[1989] FONSECA, I., Interfacial energy and the Maxwell rule, *Archive for Rational Mechanics and Analysis*, **106**, 63–95.

[1989] JIANG, Q., A continuum model for phase transformation in thermoelastic solids, *Ph.D. Thesis*, California Institute of Technology.

[1989] LANGER, J.S., Dendrites, viscous fingers, and the theory of pattern formation, *Science*, **243**, 1150–1156.

[1989] LEO, P.H. & R.F. SEKERKA, The effect of surface stress on crystal-melt and crystal-crystal equilibrium, *Acta Metallurgica*, **37**, 3119–3138.

[1989] VISINTIN, A., Stefan problem with surface tension, *Mathematical Models for Phase Change Problems, International Series of Numerical Mathematics, 88* (ed. J.F. Rodrigues), Birkhauser Verlag, Basel.

[1990a] ABEYARATNE, R. & J.K. KNOWLES, On the driving traction acting on a surface of strain discontinuity in a continuum, *Journal of the Mechanics and Physics of Solids* **38**, 345–360.

[1990b] ABEYARATNE, R. & J.K. KNOWLES, Implications of viscocity and strain gradient effects for the kinetics of propagating phase boundaries, *Technical Report 11, ONR Grant N00014-87-K-0017.*

[1990c] ABEYARATNE, R. & J.K. KNOWLES, On the propagation of maximally dissipative phase boundaries in solids, *Technical Report 1, ONR Grant N00014-90-J-1871.*

[1990] DENG, Y. & G.S. ANSELL, Investigation of thermoelastic martensitic transformation in a Cu-Zn-Al alloy, *Acta Metallurgica*, **38**, 77–93.

[1990] GURTIN, M.E. & A. STRUTHERS, Multi-phase thermomechanics and interfacial structure 3. Evolving phase boundaries in the presence of bulk deformation, *Archive for Rational Mechanics and Analysis*, **112**, 97–160.

[1990] GURTIN, M.E., A mechanical theory of crystallization of a rigid solid in a liquid melt; melting-freezing waves, *Archive for Rational Mechanics and Analysis*, **110**, 287–312.

[1990] ROITBURD, A.L., On the thermodynamics of martensite nucleation, *Materials Science and Engineering*, **A127**, 229–238.

[1990] ROSAKIS, P., Ellipticity and deformations with discontinuous gradients in finite elastostatics, *Archive for Rational Mechanics and Analysis*, **109**, 1–37.

[1990] SLATTERY, J.C., *Interfacial Transport Phenomena*, Springer-Verlag, New York.

[1990] STRAIN, J., Velocity effects in unstable solidification, *SIAM Journal of Applied Math*, **50**, 1–15.

[1990] TANNER, L.E. & M. WUTTIG, Workshop on first-order displacive phase transformations: review and recomendations, *Materials Science and Engineering*, **A127**, 137–144.

[1990] XIE, W., The stefan problem with a kinetic condition at the free boundary, *SIAM Journal of Mathematical Analysis*, **21**, 362–373.

[1991] ABEYARATNE, R. & J.K. KNOWLES, Wave propagation in linear, bilinear and trilinear elastic bars, *Technical Report 3, ONR Grant N00014-90-J-1871.*

[1991] CHAUDHRY, Z. & C.A. ROGERS, Bending and shape control of beams using SMA actuators, *Journal of Intelligent Material Systems and Structures*, **2**, 581–602.

[1991a] FRIED, E., On the construction of two-phase equilibria in a non-elliptic hyperelastic material, *Journal of Elasticity.* To appear.

[1991b] FRIED, E., Linear stability analysis of a two-phase process involving a steadily propagating planar phase boundary in a solid, Part 1: Purely mechanical case, *Technical Report 4, ONR Grant N00014-90-J-1871.*

[1991c] FRIED, E., Linear stability analysis of a two-phase process involving a steadily propagating planar phase boundary in a solid, Part 2: Thermomechanical case, *Technical Report 5, ONR Grant N00014-90-J-1871.*

[1991] MULLER, I. & H. XU, On the pseudo-elastic hysteresis, *Acta Metallurgica*, **39**, 263–271.

[1991] PENCE, T., On the encounter of an acoustic shear pulse with a phase boundary in an elastic material: reflection and transmission behavior, *Journal of Elasticity*, **25**, 31–74.

[1991] ROGERS, C.A., C. LIANG, & C.R. FULLER, Modeling of shape-memory alloy hybrid composites for structural acoustic control, *Journal of the Acoustical Society of America*, **89**, 210–220.

[1991] ROSAKIS, P., Compact zones of shear transformation in an anisotropic body, *Journal of the Mechanics and Physics of Solids.* To Appear.

[1991] WANG, B-T & C.A. ROGERS, Modeling of finite-length, spatially-distributed, induced strain actuators for laminate beams and plates, *Journal of Intelligent Material Systems and Structures*, **2**, 38–58.

[1992] AMATO, I., Animating the material world, *Science*, **30**, 284–286.

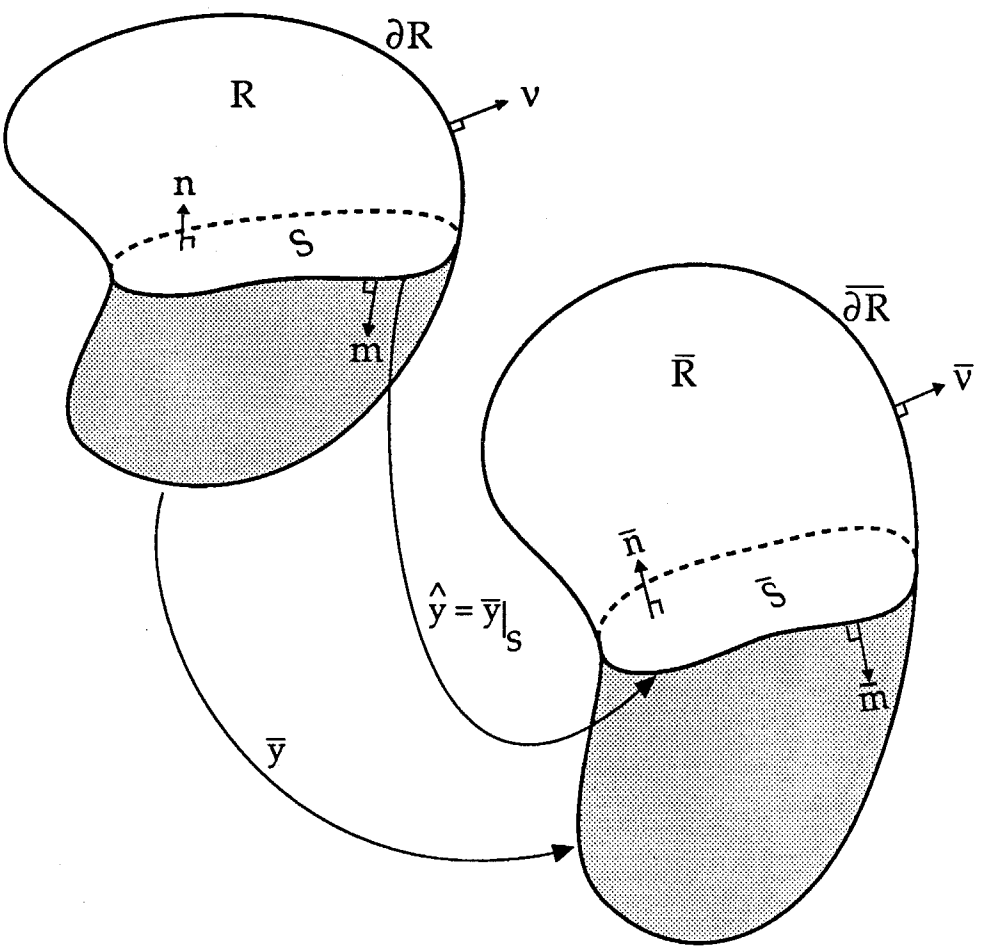

Figure 1. A two-phase deformation, $\bar{y}$, and its restriction, $\hat{y}$, to the interface, S.

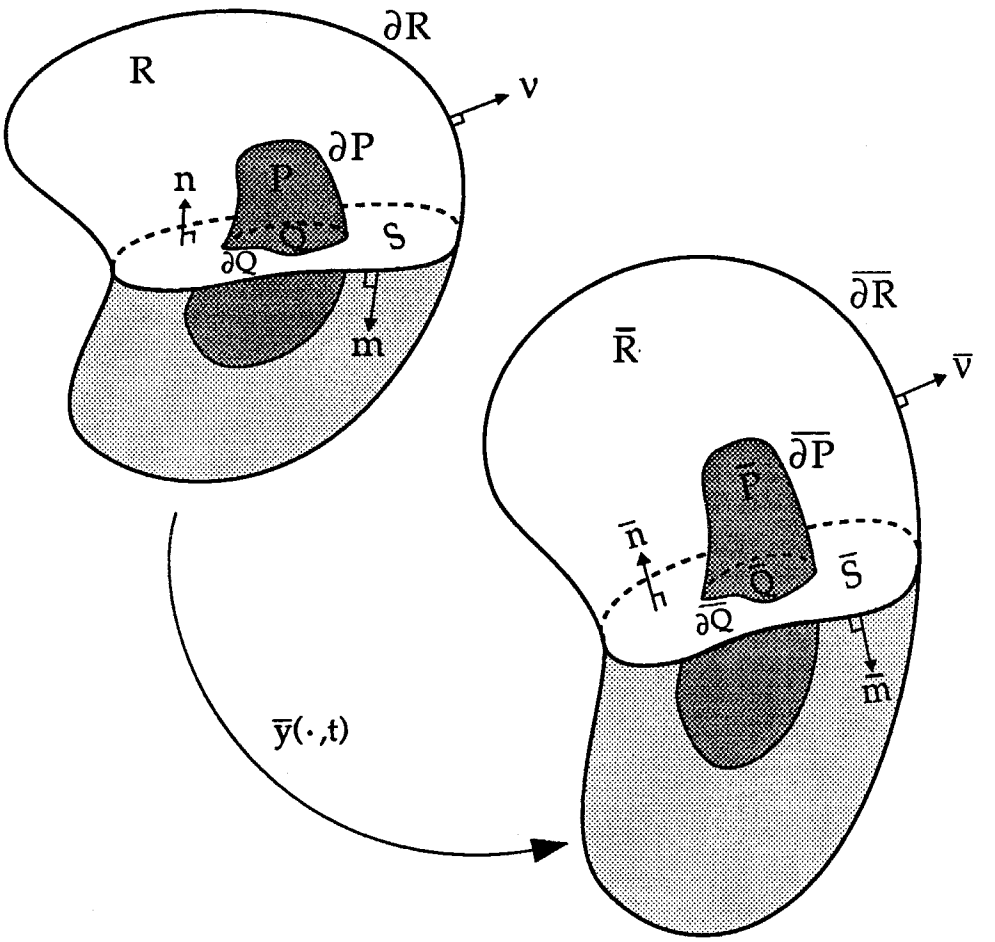

Figure 2. Subregions P and Q(t) of R and S(t), respectively, and their images, $\bar{P}(t)$ and $\bar{Q}(t)$.

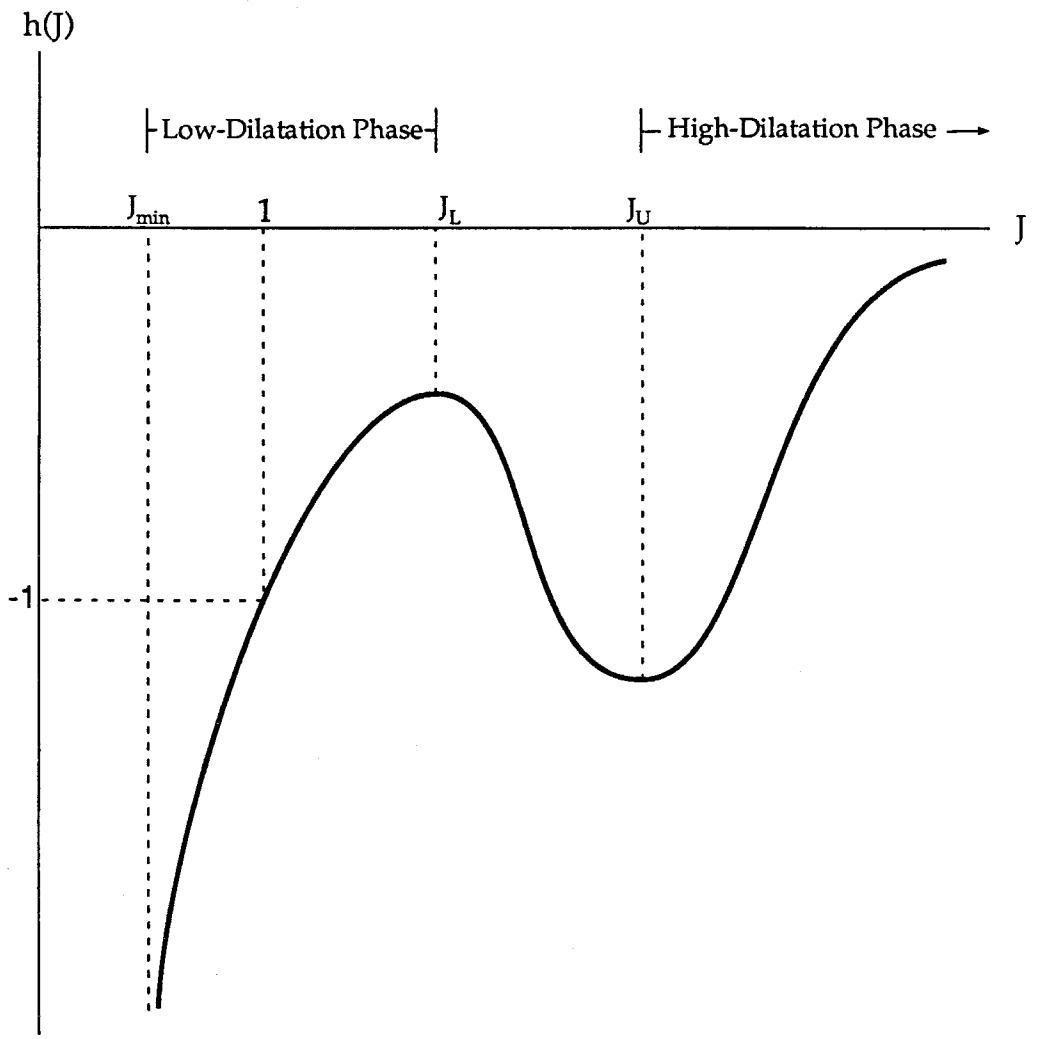

Figure 3. Graph of stress response function, h, for 3-PD solids.

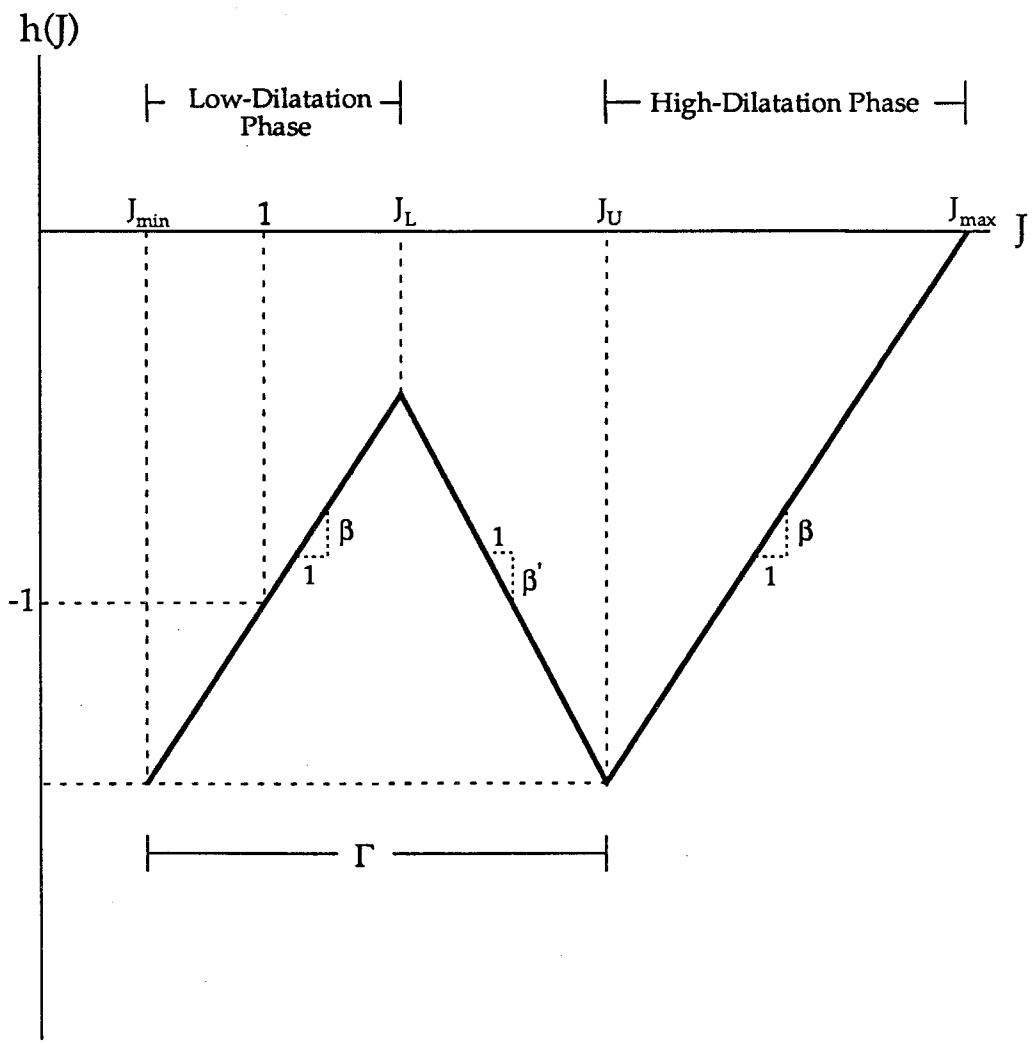

Figure 4. Graph of stress response function, h, for 3-PLD solids.

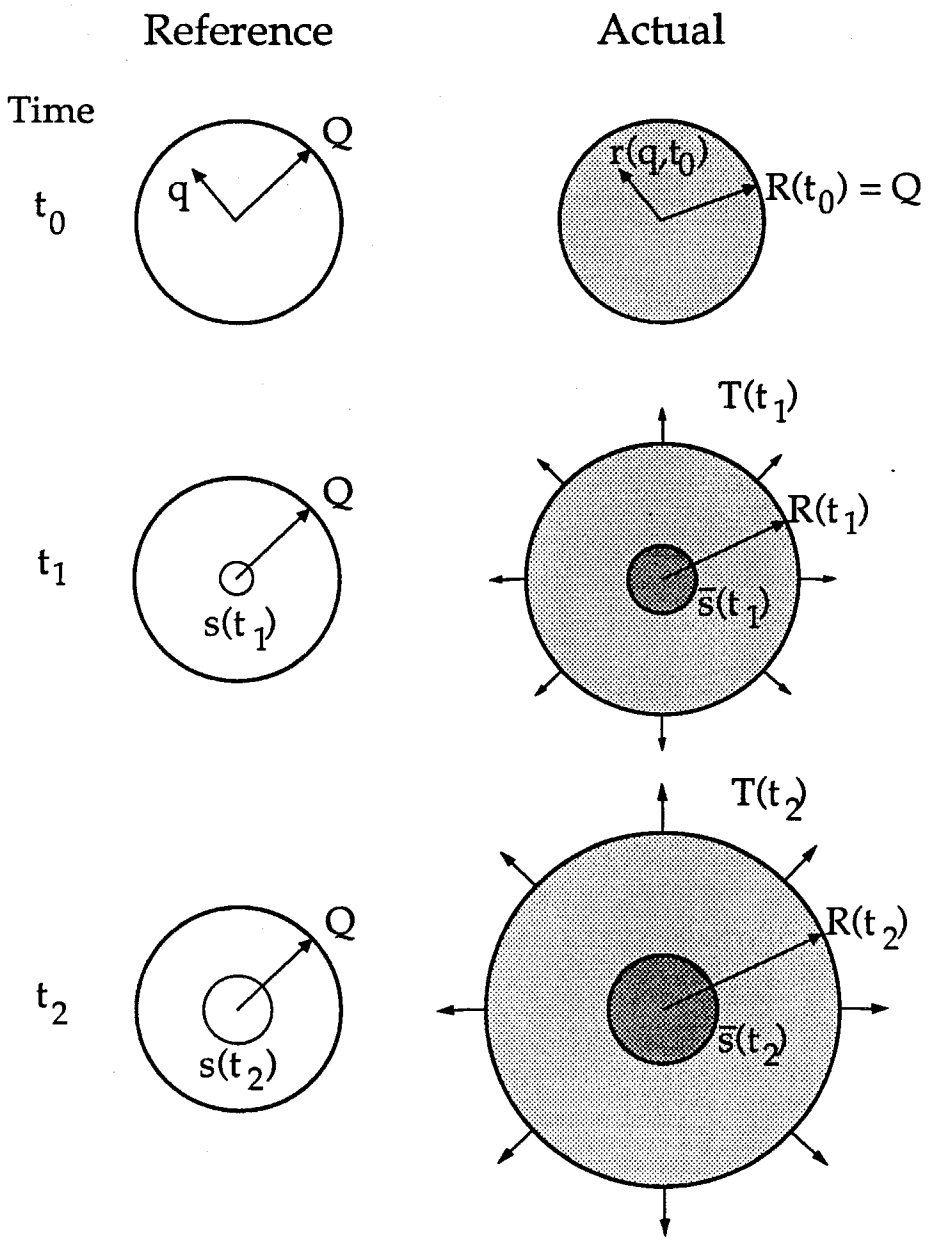

Figure 5. The Cylinder Problem.

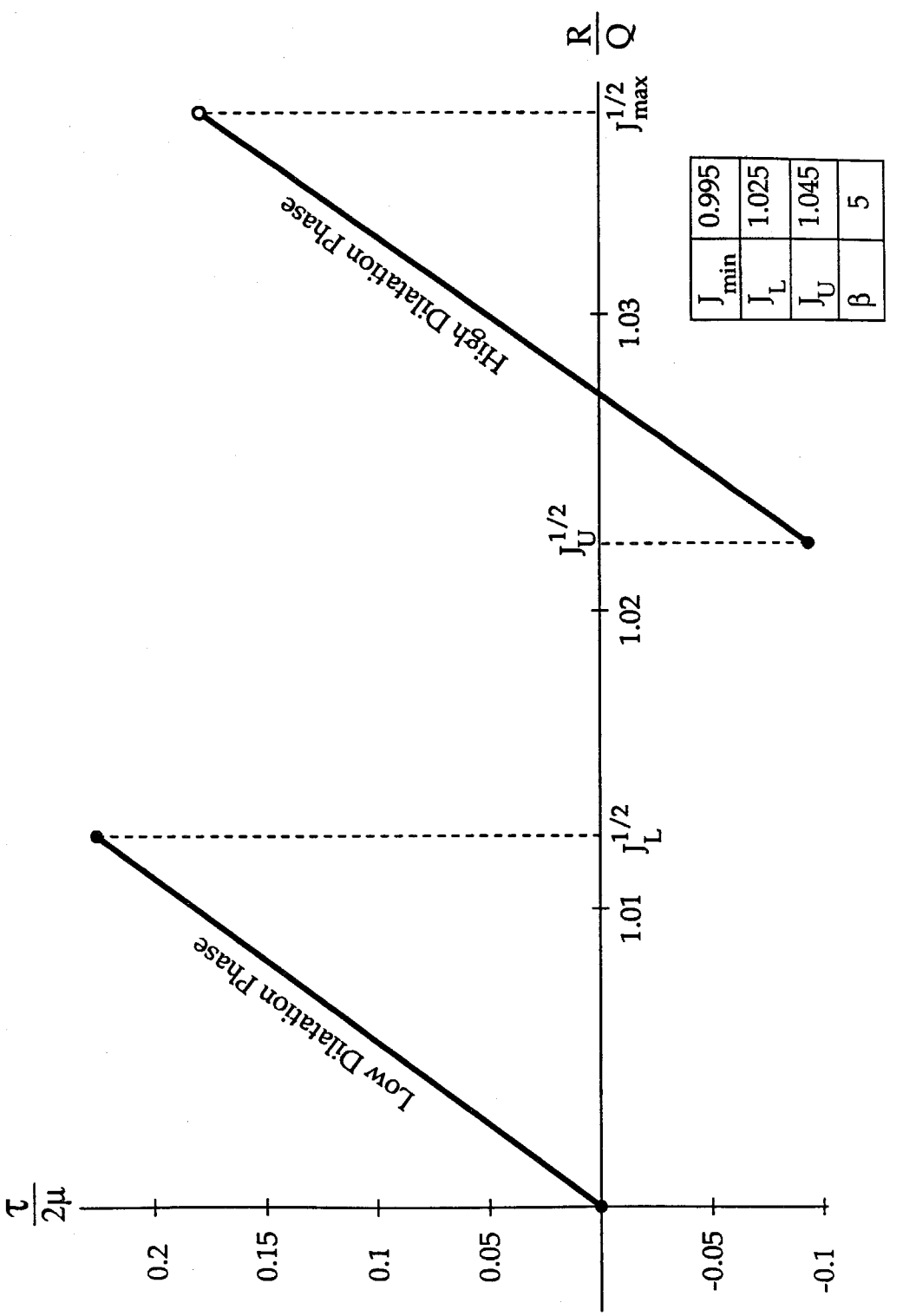

Figure 6. Single-phase macroscopic responses for the cylinder problem.

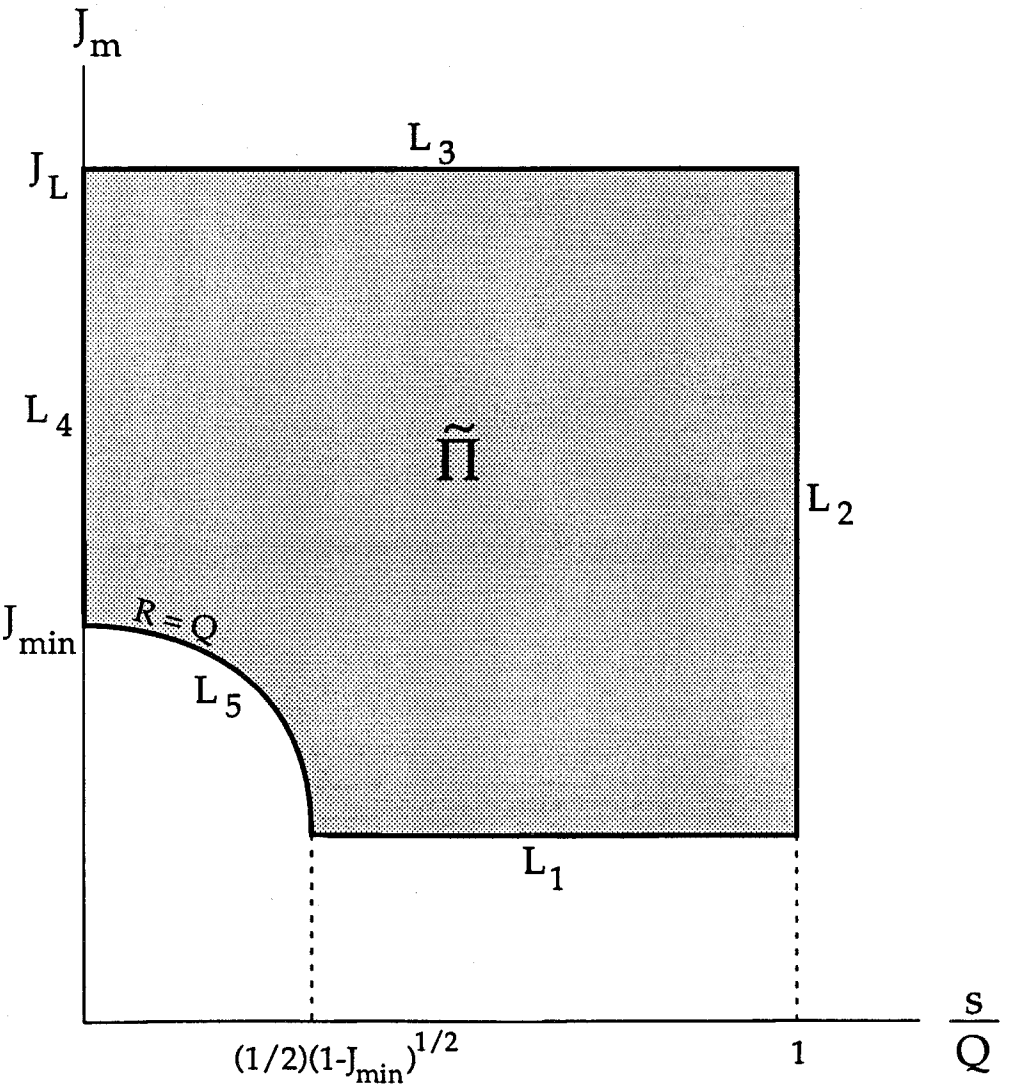

Figure 7. The set, $\tilde{\Pi}$, of all (s, J_m) pairs for which the phase segregation constraints are satisfied under extension; no surface fields.

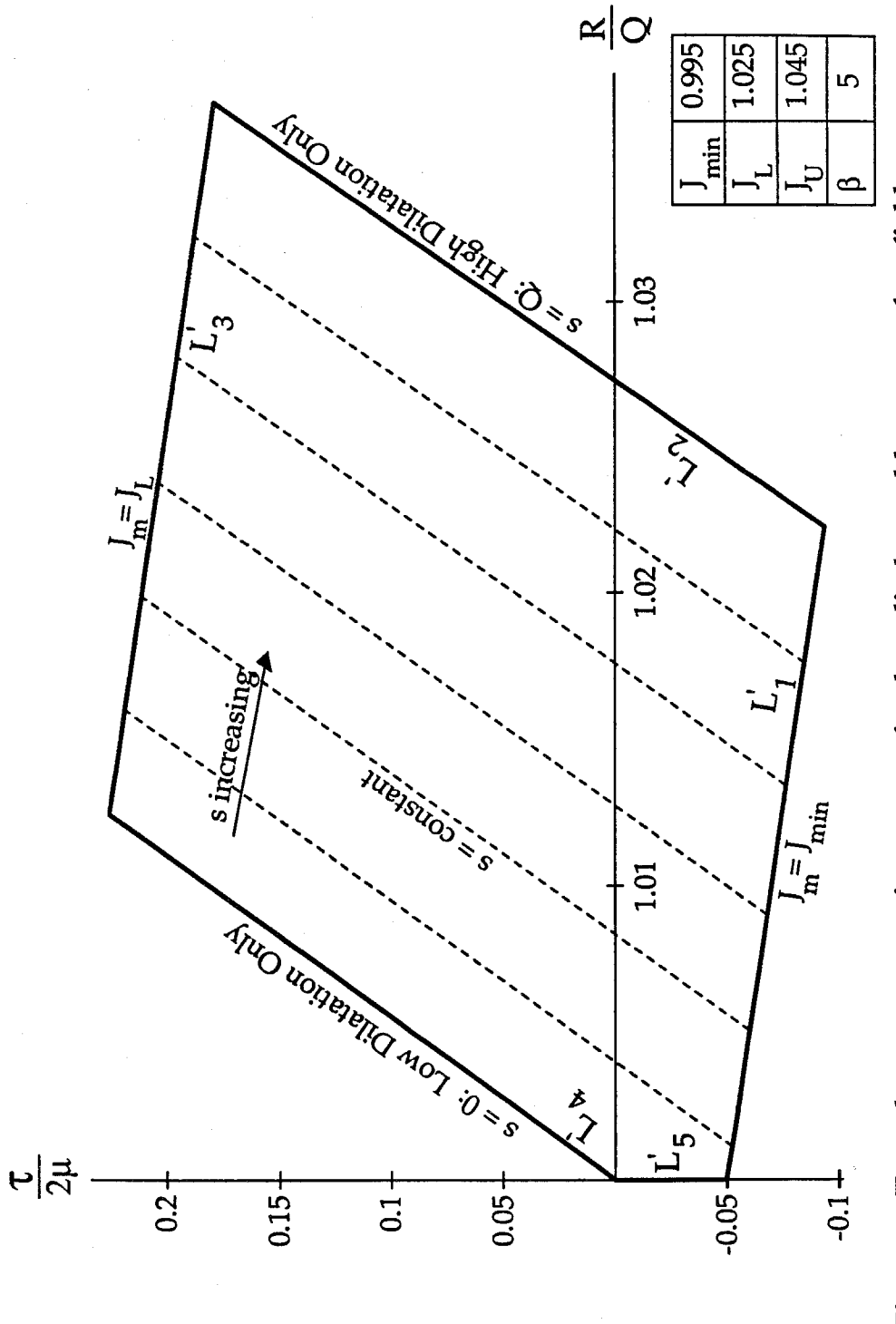

Figure 8. Two-phase macroscopic response for the cylinder problem; no surface fields.

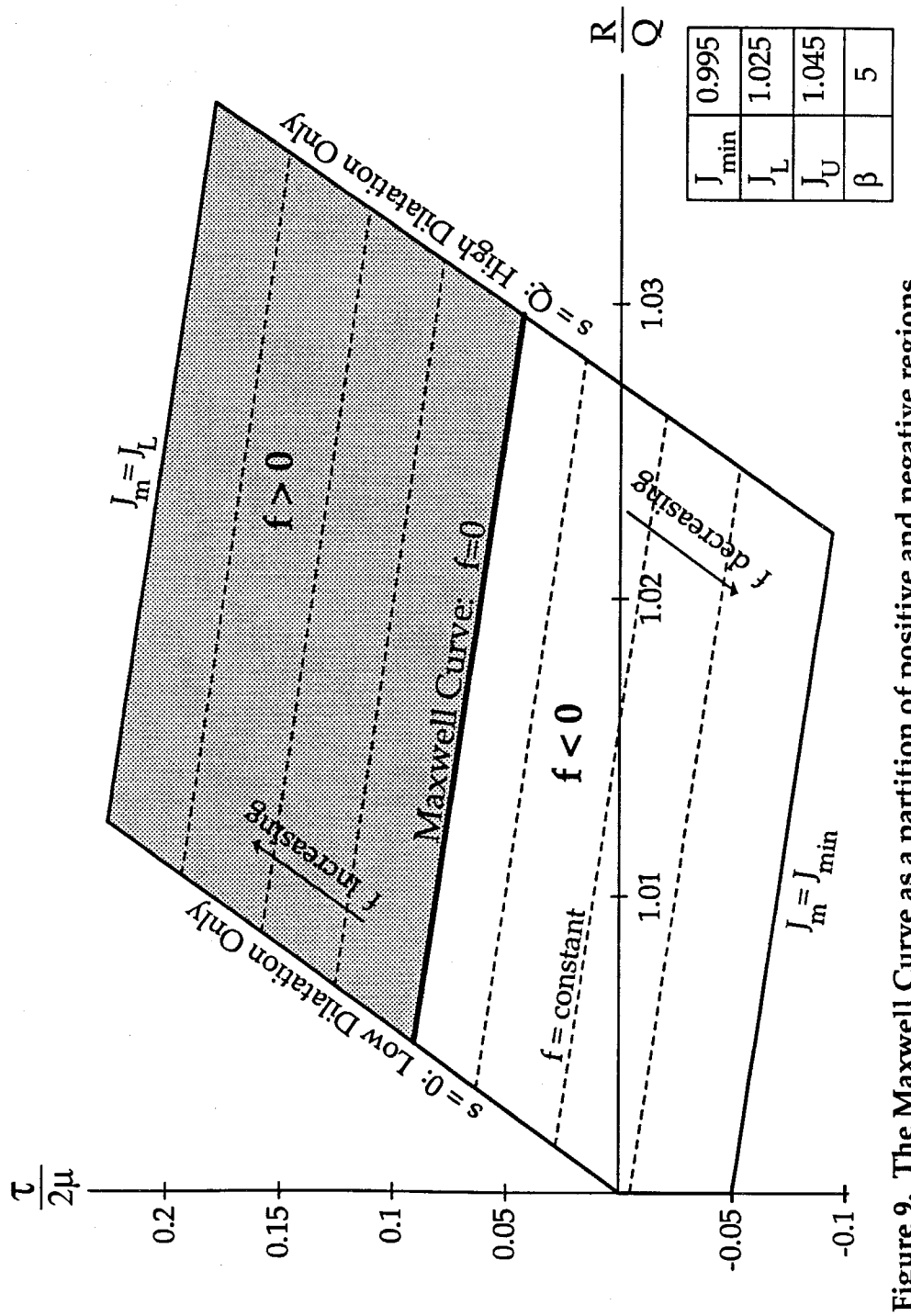

Figure 9. The Maxwell Curve as a partition of positive and negative regions of driving traction; no surface fields.

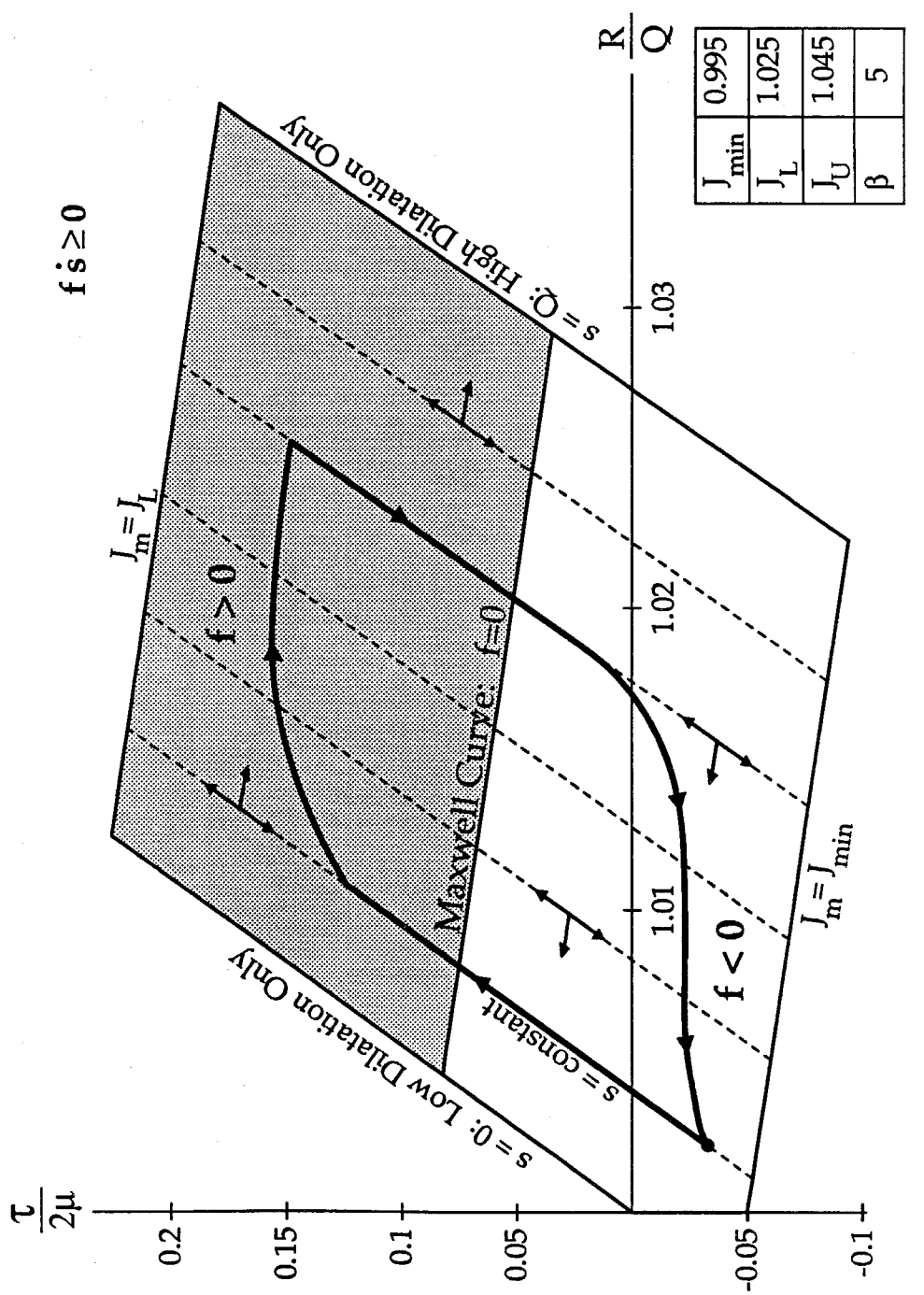

Figure 10. A sample two-phase motion satisfying the dissipation inequality restriction (shown by arrows); no surface fields.

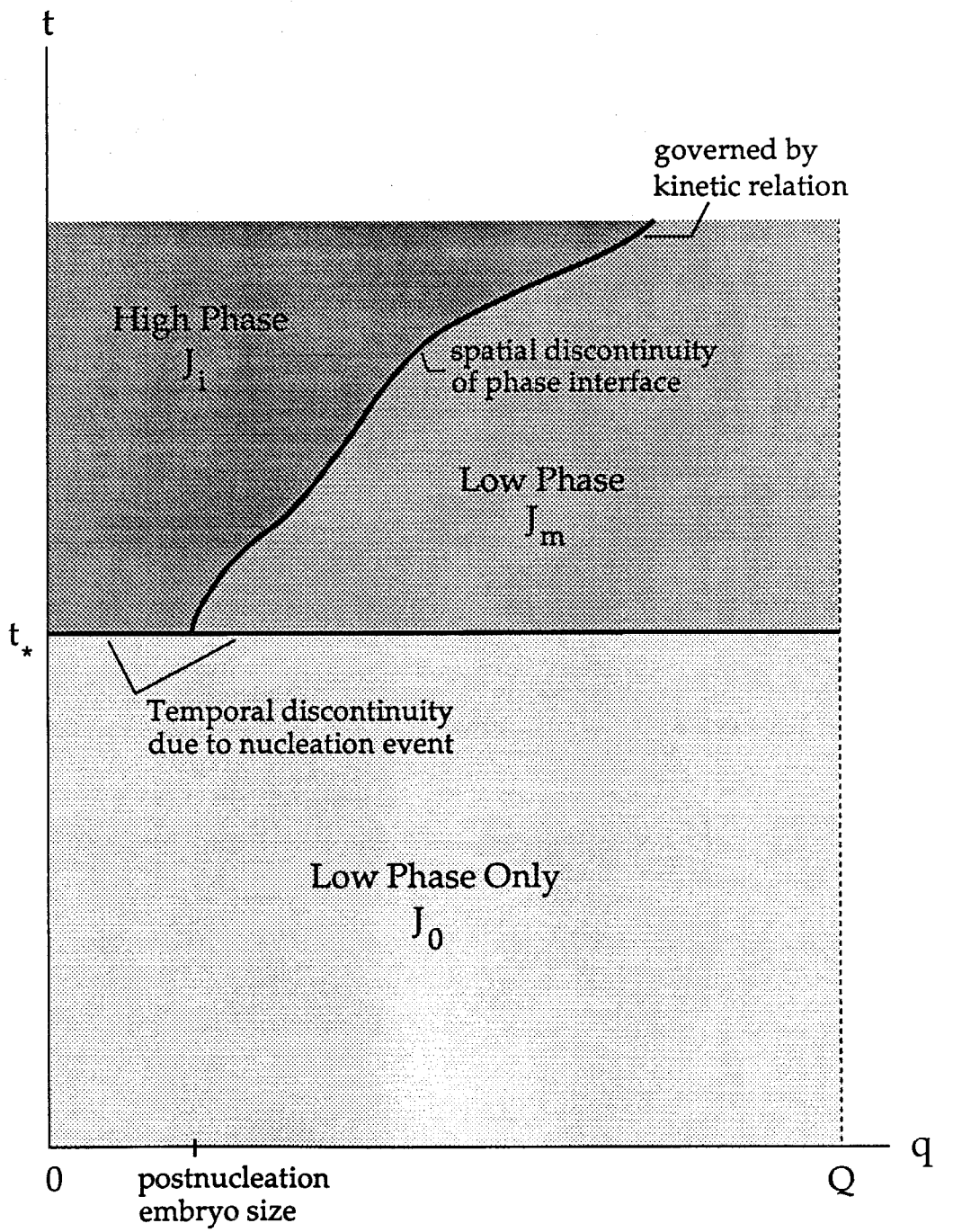

Figure 11. Time-position diagram of the nucleation and growth process showing both the interface and nucleation *shocks*.

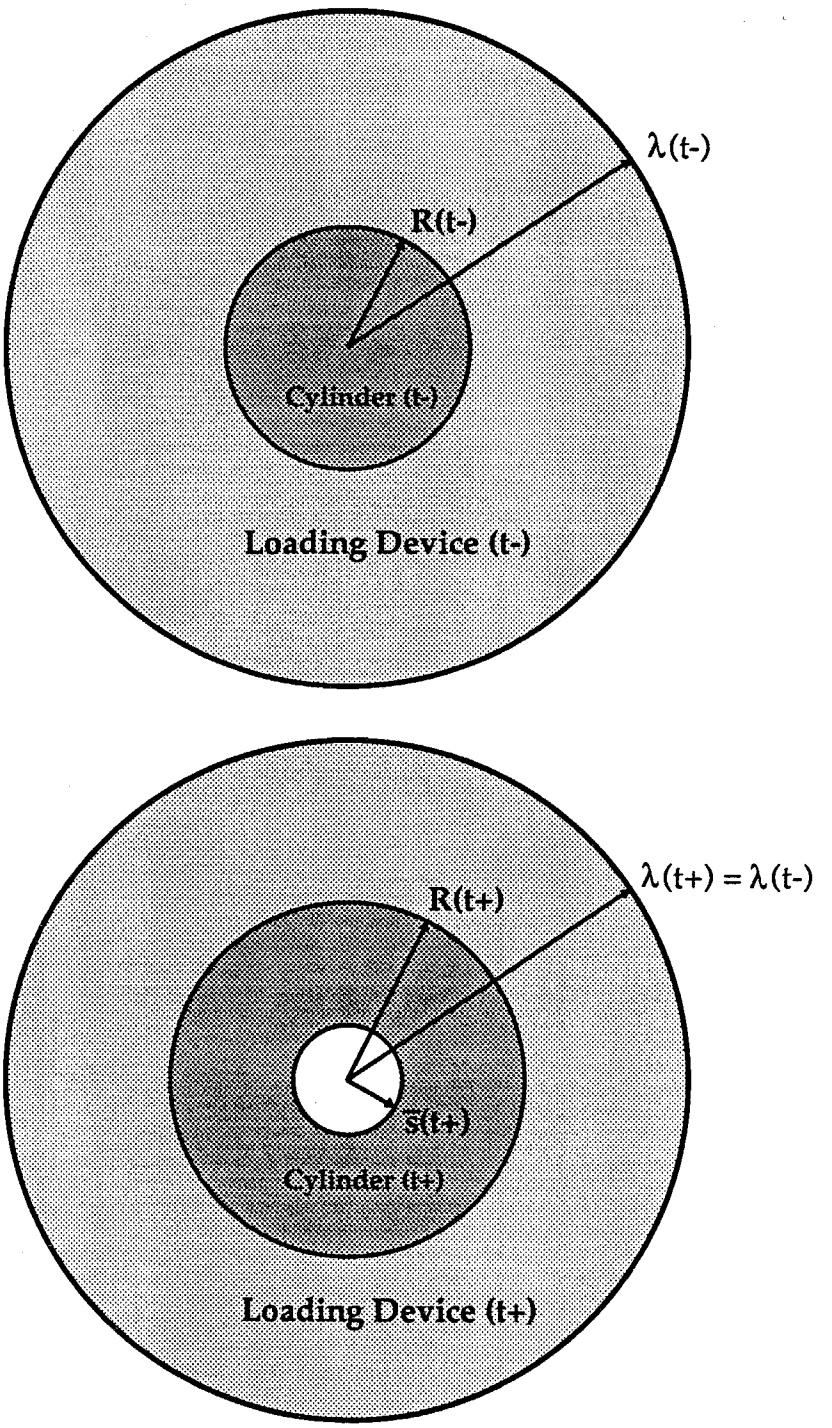

Figure 12. An interpretation of the Specialized Mixed Loading condition, where the exterior of the loading device is fixed during a nucleation event.

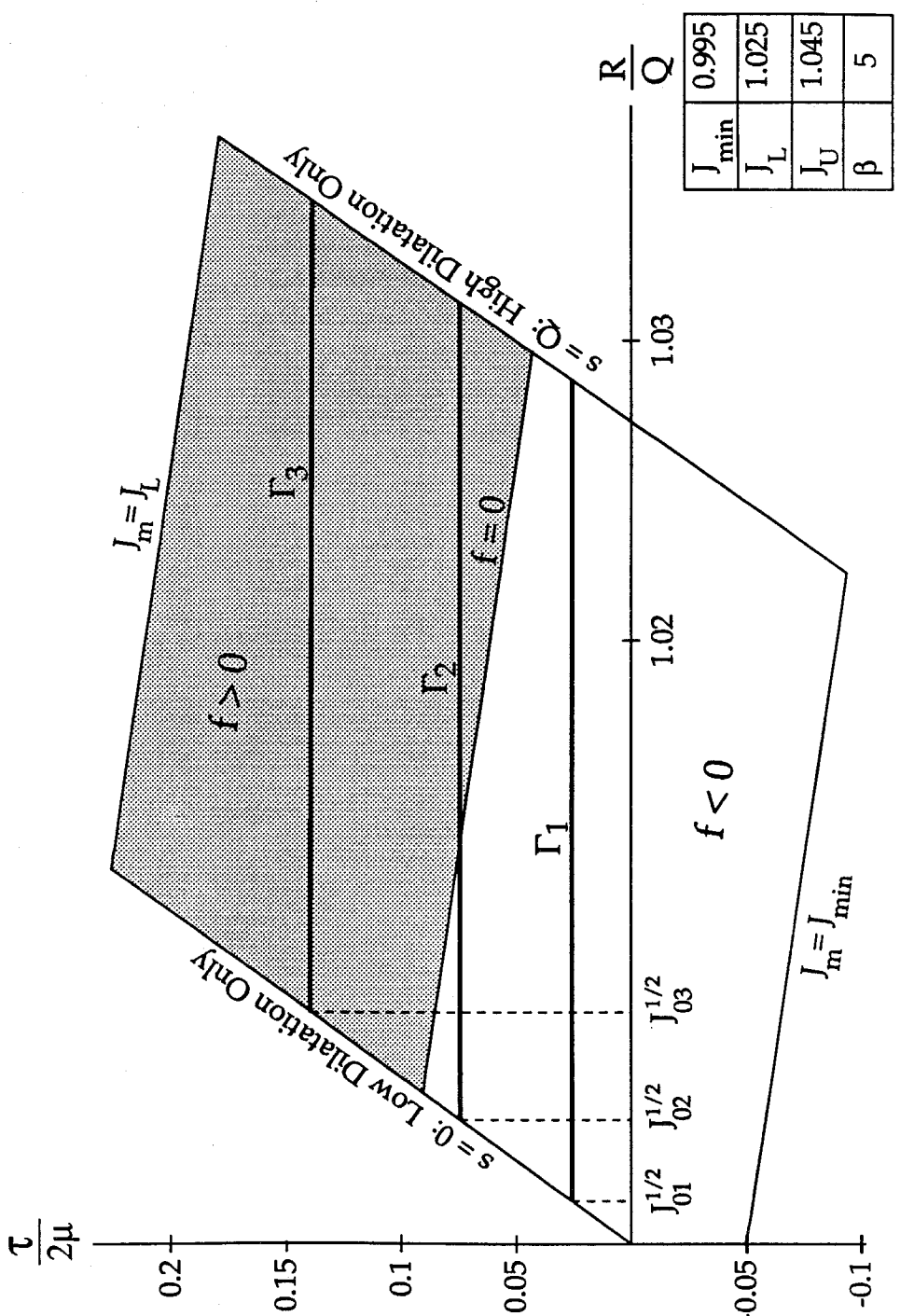

Figure 13(a). The two-phase states, Γ_k, to which the cylinder can nucleate from dilatation, J_{0k}, under soft loading; no surface fields.

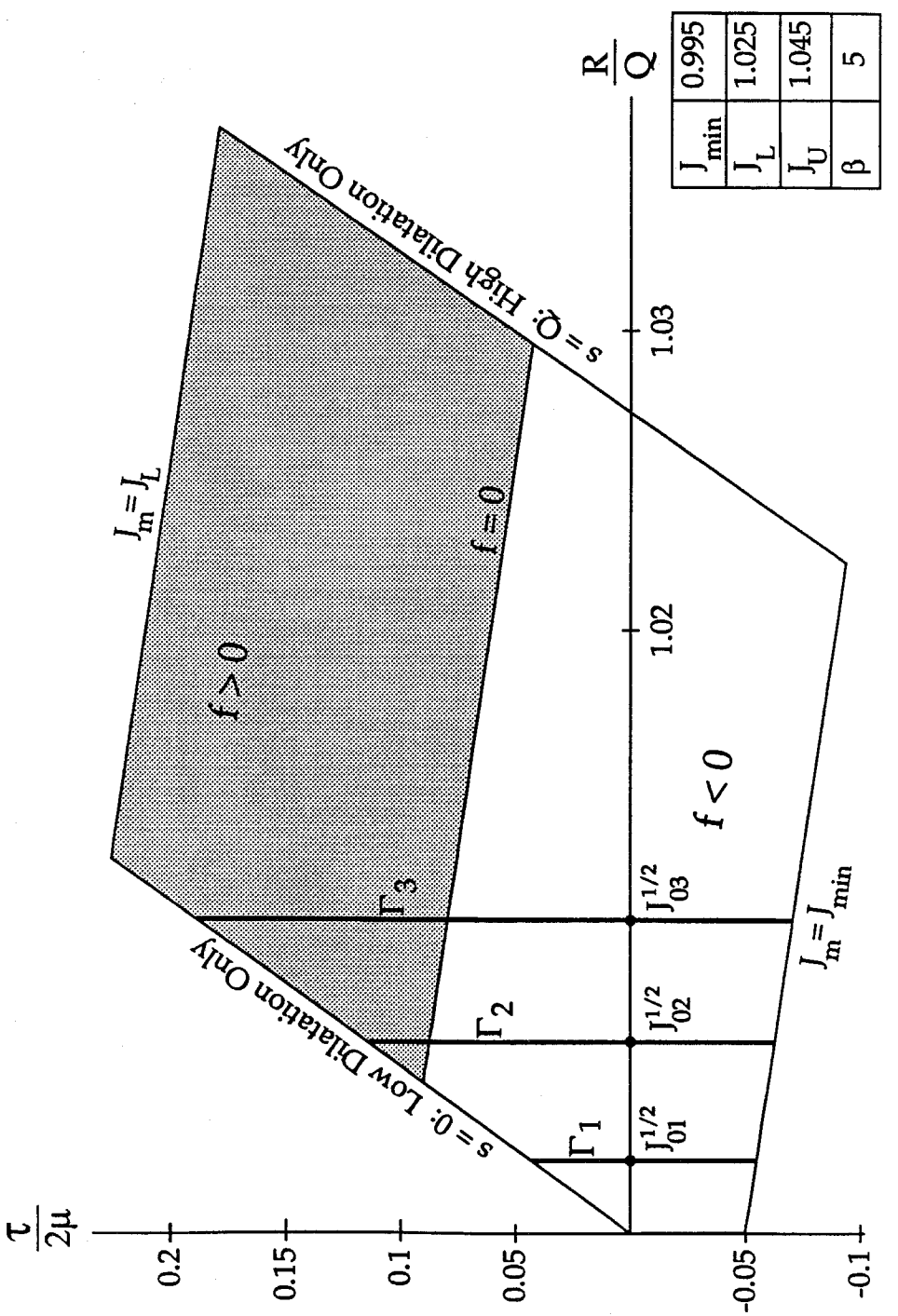

Figure 13(b). The two-phase states, Γ_k, to which the cylinder can nucleate from dilatation, J_{0k}, under hard loading; no surface fields.

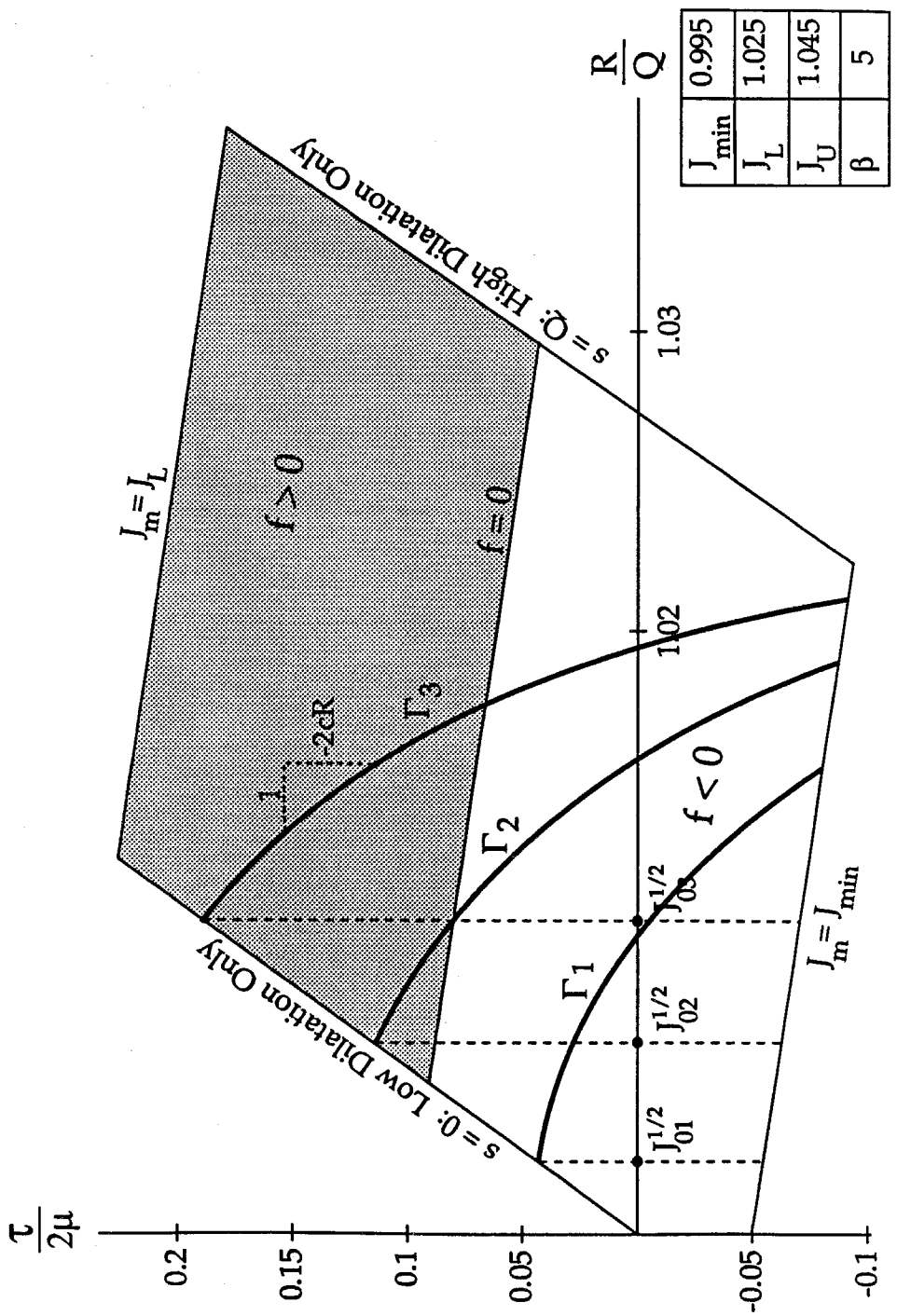

Figure 13(c). The two-phase states, Γ_k', to which the cylinder can nucleate from dilatation, J_{0k}' under specialized mixed loading; no surface fields.

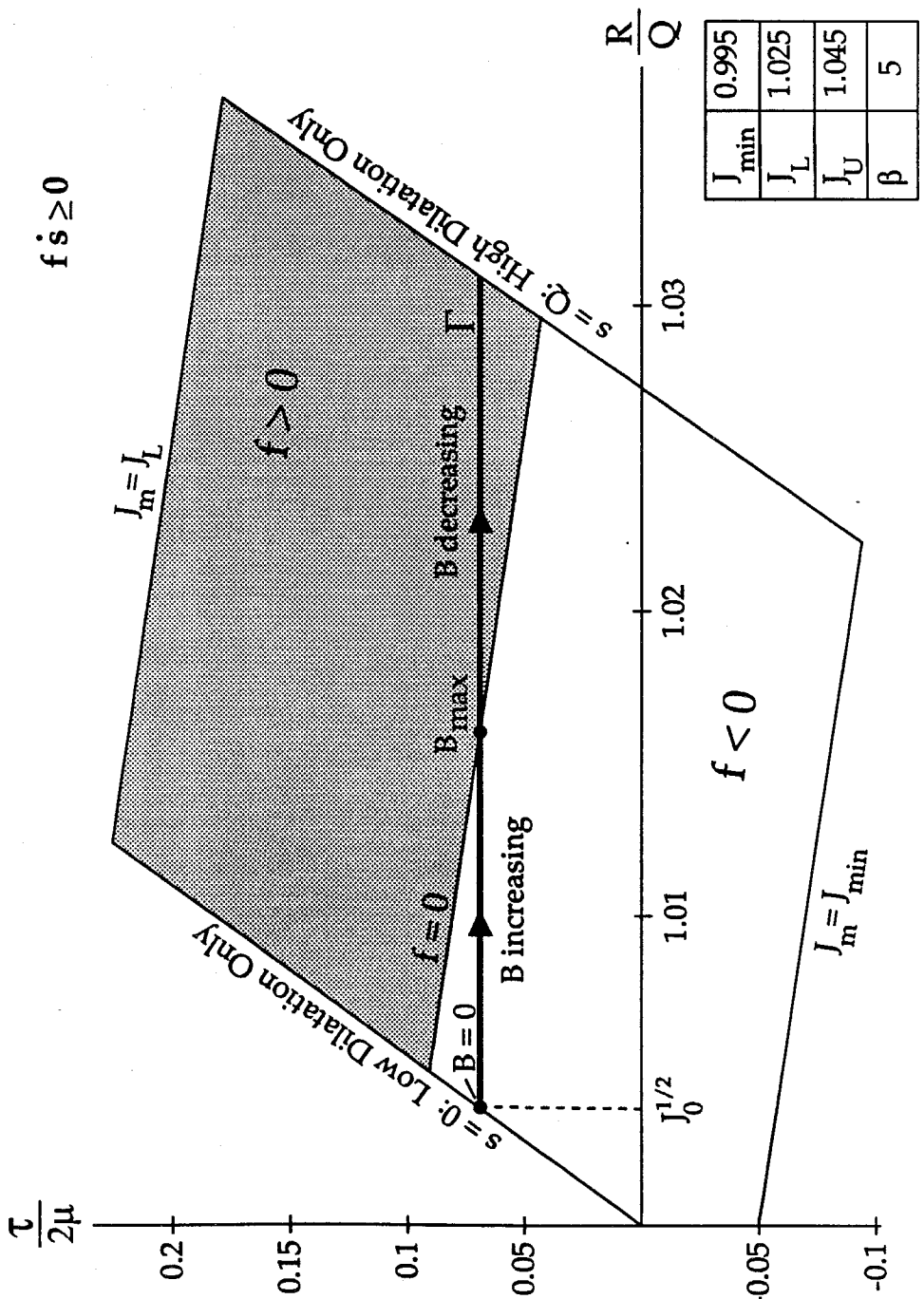

Figure 14. The relationship between B and f, illustrated for soft loading; no surface fields.

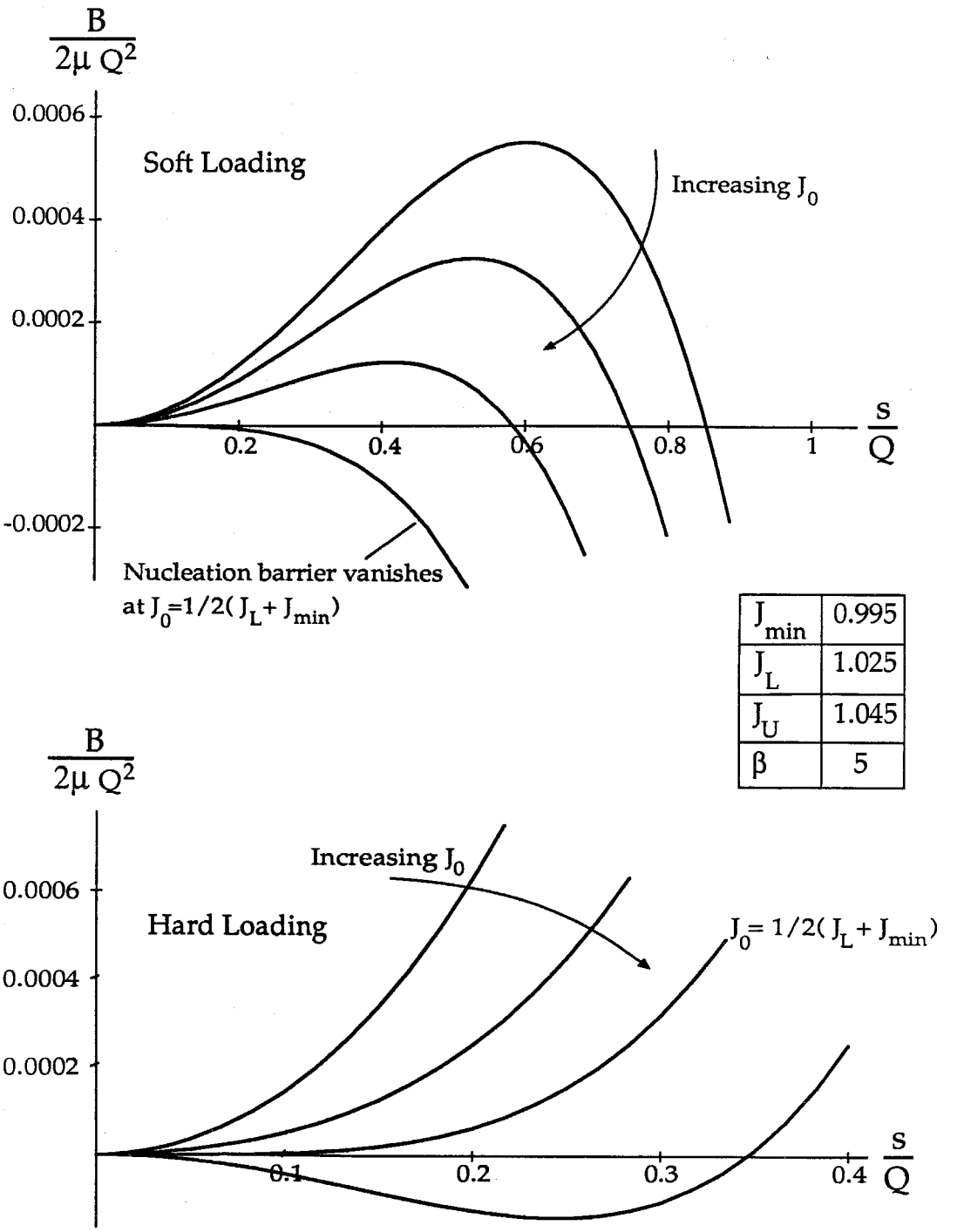

Figure 15. Profiles of nucleation energy, B, for both soft and hard loading; no surface fields.

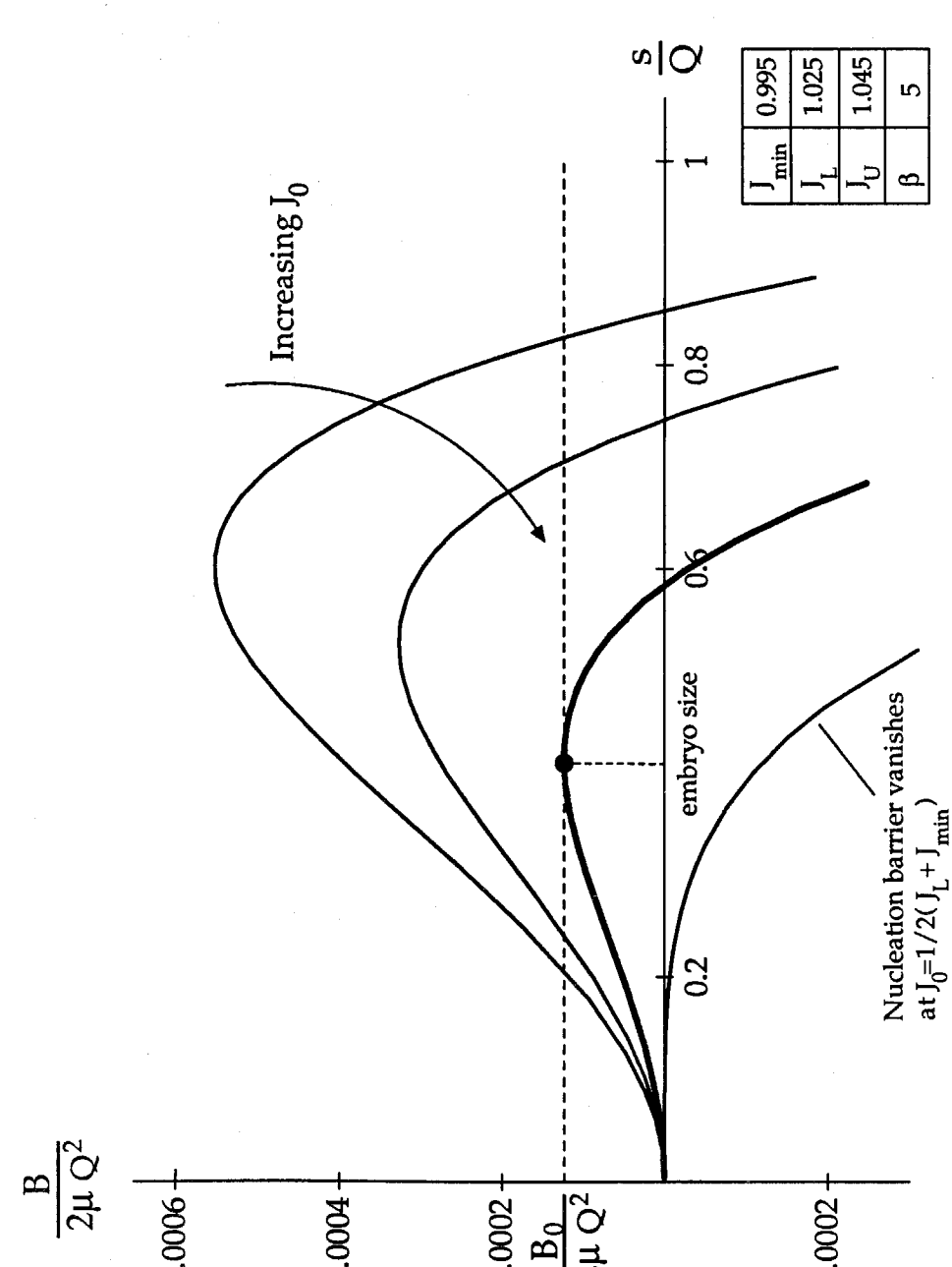

Figure 16(a). Nucleation under soft loading with no surface fields. Under increasing J_0, the nucleation barrier eventually drops to B_0 and nucleation occurs.

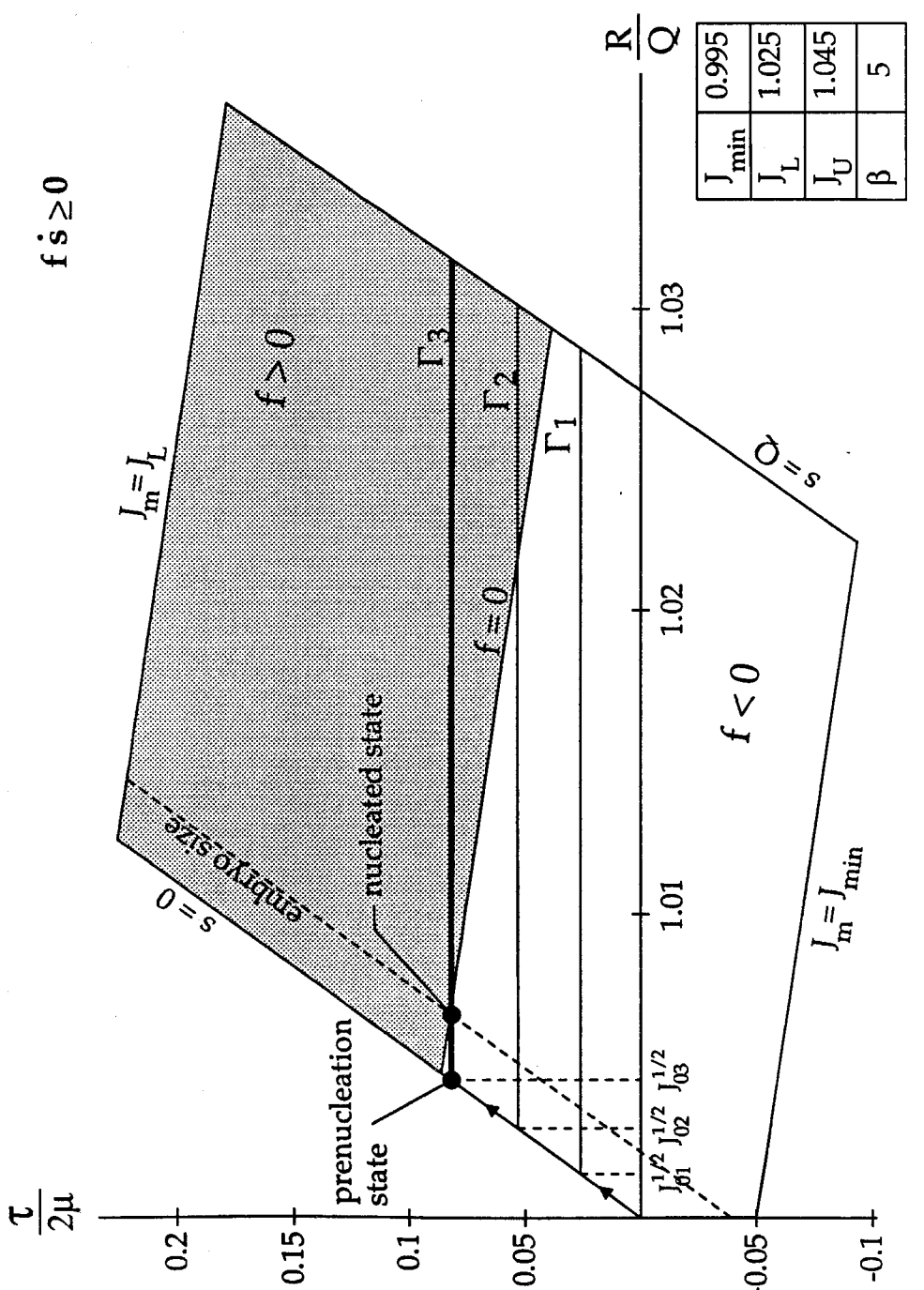

Figure 16(b). Nucleation event under soft loading; no surface fields.

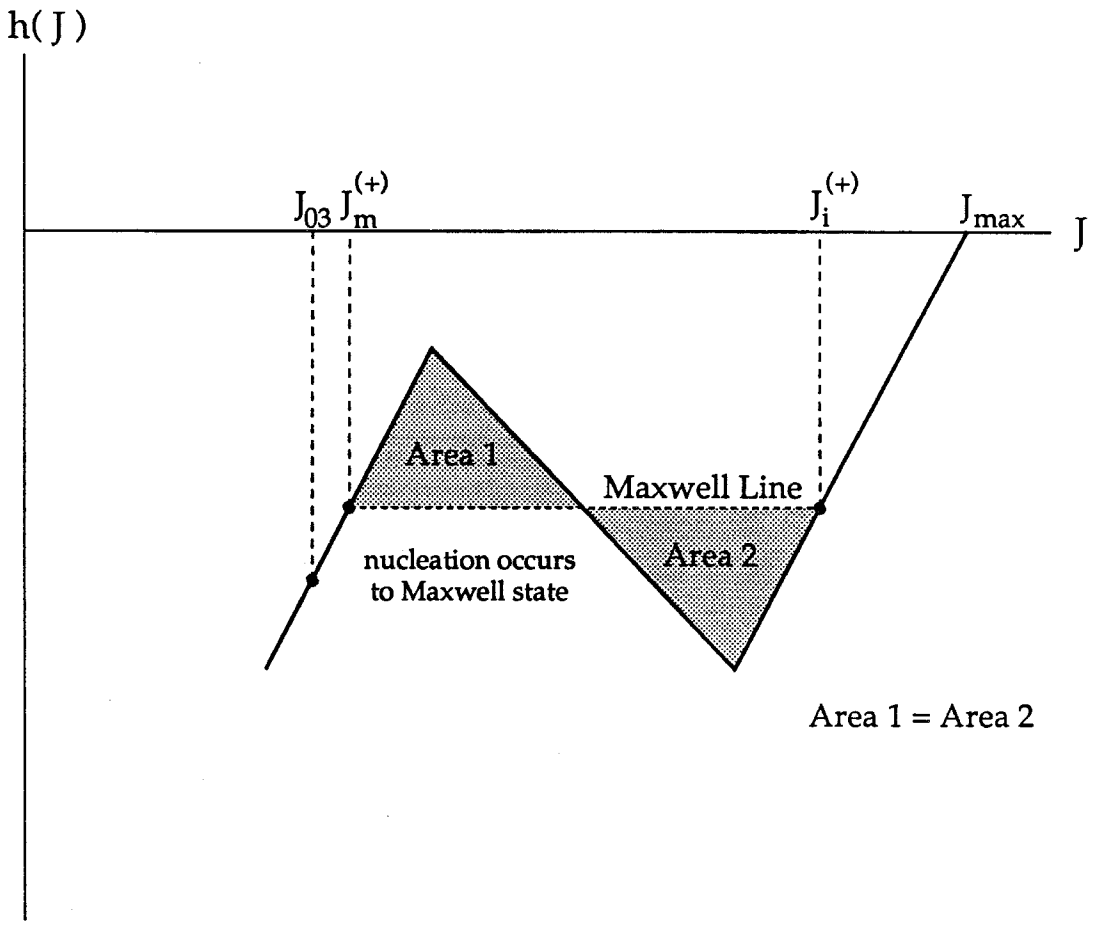

Figure 16(c). Nucleation event under soft loading; no surface fields.

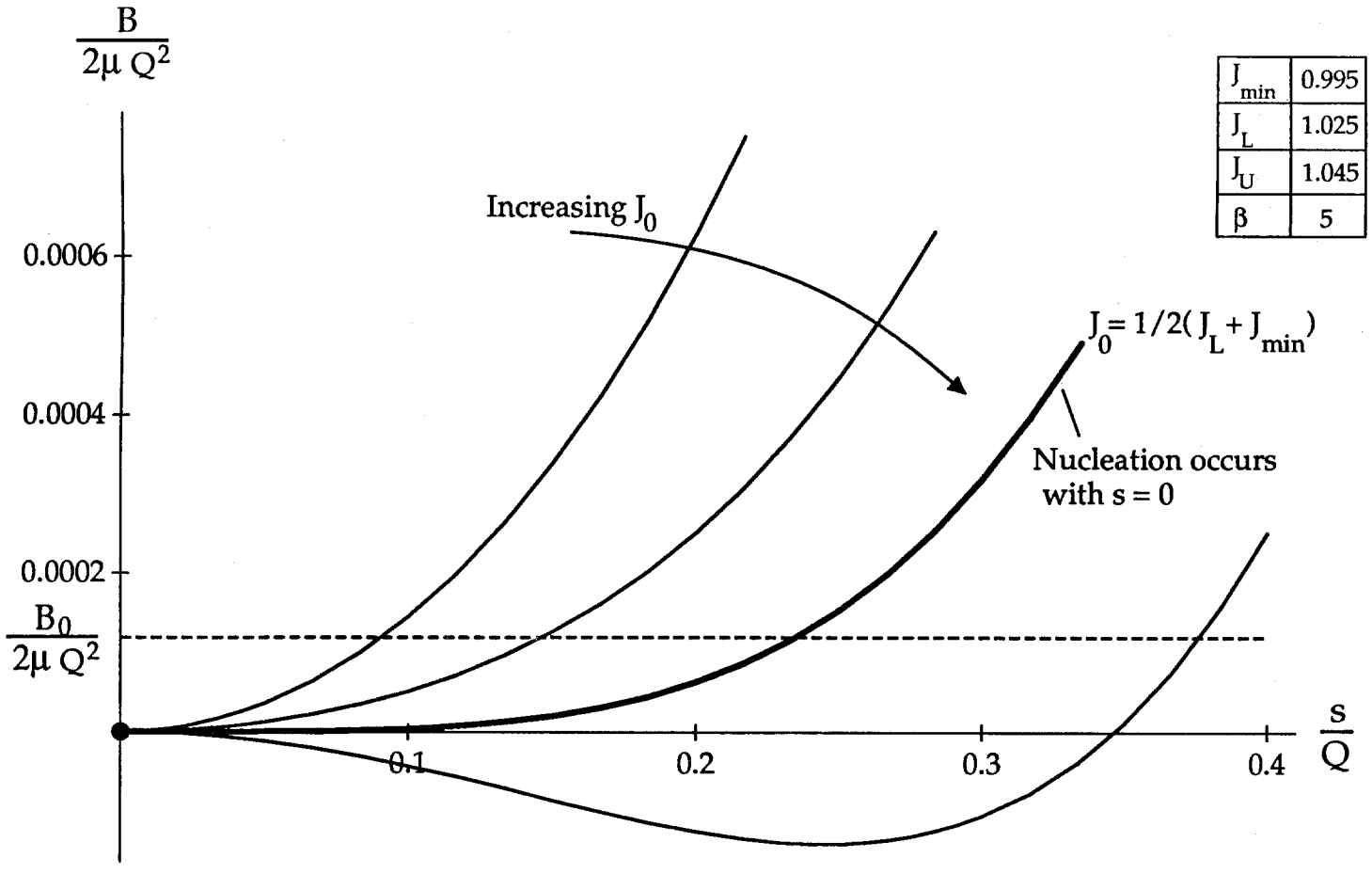

Figure 17(a). Nucleation under hard loading with no surface fields. Under increasing J_0, the convexity of $\tilde{B}(\cdot, J_0)$ decreases. Nucleation occurs with an embryo of zero measure when the convexity becomes zero.

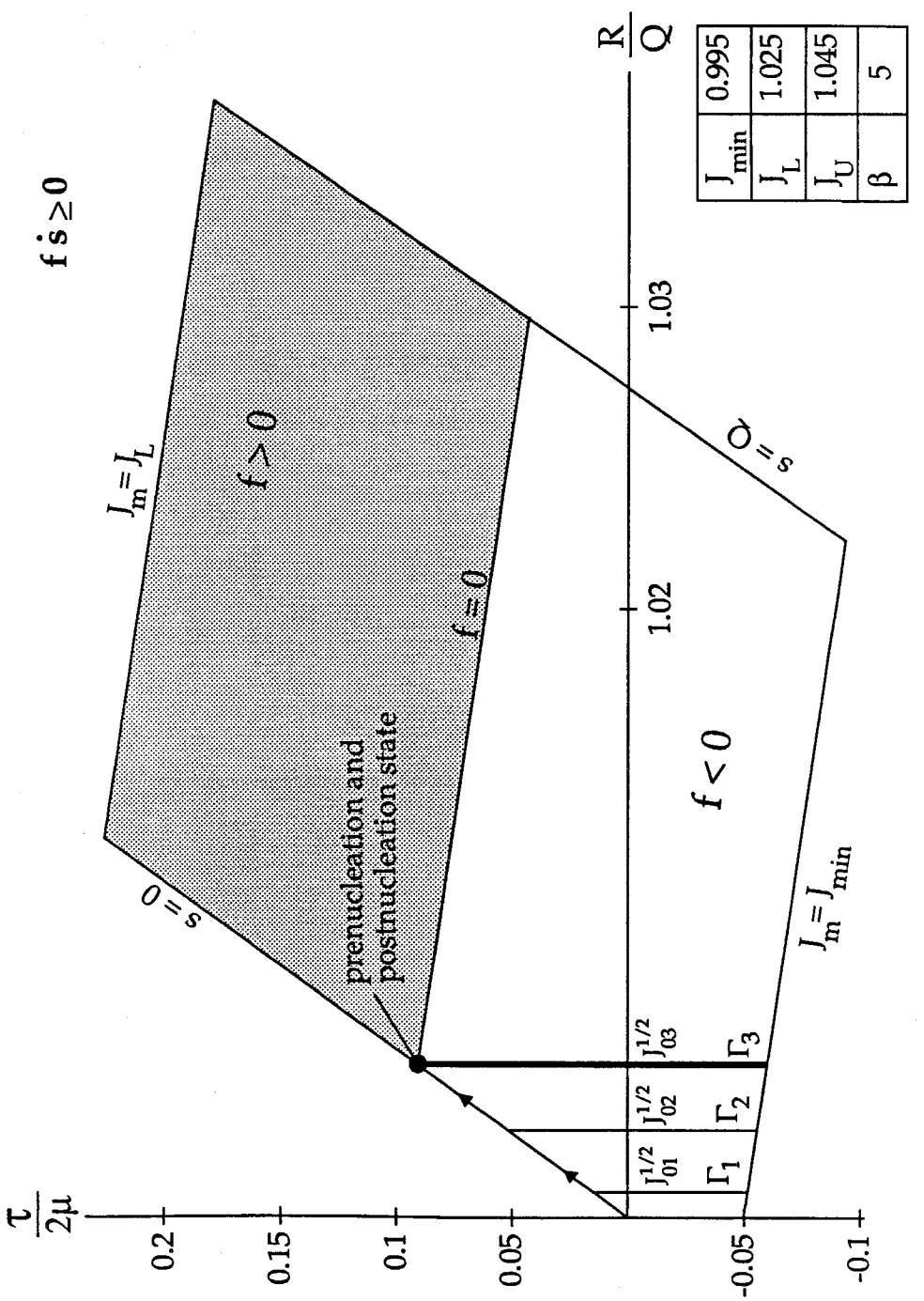

Figure 17(b). Nucleation event under hard loading; no surface fields.

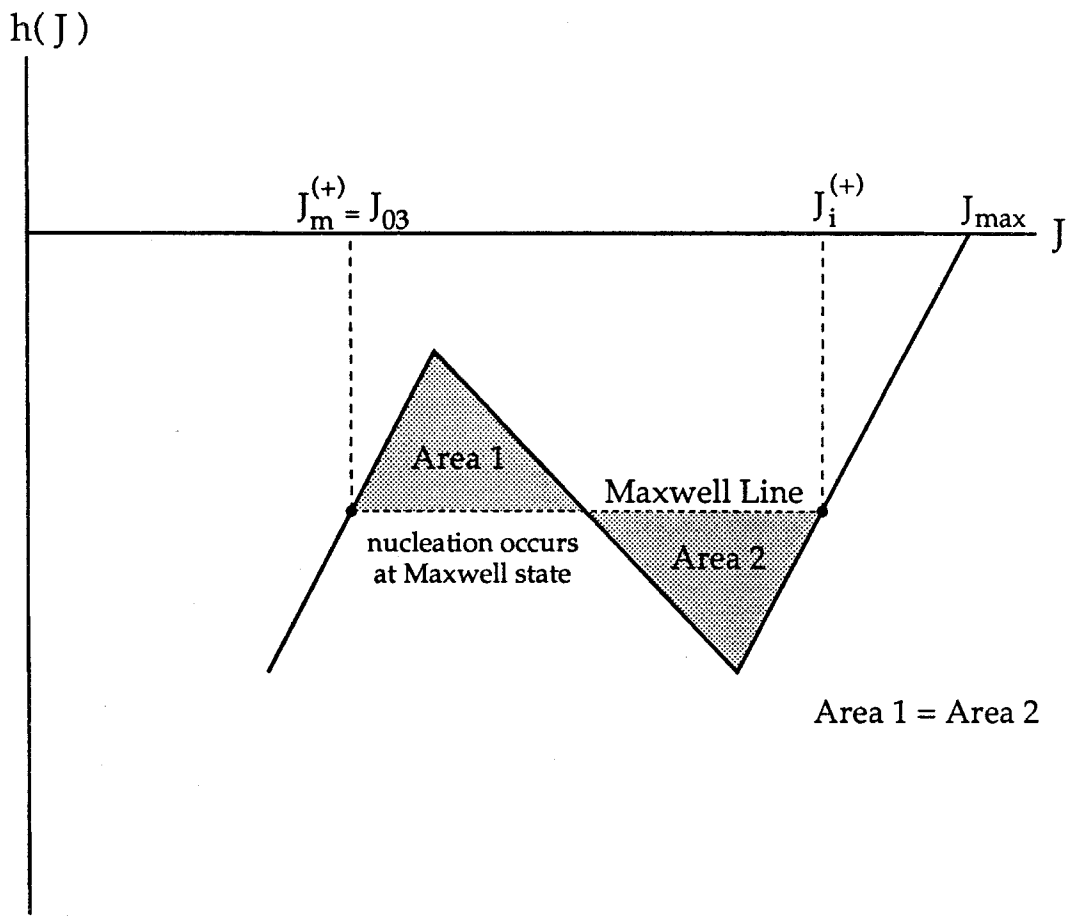

Figure 17(c). Nucleation event under hard loading; no surface fields.

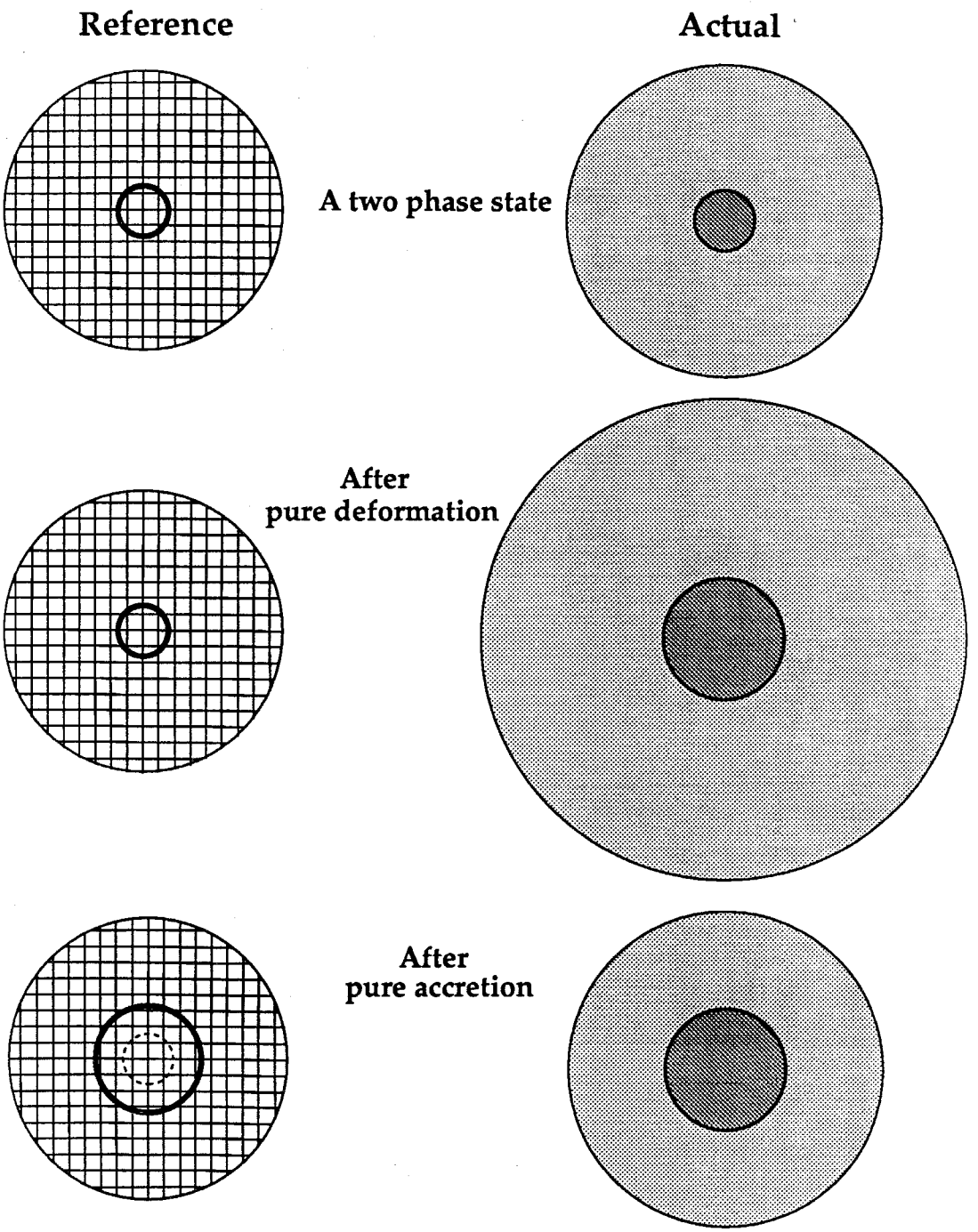

Figure 18. An atomistic interpretation of bonding energy. Pure deformation does not increase the total interface energy while pure accretion does. (Note that in actuality, accretion cannot occur without some deformation.)

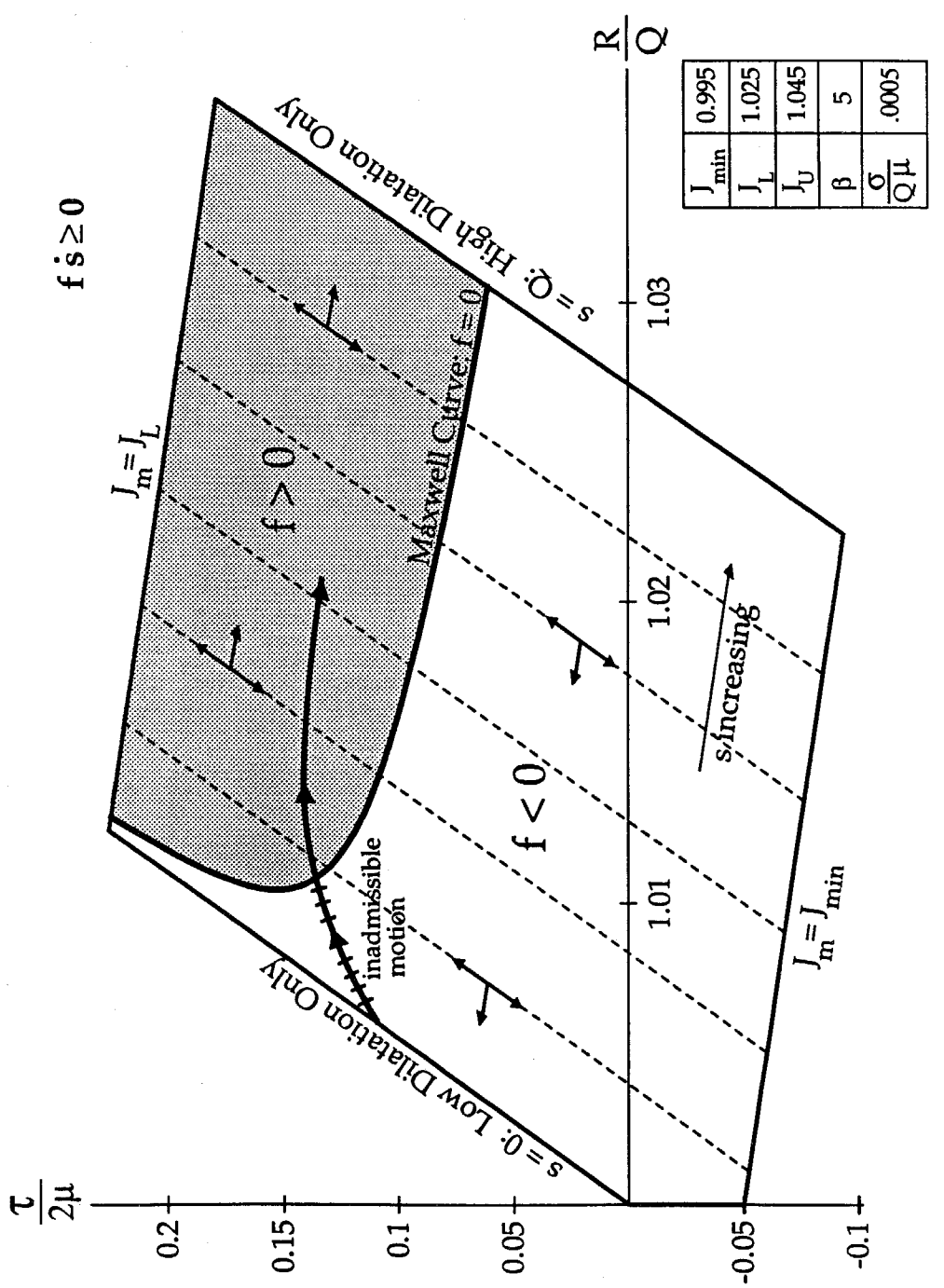

Figure 19. Macroscopic response curve for the interface with bonding energy.

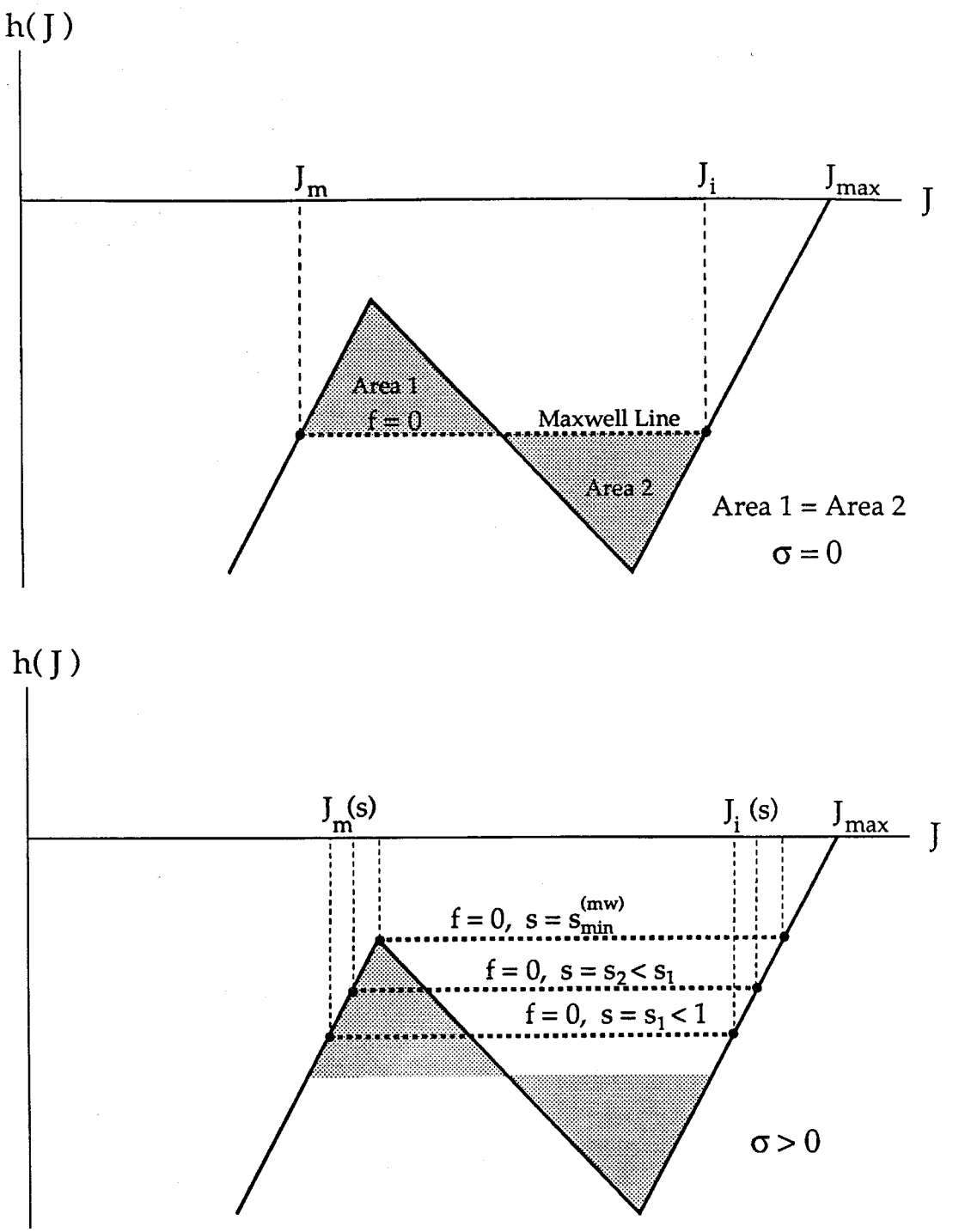

Figure 20. The Equal Area Rule , Figure (a), and its violation due to interface bonding energy, Figure (b).

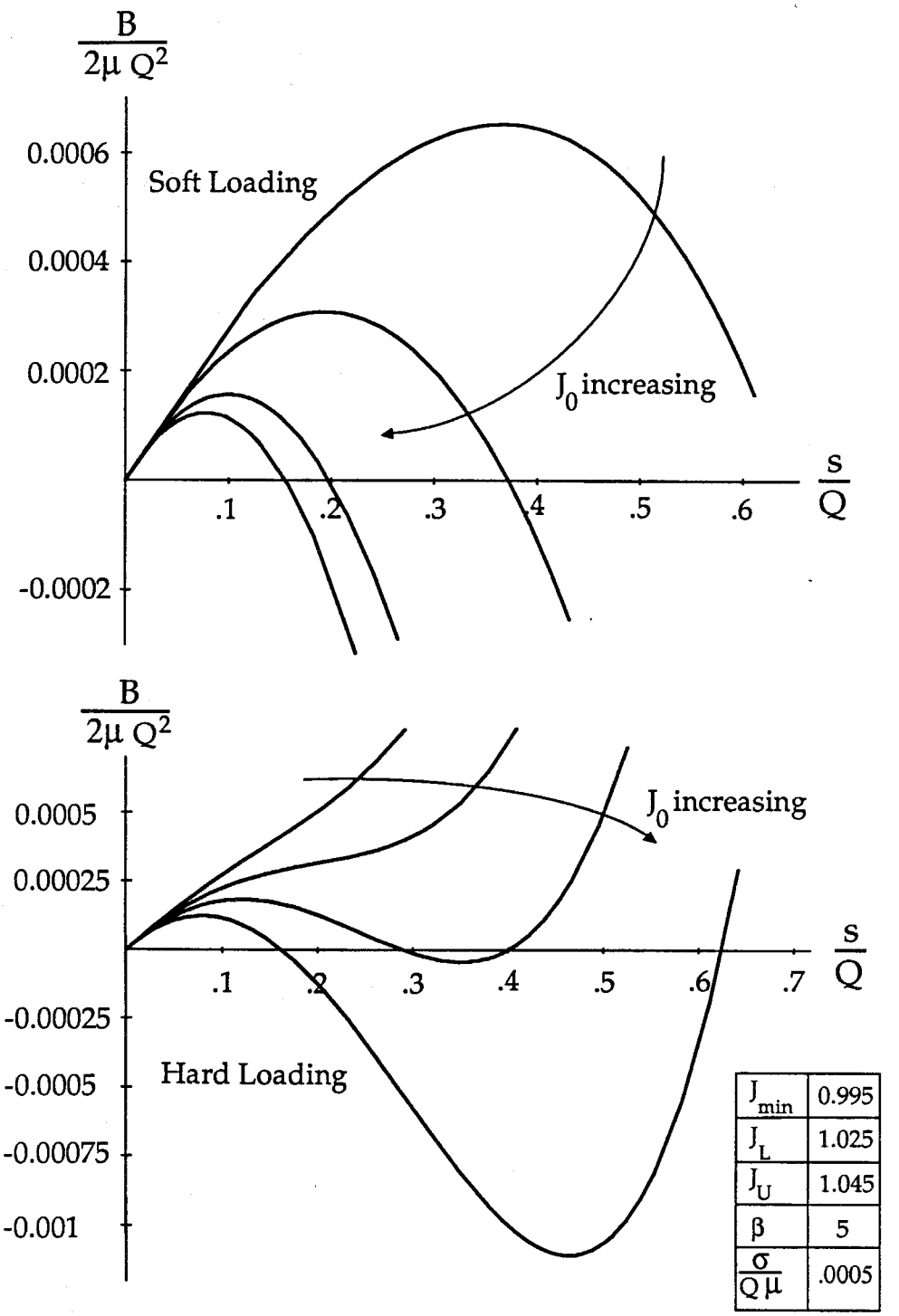

Figure 21. Profiles of nucleation energy, B, for both soft and hard loading; interfaces with bonding energy.

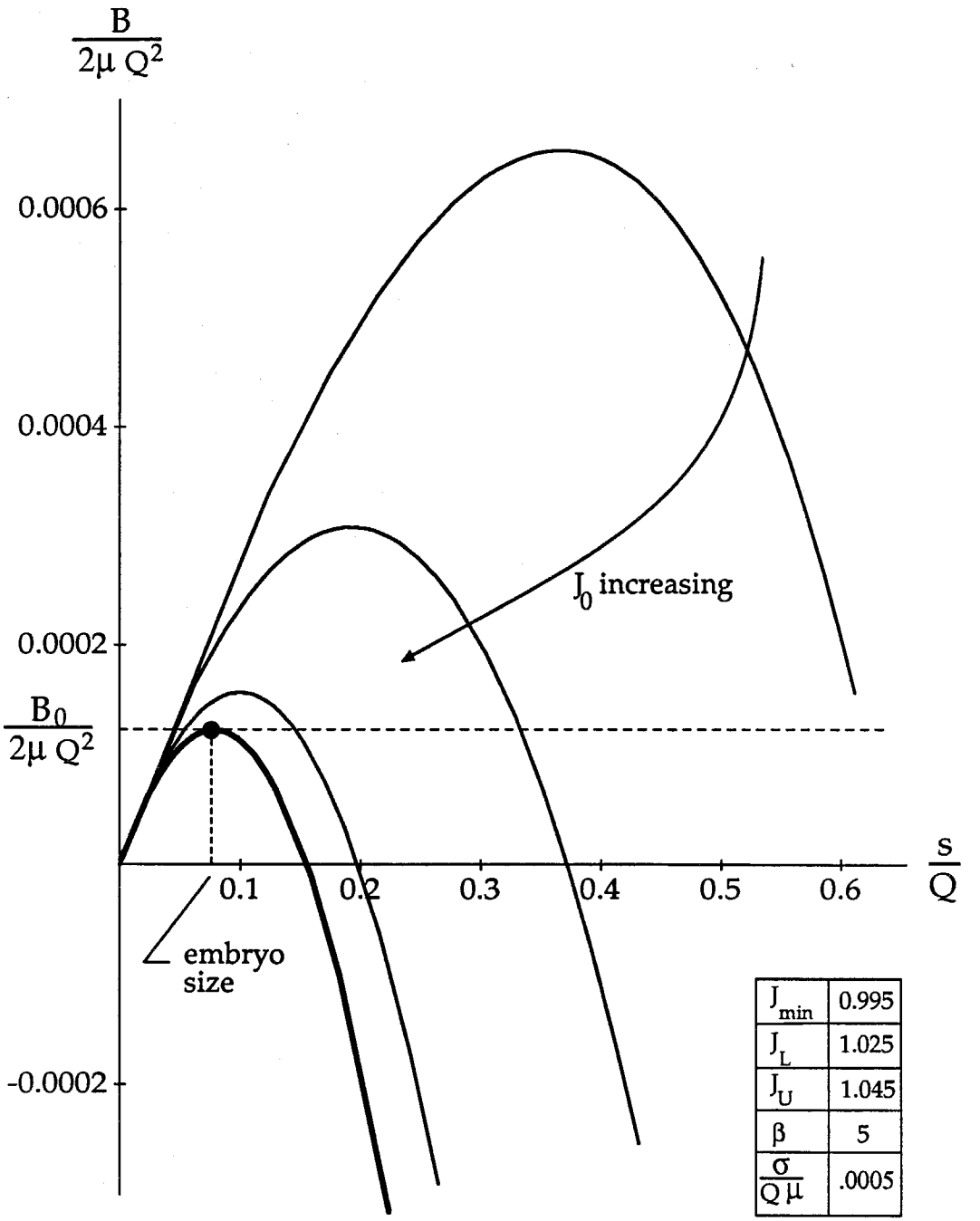

Figure 22(a). Nucleation under soft loading with interface bonding energy. Under increasing J_0, the nucleation barrier *may* eventually drop to B_0, at which point nucleation occurs.

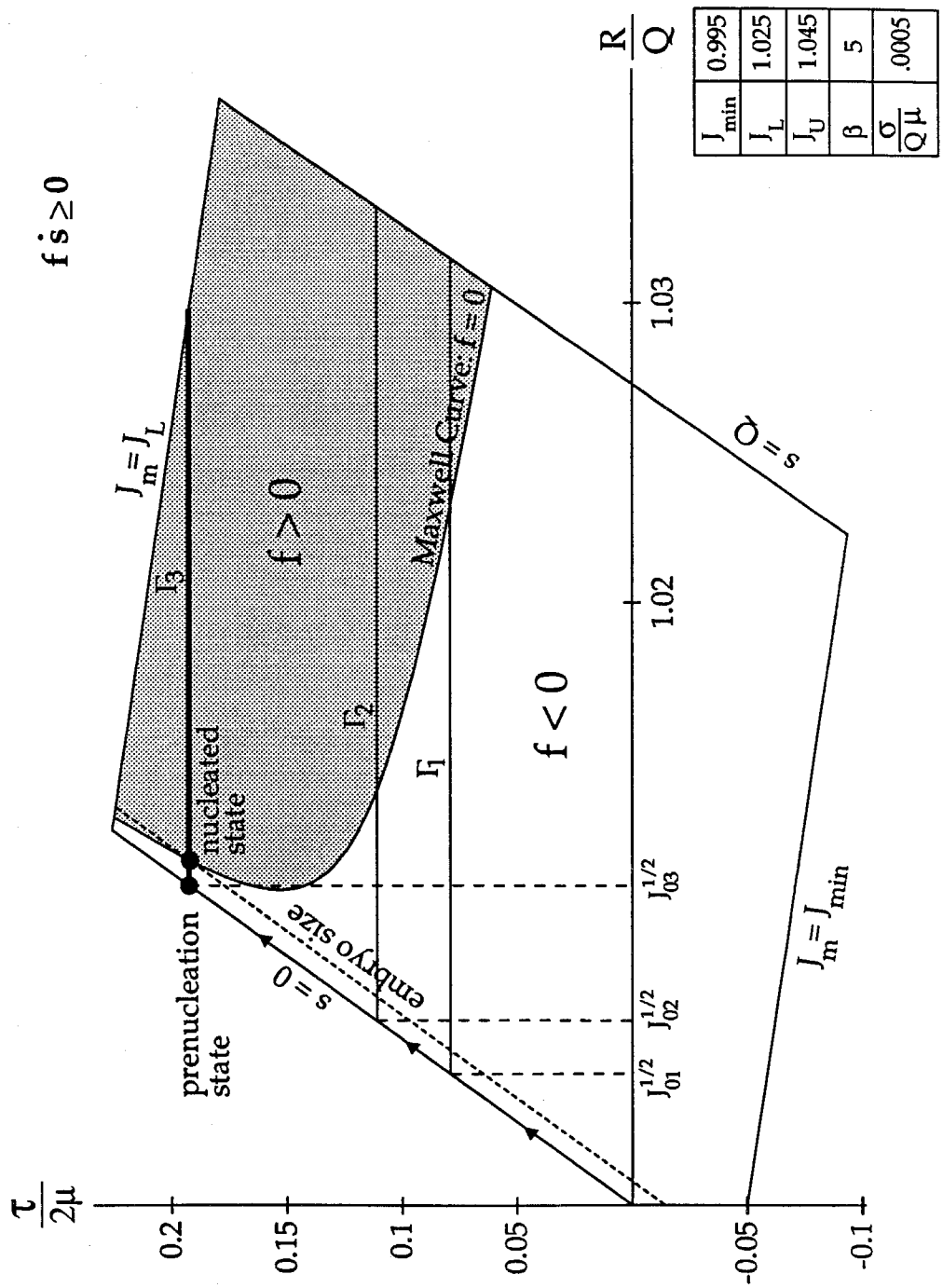

Figure 22(b). Nucleation event under soft loading for interfaces with bonding energy.

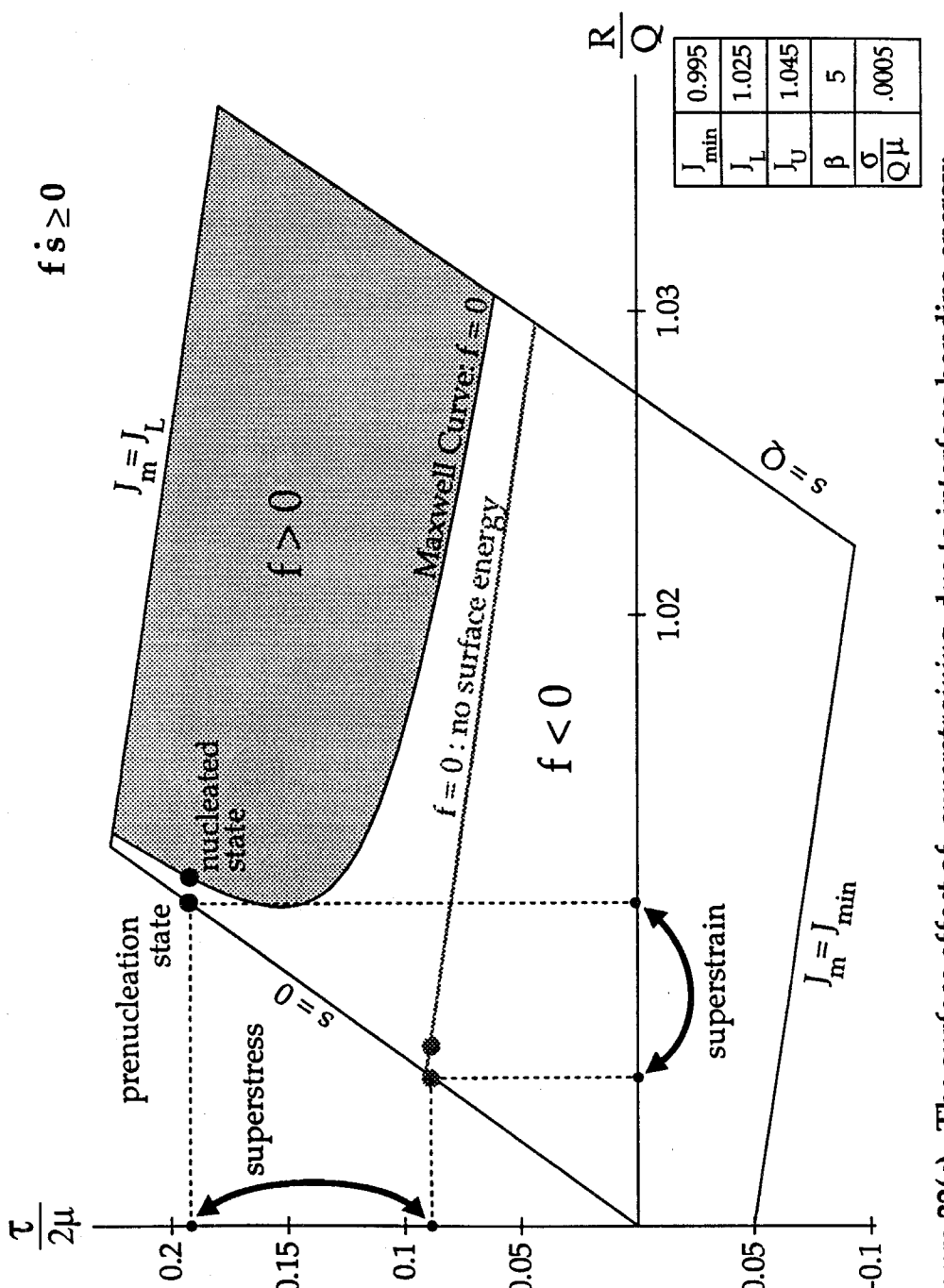

Figure 22(c). The surface effect of *superstraining* due to interface bonding energy; soft loading.

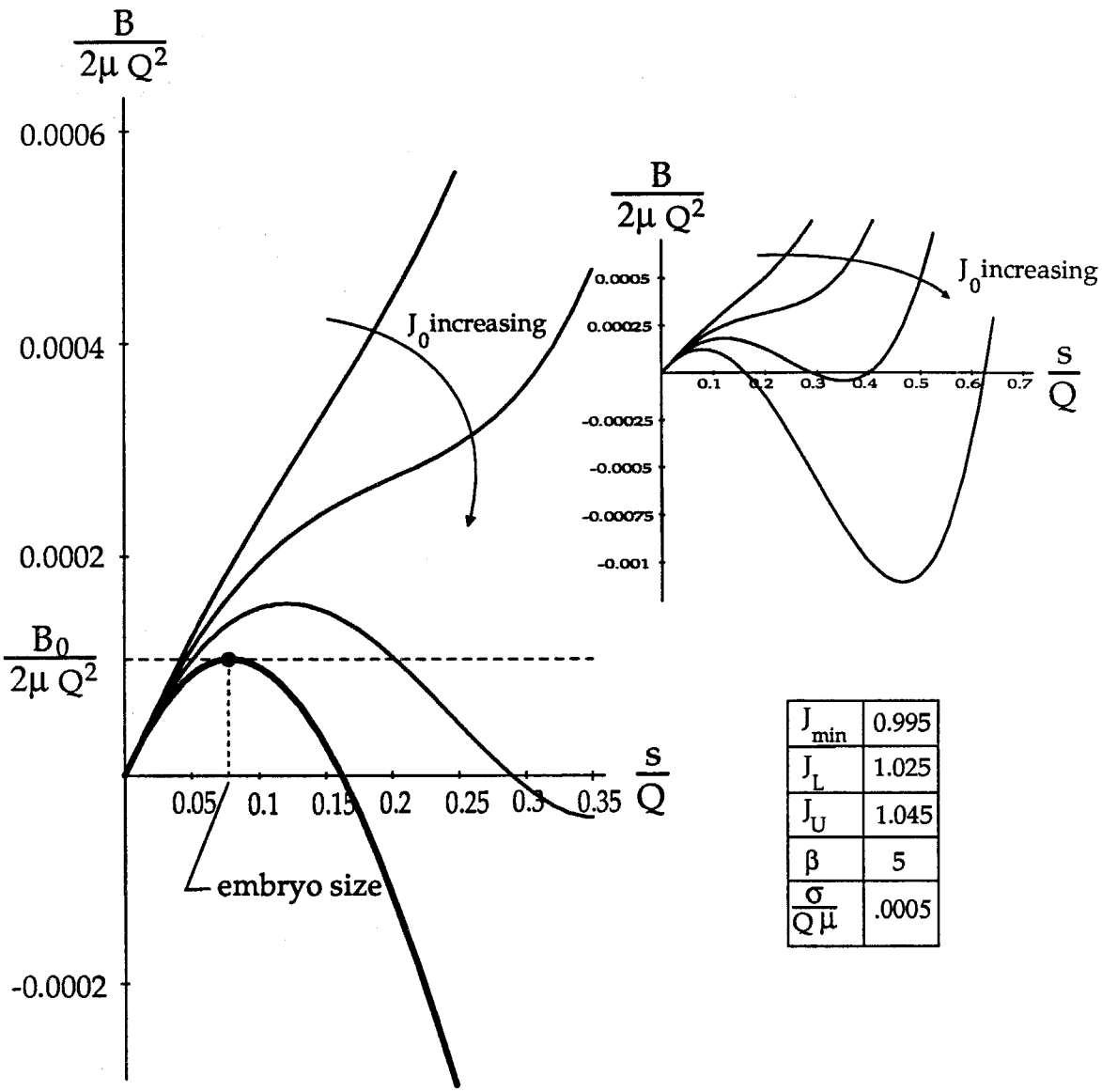

Figure 23(a). Nucleation under hard loading with interface bonding energy. Under increasing J_0, the nucleation barrier *may* eventually drop to B_0, at which point nucleation occurs.

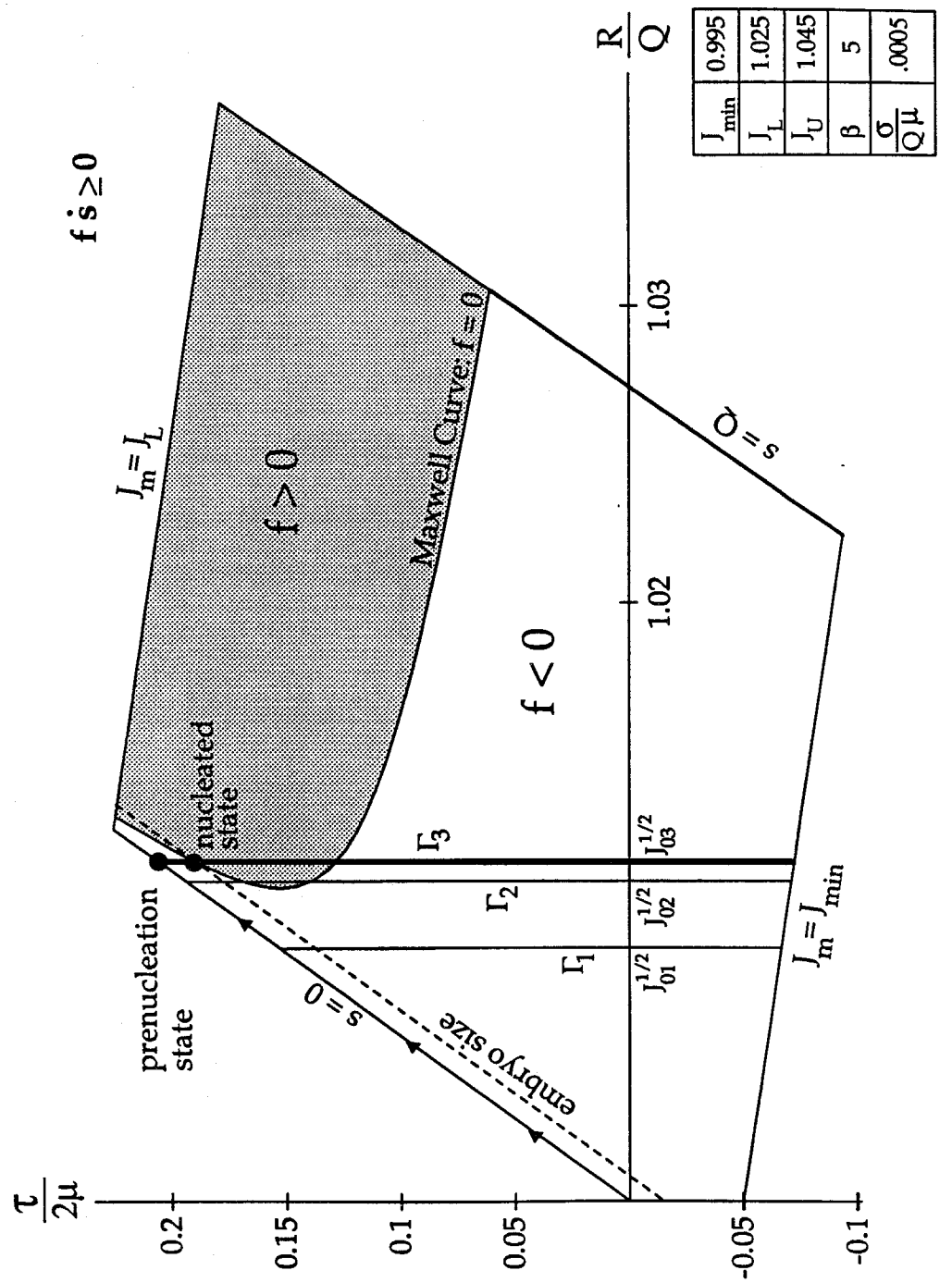

Figure 23(b). Nucleation event under hard loading for interfaces with bonding energy.

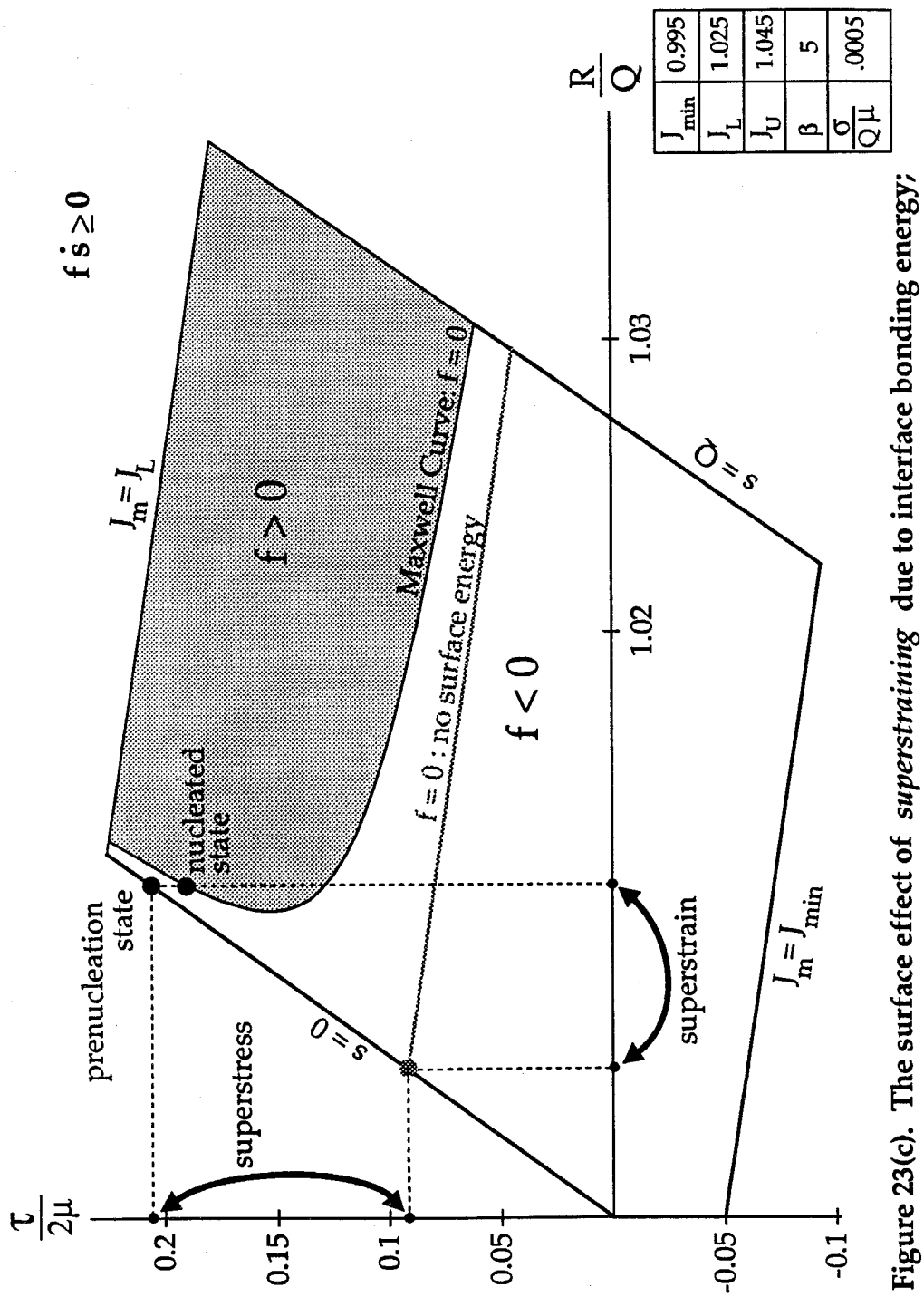

Figure 23(c). The surface effect of *superstraining* due to interface bonding energy; hard loading.

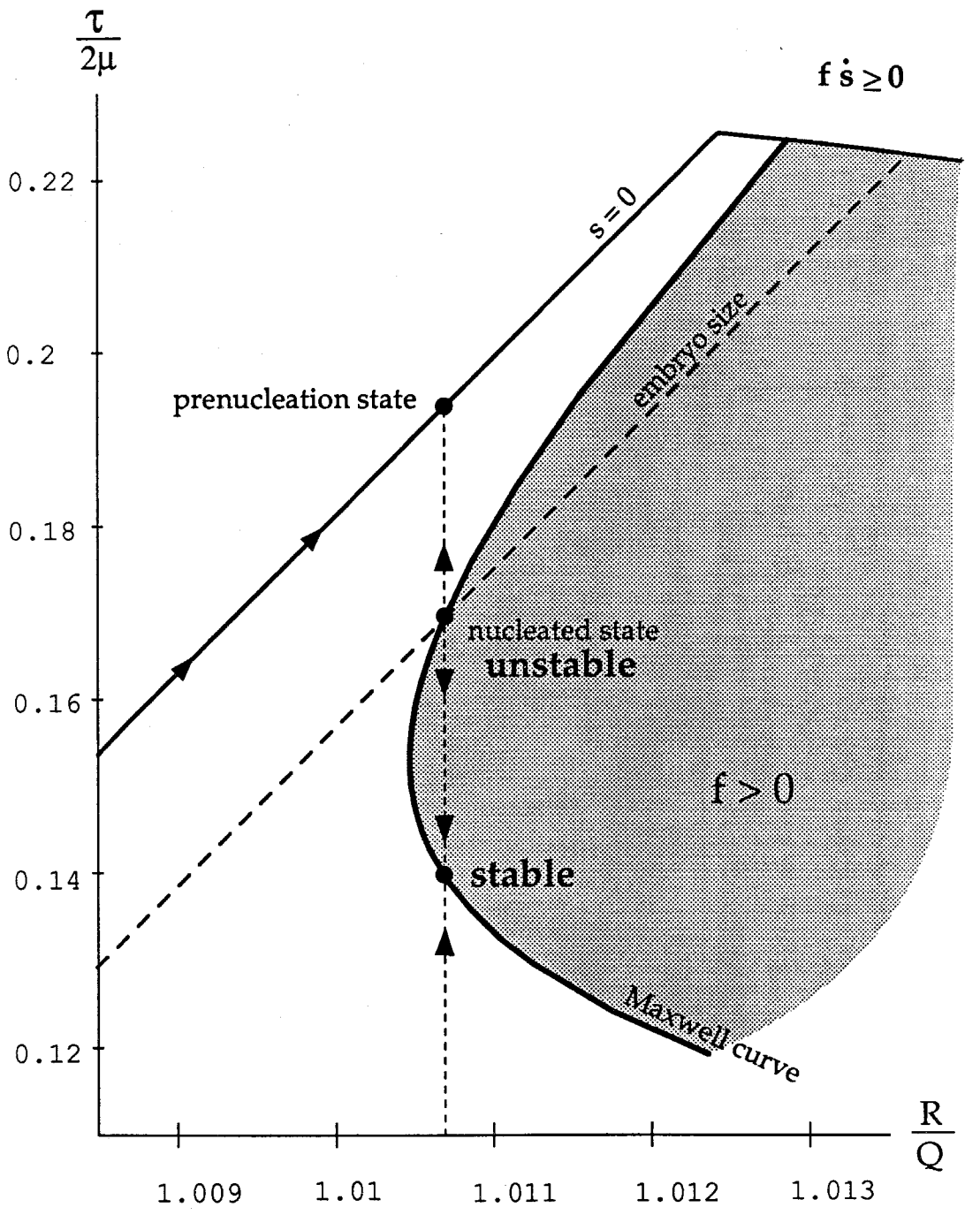

Figure 23(d). Close-up look at hard-loading nucleation event as illustrated on system macroscopic response; interfaces with bonding energy. Here the associated stable and unstable nuclei are illustrated.

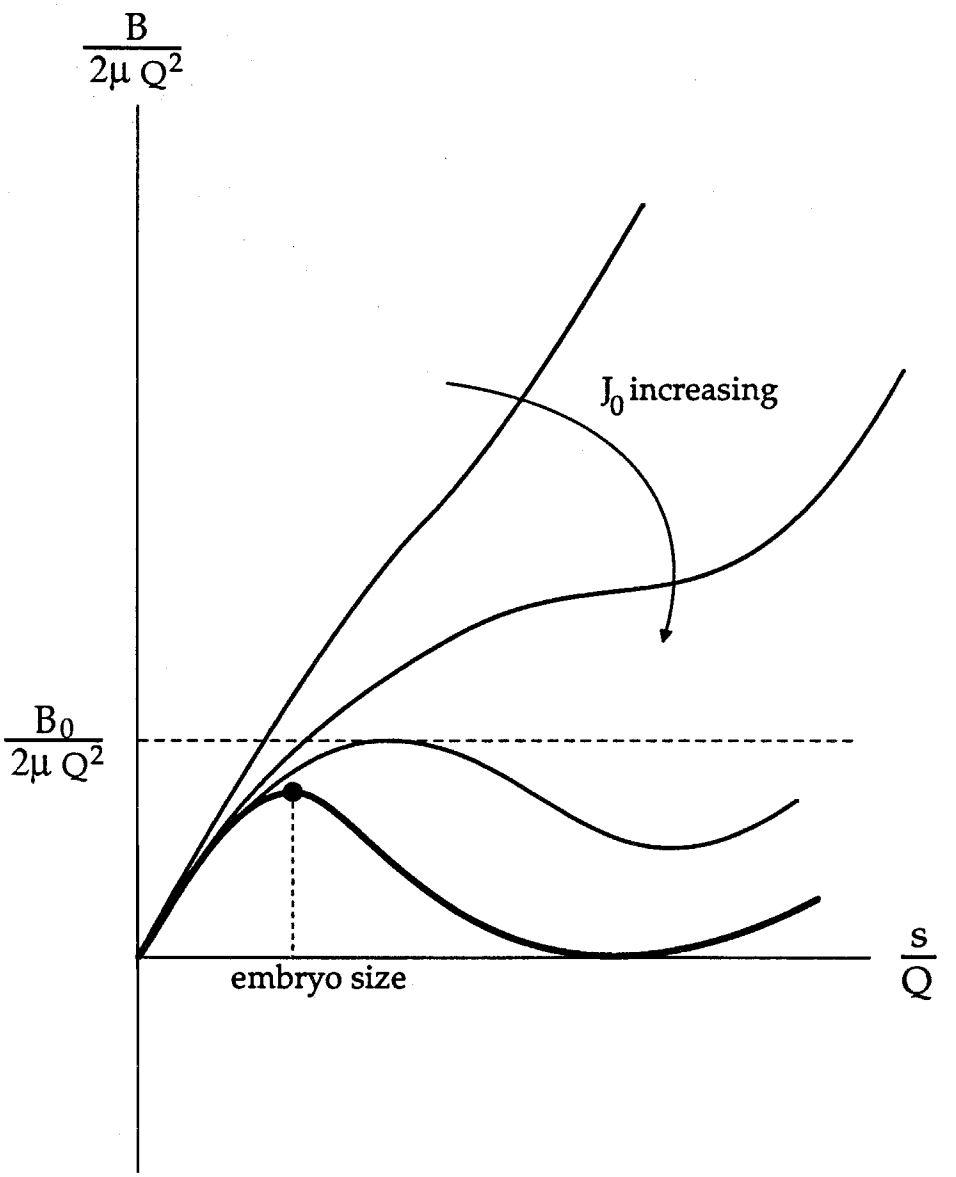

Figure 24. Illustration of how part (ii) of the nucleation criterion may prevent nucleation from occurring at B_0. (The plot shown is a drawing, and was not generated using a particular set of parameters.)

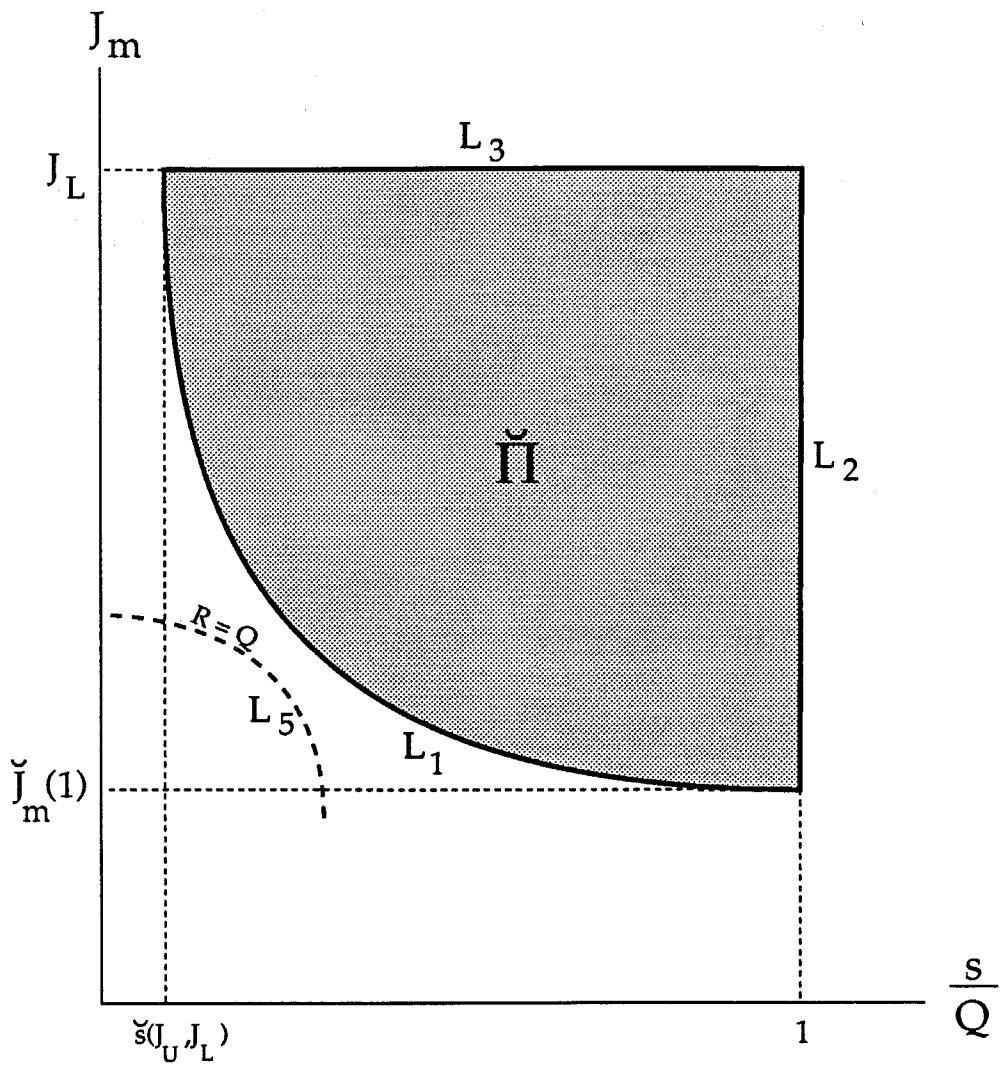

Figure 25. The set, $\breve{\Pi}$, of all (s, J_m) pairs for which the phase segregation constraints are satisfied under extension; fluid-like interfaces. For clarity, it is assumed that L_1 does not intersect L_5, the curve for which R = Q.

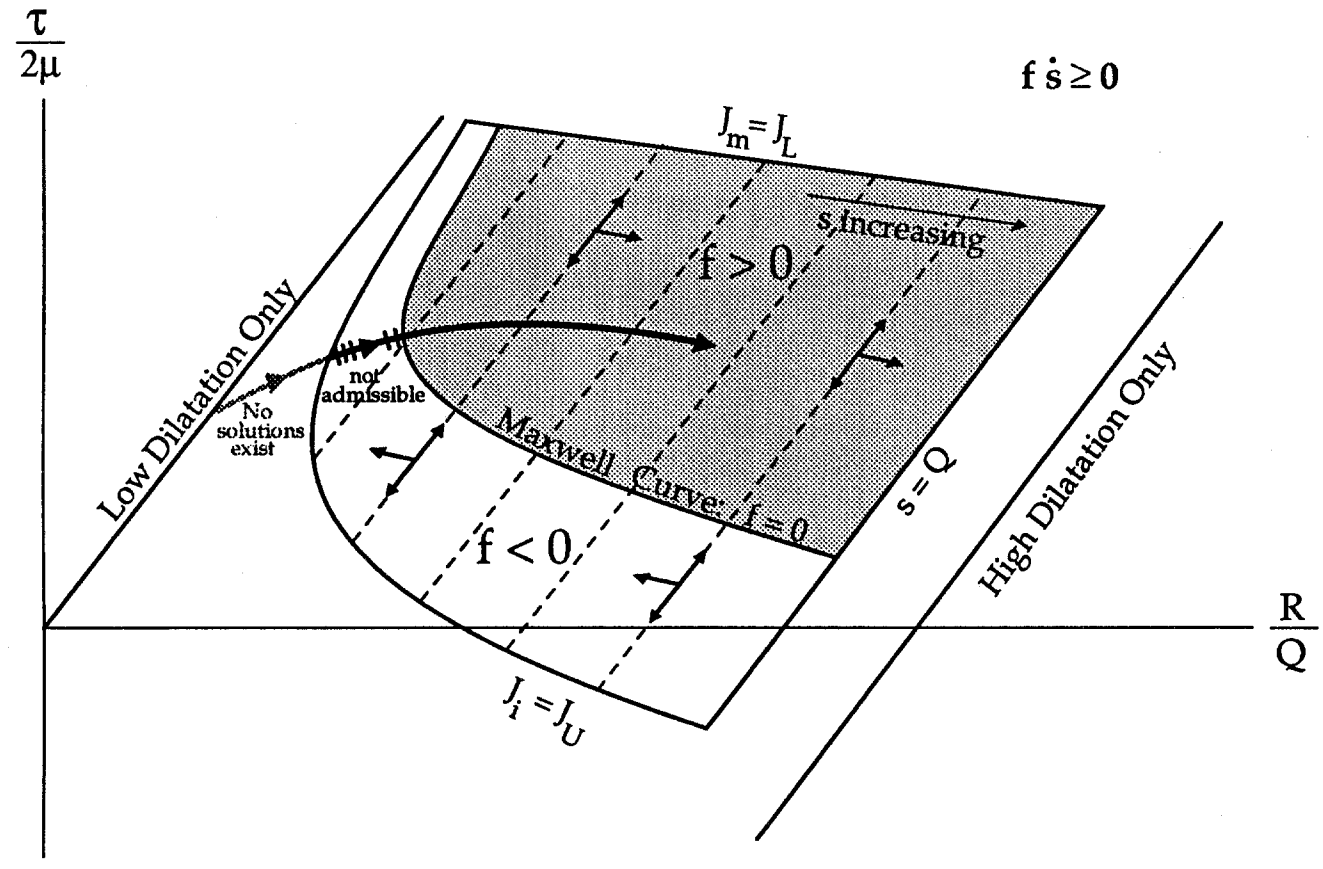

Figure 26. Macroscopic response curve for fluid-like interfaces. A sample two-phase motion is shown to exhibit regions where no two-phase solutions exist, where embryo growth is prohibited, and also where growth is admissible. (This drawing was provided instead of data generated from a particular set of parameters only so that each of these regions is clearly identified on a single plot.)

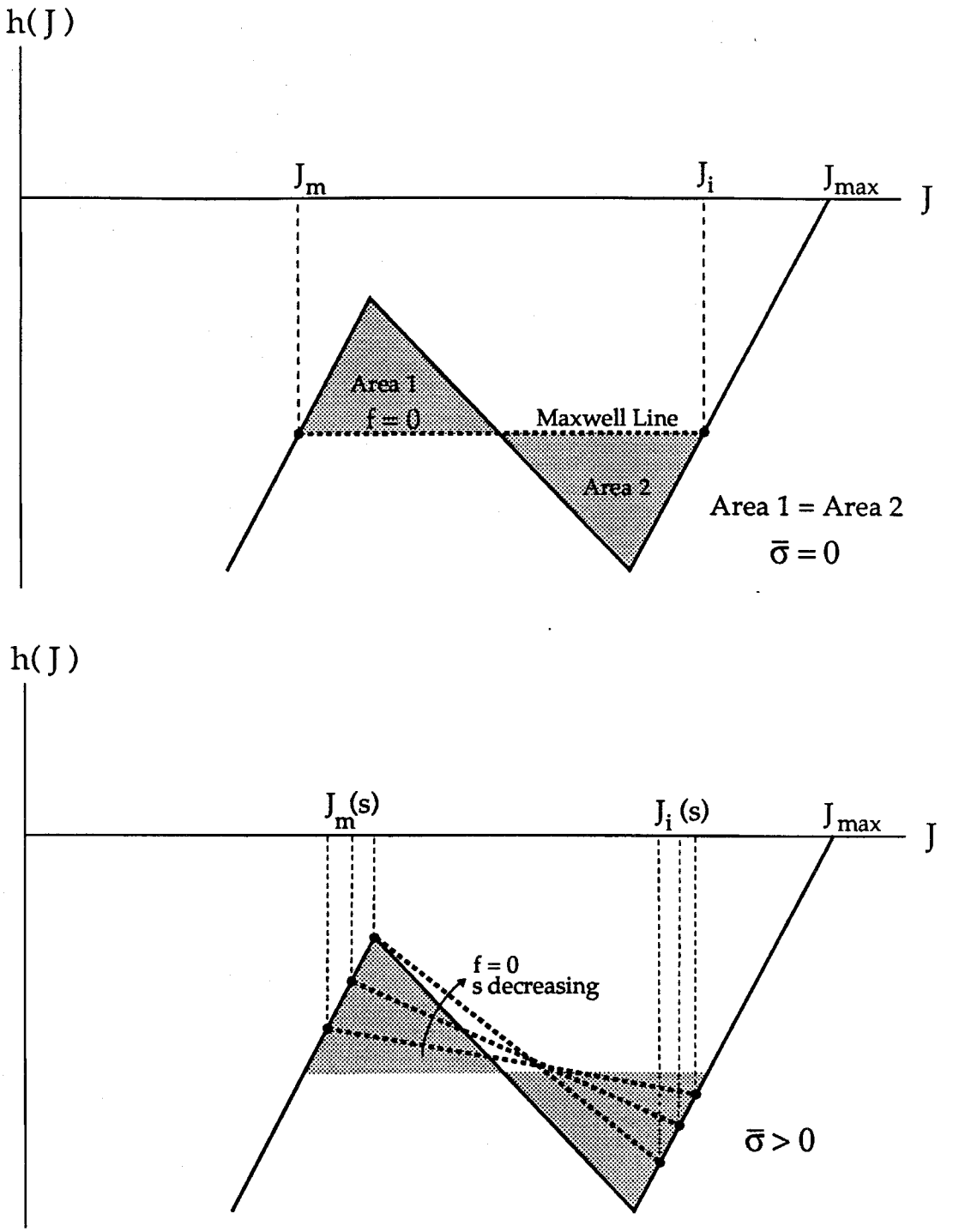

Figure 27. The Equal Area Rule , Figure (a), and its violation for materials with fluid-like interfaces, Figure (b).

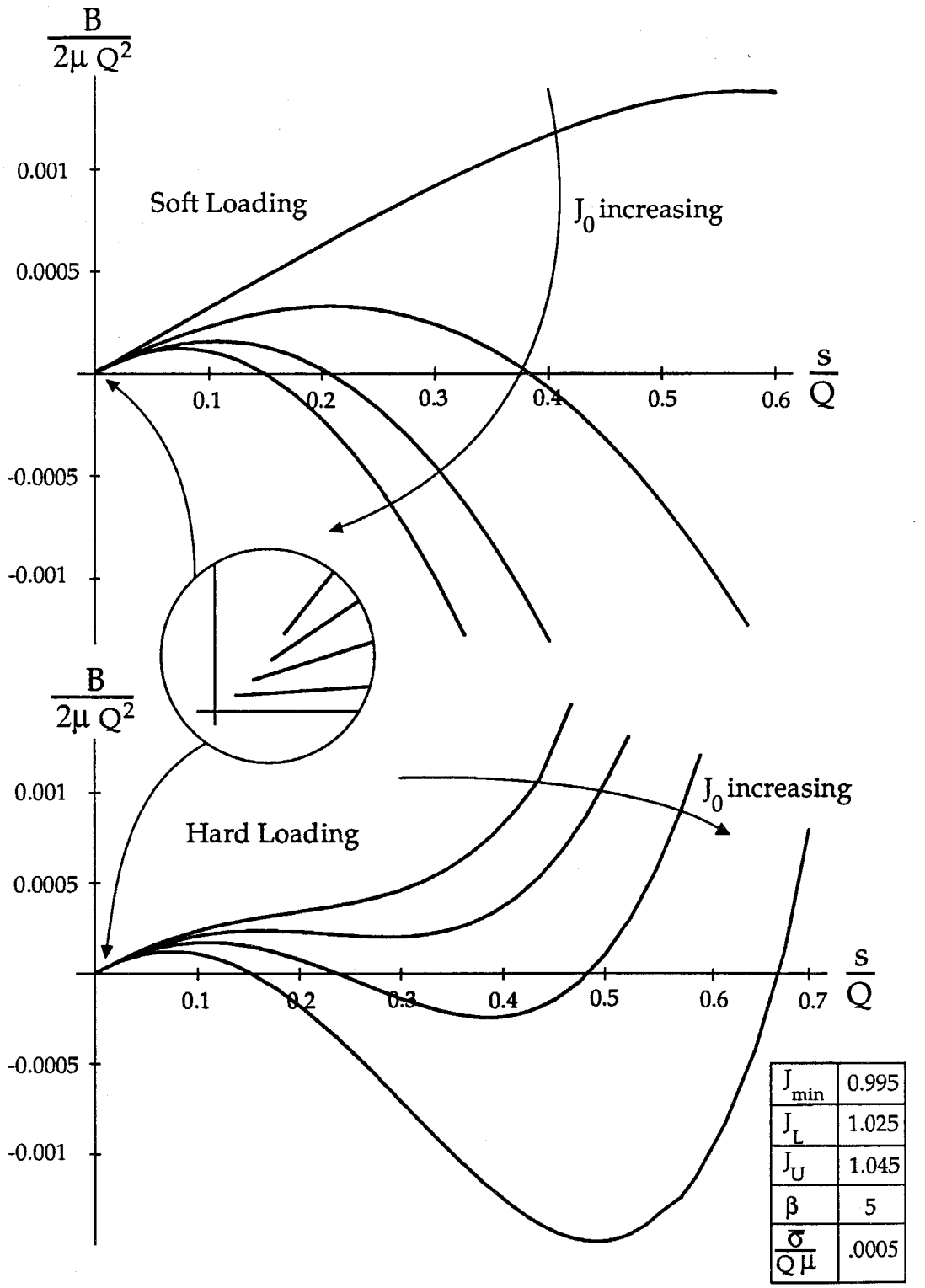

Figure 28. Profiles of nucleation energy, B, for both soft and hard loading; fluid-like interface.

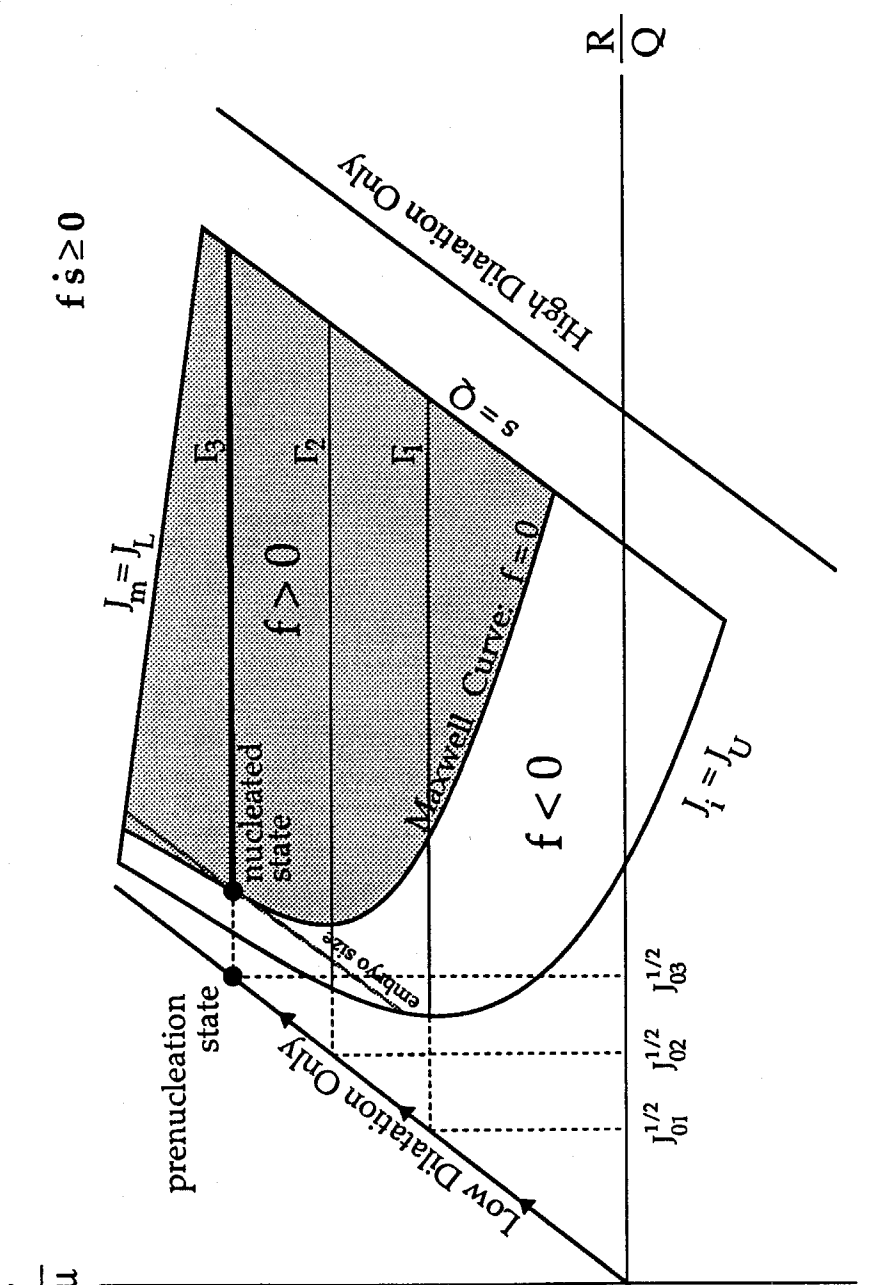

Figure 29. Nucleation event under soft loading for fluid-like interfaces.

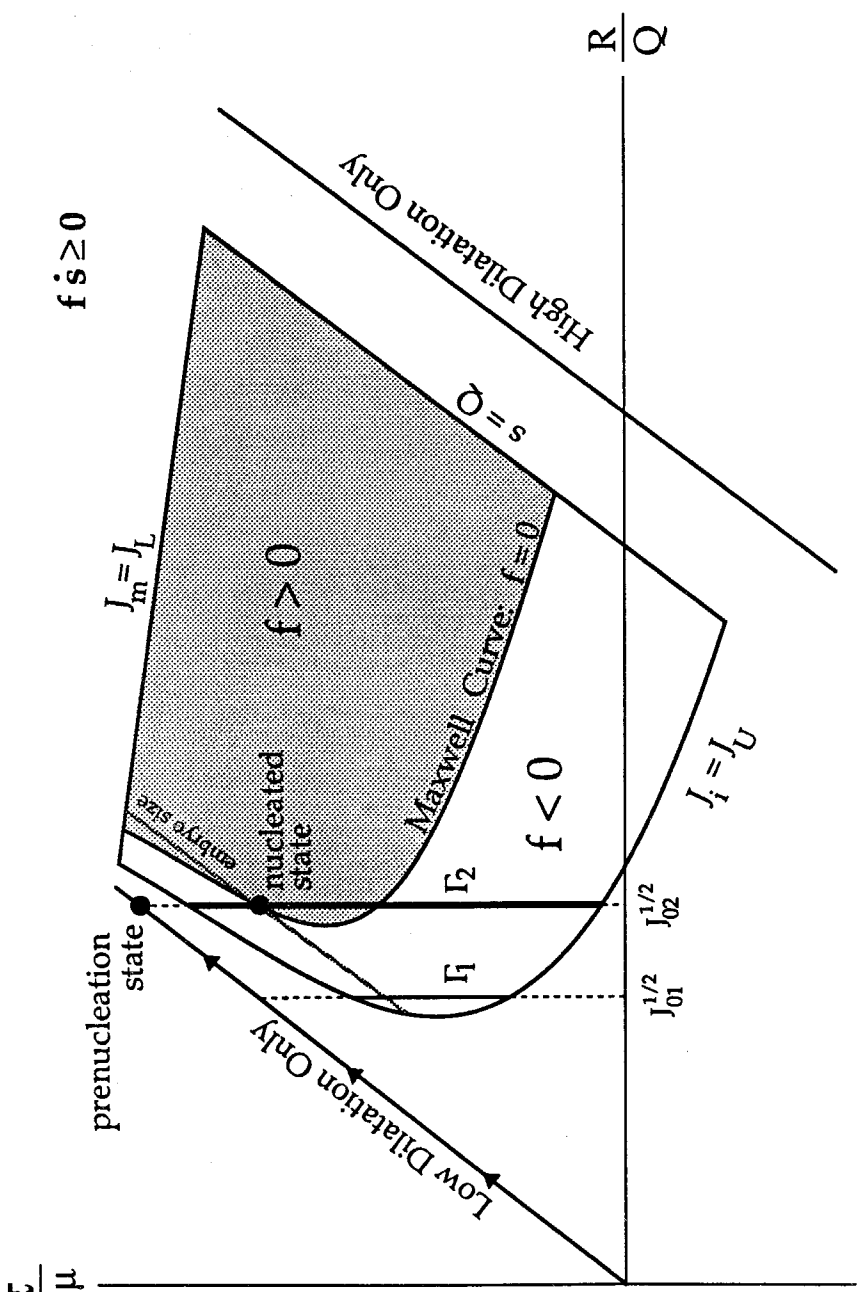

Figure 30. Nucleation event under hard loading for fluid-like interfaces.